Sensitivity-based Pricing and Multiobjective Control for Energy Management in Power Distribution Systems

by

Bharadwaj Ranganathan Sathyanarayana

A Dissertation Presented in Partial Fulfillment
of the Requirements for the Degree
Doctor of Philosophy

Approved July 2012 by the
Graduate Supervisory Committee:

Gerald Heydt, Chair
Vijay Vittal
Raja Ayyanar
Junshan Zhang

ARIZONA STATE UNIVERSITY

August 2012

ABSTRACT

In the deregulated power system, locational marginal prices are used in transmission engineering predominantly as near real-time pricing signals. This work extends this concept to *distribution engineering* so that a distribution class locational marginal price might be used for real-time pricing and control of advanced control systems in distribution circuits. A formulation for the distribution locational marginal price signal is presented that is based on power flow sensitivities in a distribution system. A Jacobian-based sensitivity analysis has been developed for application in the distribution pricing method.

Increasing deployment of distributed energy sources is being seen at the distribution level and this trend is expected to continue. To facilitate an optimal use of the distributed infrastructure, the control of the energy demand on a feeder node in the distribution system has been formulated as a multiobjective optimization problem and a solution algorithm has been developed. In multiobjective problems the Pareto optimality criterion is generally applied, and commonly used solution algorithms are decision-based and heuristic. In contrast, a mathematically-robust technique called normal boundary intersection has been modeled for use in this work, and the control variable is solved via separable programming.

The Roy Billinton Test System (RBTS) has predominantly been used to demonstrate the application of the formulation in distribution system control. A parallel processing environment has been used to replicate the distributed nature of controls at many points in the distribution system. Interactions between the real-time prices in a distribution feeder and the nodal prices at the aggregated load

bus have been investigated. The application of the formulations in an islanded operating condition has also been demonstrated. The DLMP formulation has been validated using the test bed systems and a practical framework for its application in distribution engineering has been presented. The multiobjective optimization yields excellent results and is found to be robust for finer time resolutions. The work shown in this report is applicable to, and has been researched under the aegis of the Future Renewable Electric Energy Delivery and Management (FREEDM) center, which is a generation III National Science Foundation engineering research center headquartered at North Carolina State University.

“Your whole question is, ‘What do I do?’. I have no answer.”

H. H. Sri Sri Ravi Shankar

Dedicated to all spiritual masters - past, present and future;

though too insignificant an offering, this is a humble reminder to the self

of all the timeless moments this work has made possible.

ACKNOWLEDGMENTS

I express my sincere gratitude to my advisor Dr. Gerald Heydt for his guidance and leadership throughout my graduate studies. This work would not be the same without his superior insight and knowledge. His commitment to education and research is an inspiration. I am grateful to National Science Foundation and the Future Renewable Electric Energy Delivery and Management systems center under grant EEC-08212121 for its continued support through the duration of this work. I appreciate the contributions of Dr. Alex Huang, Dr. Raja Ayyanar, Dr. Mariesa Crow and Dr. Bardul Chowdhury; and the FREEDM working group student members at Florida State University towards this research. Gratitude is also due to my graduate supervisory committee, comprising of Dr. Junshan Zhang, Dr. Raja Ayyanar and Dr. Vijay Vittal for their time and support.

I also take this opportunity to thank the distinguished faculty of the power engineering program at Arizona State University, for their many contributions towards my comprehensive growth over the period of my education here. Appreciations are also due to all my fellow students at Arizona State University, and FREEDM systems center for their support. I am also grateful for my brother Lakshminarayan Bharadwaj at Indian Institute of Technology, Kanpur for all the hours spent proofreading and offering corrections to this document, and my loving parents without whom nothing would be the same.

TABLE OF CONTENTS

Page

CHAPTER Page

APPENDIX Page

LIST OF TABLES

Table Page

Table Page

LIST OF FIGURES

Figure Page

Figure Page

Figure Page

Figure Page

NOMENCLATURE

A	Non-directed bus-line incidence matrix
A_{eq}, $A_{in\text{-}eq}$	Equality and inequality matrices in optimization
b, b_{eq}	Right hand side of inequality and equality equations in optimization
b^{sh}_{ij}	Total primitive line charging susceptance in the line between buses i and j
B	Bus susceptance matrix referenced to ground
B'	Bus susceptance matrix referenced to swing bus
C	Optimal power flow cost function
C_0, C_1	Generator cost function coefficients
C_e, C_ℓ, C_g	Empirical constants for distribution locational marginal price terms
CAISO	California Independent System Operator
CCE	Cumulative cost of energy
CF	Capacity factor
d	Distance along a normal from the convex hull to the objective boundary
d_n	Number of subtransmission supply points to a distribution system
DER	Distributed energy resource
DESD	Distributed energy storage device
DGI	Distributed grid intelligence
DLMP	Distribution locational marginal price
DMS	Distribution management system

$E_{s,max}$	Maximum installed energy storage capacity
EMS	Energy management system
ERCOT	Electric Reliability Council of Texas
f	Objective function
FERC	Federal Energy Regulatory Commission
FID	Fault interruption device
FREEDM	Future Renewable Electric Energy Distribution and Management
g_{ij}, b_{ij}	Primitive line conductance and susceptance of line between buses i and j
G^C	Generator fuel cost function
GSF	Generation shift factor
H	Set of all generating units in the transmission network
H_b	Primitive branch admittance matrix
I^b	Vector of bus current magnitudes
I^l	Vector of line current magnitudes
IEEE	Institute of Electrical and Electronics Engineers
IEM	Intelligent energy management
IFM	Intelligent fault management
ISO	Independent System Operator
ISO-NE	Independent System Operator-New England
J	Jacobian matrix of the Newton-Raphson power flow algorithm
J_{agg}	Aggregated objective function in a multiobjective optimization

J_1 - J_4	Submatrices within the power flow Jacobian matrix
ℓ	Directed bus-line incidence matrix
L	Modified form of the directed bus-line incidence matrix
LMP	Locational marginal price
MOP	Multiobjective optimization problem
n_l, n_b	Number of branches (lines), nodes (buses) in the distribution circuit
n	Number of steps in the optimization time horizon
n_s	Number of single-variable functions in a separable program
NBI	Normal boundary intersection
NSF	National Science Foundation
NY ISO	New York Independent System Operator
OPF	Optimal power flow
p	Number of objectives in the multiobjective optimization
p_b	Number of breakaways in a separable program
P^b, Q^b	Vectors of active and reactive power bus injections
P^g, Q^g	Vectors of generator active and reactive power outputs
P^l, Q^l	Vectors of active and reactive power line flows
P_{ld}	Peak rating of the net load in the distribution system
P_{loss}	Branch active power loss
P_{max}	Maximum power rating of storage interface converters
P_r	Sum of peak power ratings of the distributed resources in the system
P_R	Branch MVA rating

PK	Time window denoting the peak load duration
PCC	Point of common coupling
PES	Power and Energy Society
PLL	Phase locked loop
PTDF	Power transfer distribution factor
PWM	Pulse width modulation
R_l, X_l	Branch resistance and reactance
RBTS	Roy Billinton Test System
RTO	Regional Transmission Operator
RSC	Reliable and secure communication
s, s_0	State of charge and initial condition on the state of charge
S	Line flow sensitivity matrix
S^l	Vector of complex line flows
S_1 - S_4	Submatrices within the line flow sensitivity matrix
SOC	State of charge
SCADA	Supervisory control and data acquisition
SP	Separable programming
SST	Solid state transformer
T	Time horizon of study
u	Unit normal constructed to a convex hull
V	Vector of bus voltage magnitudes
V^-, V^+	Negative and positive sequence voltages

W	Vector of weights for objectives in normal boundary intersection
x, X	A single control variable and a vector of control variables
X_d	Vector representing the active power demand at each time step in the time horizon
X_{load}	Vector representing the load at each time step in the time horizon
X_{DG}	Vector representing the renewable power output
X_S	Vector representing the storage charging rates
Y_{bus}	Bus admittance matrix
z	Objective function f_1 represented as an additional control variable
Z	Branch impedance
Z_{bus}	Bus impedance matrix
$\{.\}^*$	Representation of an optimal solution
$\{.\}^T$	Matrix transpose operation
α	Weight of breakaways in a separable program
ΔP, ΔQ	Vectors of active and reactive power bus mismatches
ΔP^b, ΔQ^b	Vectors of active and reactive power bus injections
ΔP^g, ΔQ^g	Vectors of generator active and reactive power outputs
ΔP^l, ΔQ^l	Vectors of active and reactive power line flows
Δt	Time duration of each step in optimization
ΔT	Time delay in calculating the forecasts of the system dynamics
ΔV	Vector of changes in bus voltage magnitudes
$\Delta \theta$	Vector of changes in bus voltage angles

δ	Distribution locational marginal price
$\delta_{\{.\},e}$	Energy component of distribution locational marginal price
$\delta_{\{.\},c}$	Congestion component of distribution locational marginal price
$\delta_{\{.\},l}$	Loss component of distribution locational marginal price
ε	Power loss percentage in energy storage interface converters
λ	Locational marginal price
$\lambda_{\{.\},e}$	Energy component of locational marginal price
$\lambda_{\{.\},c}$	Congestion component of locational marginal price
$\lambda_{\{.\},l}$	Loss component of locational marginal price
μ	Lagrange multiplier in optimal dispatch for line real power flow constraints
υ	Renewable incentive in distribution location marginal price
φ	Power factor at bus
π	Participation factor of supply-end in the distribution system
Φ	Matrix representing deviations in individual objective minima
Ψ	Convex hull of individual minima
ρ	Power transfer distribution factor
ρ_{AC}	Jacobian-based AC power transfer distribution factor
χ	Reduced-form DC power flow matrix
Θ	Vector of bus voltage angles

Chapter 1

DISTRIBUTION SYSTEM OPERATIONS

1.1 Motivation

Traditional operational objectives in a power distribution system include voltage regulation, loss reduction, and maintaining distribution asset loading within rated limits. Most *legacy* distribution systems have minimal control possibilities – mainly shunt capacitor switching for voltage regulation, and possible tap changing at the substation end of distribution primary feeders. Other typical operations belong in the category of distribution system protective devices like fuses and reclosers. Load management and restoration also constitute common operations for distribution systems, as implemented by several utilities. Therefore, in general distribution system operations are mainly centered towards the reduction of disruptions in circuits and the supply, and the adequate management of electricity delivery. In recent times, special attention on increased reliability and quality of power delivered, has garnered much importance.

Under contemporary environments, additional operations and controls may be in place such as energy and power management, reactive power dispatch, and management of renewable resources. Energy storage in distribution systems has also been proposed, and this too would entail control. The optimization of the operating point in power distribution systems can be viewed as a multiobjective problem. One hobble in the traditional approach to distribution engineering has been a minimum of control possibilities; another has been a paucity of measured information; yet another has been the basic nature of radial distribution primaries.

Some of these issues are changing rapidly with the advent of the Smart Grid. Also, the potential introduction of relatively high levels of distributed energy resources and energy storage devices at residential, industrial, and commercial load sites changes the generalized approach needed in distribution engineering. The strategy that is needed for the control of energy storage devices located in the distribution system suggests the search for a control signal (or signals) that capture long term objectives.

In 2008, the U. S. National Science Foundation inaugurated an engineering research center denominated the Future Renewable Electric Energy Distribution and Management (FREEDM) center. The essence of the FREEDM energy management controls relates to the balancing or management of various objectives including: peak demand reduction from the legacy system, maximal penetration of renewable resources, low cost to the consumer, the ability to support at least part of the demand in the case of loss of power supply from the conventional distribution system, and reduction of greenhouse gas emissions. One of the main enablers of these objectives is the planned use of a solid state transformer (SST). This component is a digitally controlled converter that is capable of controlling power flow, voltage magnitude, and various phase relationships of current and voltage.

Some operating states in distribution systems are best controlled in real time (e.g., voltage magnitudes). Voltage magnitudes are largely controlled by reactive power demands and assets in the system, and all of these factors are basically real time variables. Energy demand over some time period T, and peak

power demand (e.g., daily peak) in a feeder, are both quantities that occur and can be controlled over a much longer time horizons. Figure 1.1 shows a pictorial of time horizons of some of the operations in a distribution system.

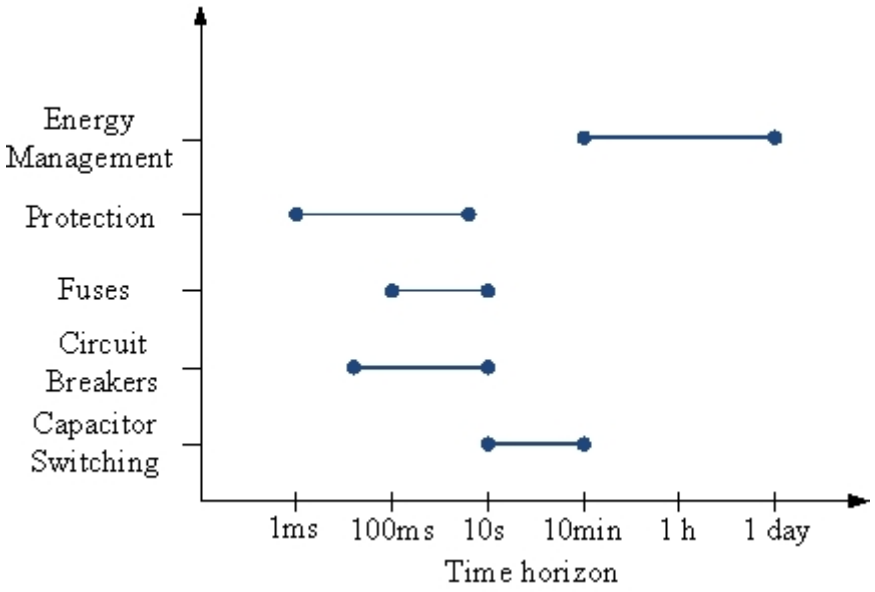

Figure 1.1 Time horizon for operations in a distribution system (approximately logarithmic scale)

In interconnected transmission networks, locational marginal prices (LMPs) are used to quantify the cost of the next megawatt hour delivered to a specified point of delivery at a given system operating point. LMPs can thus be viewed as pricing signals that in an energy market dictate the efficient or optimal functioning of the system assets to serve load and maintain balance of power in the bulk power system. In essence, LMPs appear to have characteristics that are consistent with some distribution engineering objectives related to energy flow and energy management. For purposes of this report, *distribution system control* is taken to refer to energy management, and not voltage control or system protec-

tion. The latter two subsystems occur in a high speed time horizon and presumably are decoupled from the energy management milieu.

1.2 Objectives and Scope of Research

The primary objective of this work is to develop a time-of-day pricing and control strategy for power distribution systems that would be beneficial for the optimal operation of the distribution system, both with contemporary practices and envisioned future advances. A distribution locational marginal price (DLMP) based formulation has been investigated for this purpose. A power flow sensitivity based formulation has been developed that takes into consideration the operational characteristics of power distribution systems. The optimal control of the energy demand on a distribution feeder with the presence of distributed assets has also been investigated in this work. The particular points of interest of this study are:

i. Formulate a model for distribution class locational marginal prices using a sensitivity based approach, for power distribution systems.
ii. Analyze the characteristics of such a formulation and its operational reliability in distribution systems.
iii. Develop a multiobjective optimization based control technique to minimize the energy demand on a feeder with dispersed distributed resources and storage elements.
iv. Test the DLMP and control formulations on a test case that provides the characteristics of the transmission network and details of the distribution circuits at its component buses.

v. Study possible interactions of the control formulation in the distribution system, on the bulk power system price structures.

vi. Perform extensive simulation tests on different types of test-bed systems available in contemporary literature, considering different operational scenarios common for distribution system analysis.

vii. Illustrate the DLMP for the FREEDM system.

viii. Present a roadmap for the practical application of the algorithms developed.

1.3 Literature Review

A sampling of literature accessible on the topics of interest in this study is presented here. Some of the issues relating to the controls (both existing and envisioned) for distribution systems, locational marginal prices, multiobjective optimization, and integration technologies for renewable resources and storage in the distribution system are chronicled in the follow discussions.

Controls in Distribution Systems

Power distribution system controls and operations have been a topic of study and innovation from its inception [1], more so in recent years due to the advances in the computational and technological spheres. As discussed earlier, traditional control operations in distribution systems can be predominantly typified by voltage regulation and reactive power management [2-3], protection based controls [4-6], power quality control algorithms [7-9], and the management of harmonics and non-sinusoidal loads [10].

Automation in distribution engineering using distribution management systems (DMS) was first conceptualized and used by several utilities in the 1990s, akin to its transmission engineering counterpart, the energy management system (EMS). Some of the key ideas here included supervisory control and data acquisition, automation of distribution substations and feeders, and distribution system analysis applications [11-14]. Optimal feeder reconfiguration, centralized voltage control etc. are added functionalities in a DMS, and have been discussed in great detail in reference [12]. Some DMS control functions are implemented inherently different from the transmission case. The control functionalities vary due to the following factors: distribution systems are radial feeders while transmission systems are networked; distribution system devices to be monitored are located throughout the distribution system (e.g., on pole tops) while transmission devices are predominantly localized within the substation; typical distribution systems are subject to topology changes that are more drastic and frequent than the transmission counterpart [11-13] – e.g. due to feeder reconfigurations, greater frequency of system outages, regular system expansion etc. In existing scenarios, it should also be noted that the level of automation in distribution systems is far lower than in the case of transmission networks.

Another facet of control in distribution system is demand-side management, where the dynamic response of the demand-side to fluctuations in load prices could play an important role in shaping the future of deregulated energy markets [15-16]. Some potential implications of demand response discussed in literature are the stabilization of grid frequency [17] and optimal investment in

power generation [18]. References [15-19] provide an excellent background and conceptualization of demand-side management.

The increasing penetration of distributed resources and storage devices in the distribution system is an expected phenomenon. Several electricity market operators e.g., California Independent System Operator (CAISO), have been working on integration of renewables and storage in their distribution circuits [20]. Energy storage integration in view of mitigating large energy ramps during load pick-ups in the morning and ramp down in the evening, and cases of over generation have been proposed by CAISO. Storage participation in the ancillary service markets is also being studied by several market operators [21]. Potential challenges that could be attributed to increased storage and distributed energy resource (DER) penetrations are: the need for models to forecast resources, efficient monitoring and control, integration within existing system operations, maintenance of system operating limits, and potential for inadvertent islanding [20]. Reference [22] discusses energy storage in distribution systems, and the controls of this asset.

The FREEDM Systems Research Center

The United States Department of Energy has indicated the main features of the 'Smart Grid Initiative' [23] as efficient, accommodating, motivating, opportunistic, quality focused, resilient, and '*green*'. Therefore, the Smart Grid as outlined implies that control and optimization should be used in all elements of power systems, and recently new initiatives have been put forth to control and manage energy and resources in power distribution systems. One such initiative is

the Future Renewable Electric Energy Delivery and Management system center [24].

FREEDM is a generation III Engineering Research Center sponsored by the National Science Foundation. The FREEDM center focuses on the following, listed approximately in order of priority:

i. Application of solid state devices and power electronics in power distribution systems
ii. Integration of renewable resources in power distribution systems
iii. Application of control and system theory to make power distribution systems ‘smarter’.

The work done in this dissertation constitutes some of the efforts of the FREEDM system center. Smart Grid technologies appear to be especially applicable to electric power distribution systems because there are a number of control and optimization possibilities near the point of end use. A comparison of centralized and decentralized control structures [25] is shown in Figure 1.2, for the optimized point of end use. Projected designs of future distribution systems include many control features [26-29], smart capabilities (i.e., using measurements to effectuate control) [30-32], and innovative metering and rate structures to encourage desired modes of operation [33-34].

Energy Economics

In the United States, the state of California was the first in implementing a market based environment in the energy delivery sector [35].

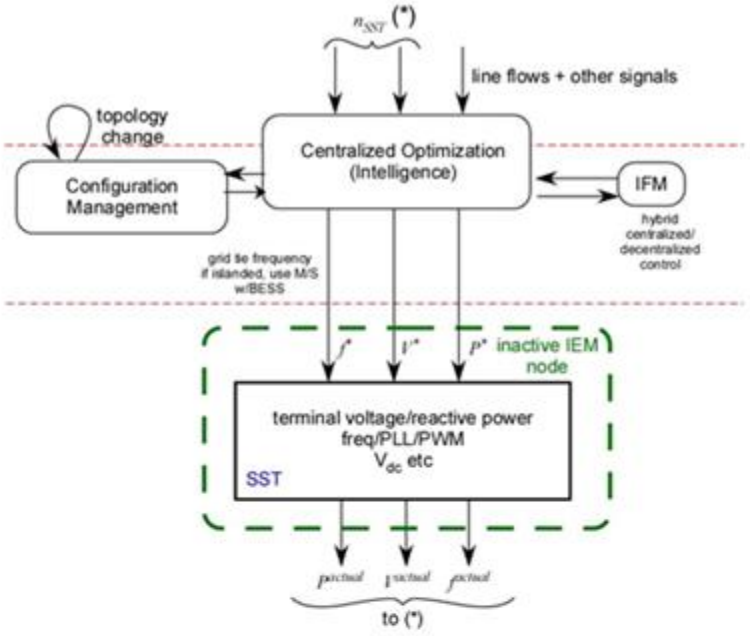

(a) Centralized control

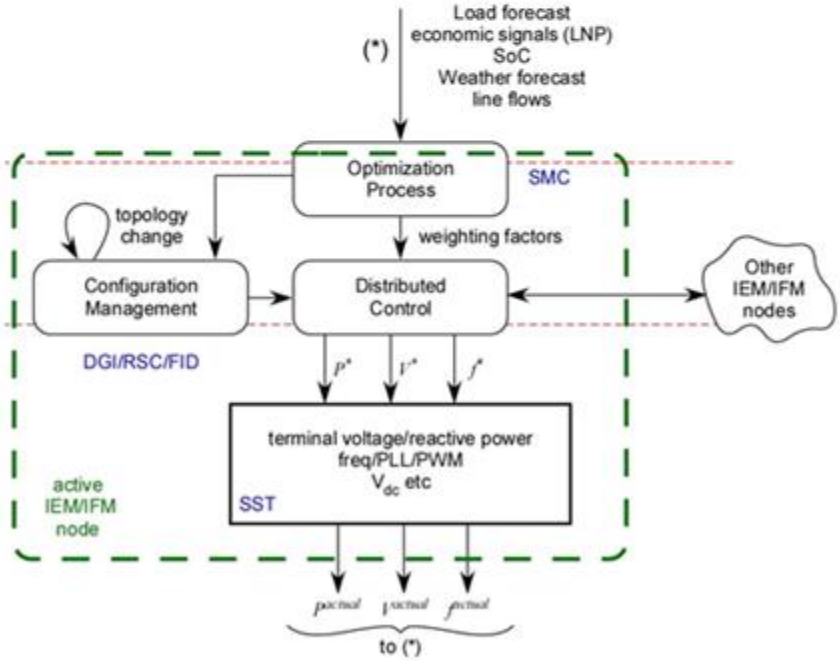

(b) Decentralized control

Figure 1.2 An example of centralized and decentralized control structures proposed for future distribution systems [25]

A wholesale electricity market implementation was undertaken in 1992 with the Federal Energy Regulatory Commission's (FERC) Transmission Open Access system, and the establishment of the Independent System Operators (ISOs) and Regional Transmission Organizations (RTOs). A detailed structure of the electricity markets and the operations of ISOs and RTOs can be found in references [36-38].

The spot price for electricity refers to the quoted price of electricity delivery in MWh for an immediate market agreement, and was first proposed by Schweppe [39]. More commonly known as locational marginal prices or nodal prices, they indicate the expectation in the direction of movement of the market prices. Hence, LMPs are viewed of as 'shadow prices' that depict the change in an objective to be optimized, when the constraints are marginally perturbed. Typical hourly day-ahead LMPs are shown in Figure 1.3, observed in the CAISO market for October 14, 2011 [40].

LMP based pricing is commonly used by most of the market operators in the US today. Some of the issues relating to an LMP based market are: the prediction of transmission congestion and prices with load variations [41], formulating a robust LMP evaluation [42], impact of wind production on LMPs [43], and they have been investigated in the references provided. References [44-45] describe how LMPs are calculated, and references [46-47] describe how they are used.

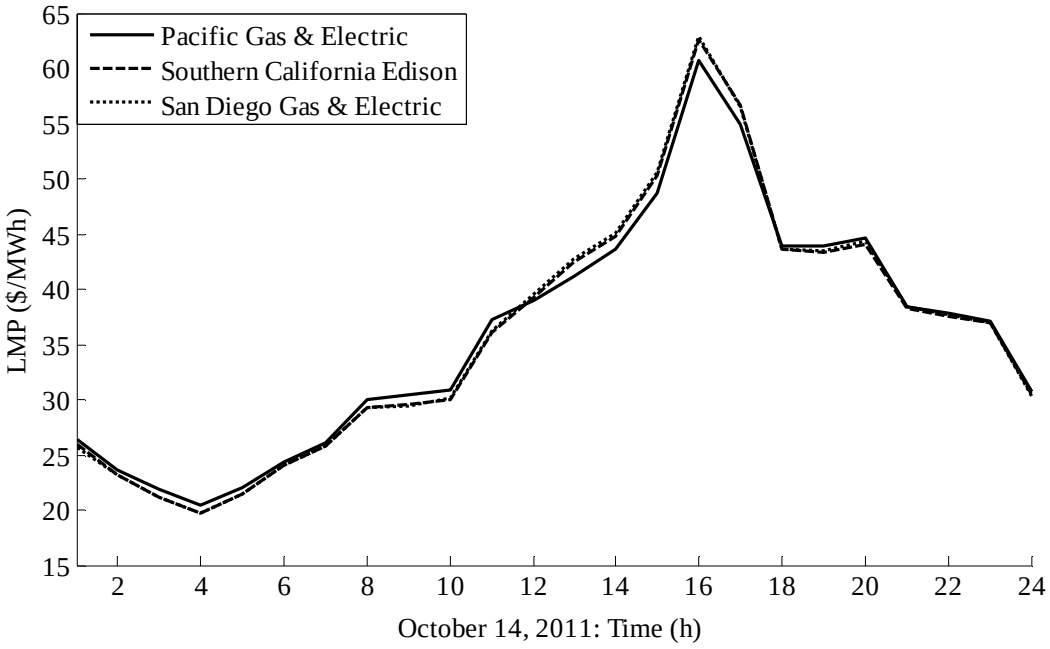

Figure 1.3 Day-ahead LMPs for utilities in the CAISO market (shown for 10.14.2011) [40]

Pricing in Distribution Systems

In view of increasing penetrations of distributed assets in the distribution system, spot pricing in distribution systems has gathered much interest. Spot prices can be evaluated considering different optimization scenarios in a feeder e.g., global benefit problem, customer benefit problem [48] etc. In distribution feeders with the presence of distributed resources, nodal prices are found to be useful in incentivizing asset owners and participants [49]. Regulation of prices in the distribution level has also been undertaken in certain cases via price-cap regulations and yardstick regulations, that are set by utilities and regulating operators. Marginal pricing in distribution systems is also important in view of distribution system expansion and planning [50]. A method of extending LMPs to distribu-

tion systems has been developed in this dissertation. The salient features and control applications have been demonstrated as well.

Furthermore, distributed generation (DG) in distribution systems could be viewed as being similar to transmission networks. Therefore, techniques for pricing for distribution systems similar to those used in transmission systems have been studied in references [49-52]. Reference [53] describes a new technique for calculation of LMP using a game theoretic approach. A uniform marginal pricing technique for distribution systems which requires much less computation as compared to other approaches has been presented in reference [54]. A new pricing technique which takes into account the reliability costs of the system is also been presented in [55]. However, this technique is computationally complex when compared to standard pricing methods, which do not incorporate unreliability tolerance of the nodes.

Renewable and Storage Integration Technologies in Distribution Systems

The integration of renewable energy resources in distribution systems poses certain issues like intermittency of the generated power. Reference [56] has proposed a storage-level solution for this problem in the form of an optimal battery storage system, and reference [57] discusses a control mechanism for linking renewable sources with the distribution system. Reliability analysis of distribution systems with renewable sources has been studied in references [58-62]. The reliability of radial feeders attached to distributed generation has also been studied [58]. References [59-61] look at the reliability of distribution systems from different renewable sources under different modes of operation. An optimal combina-

tion of different renewable sources in the system in order to minimize energy loss has also been studied [63]. Minimization of energy losses by implementing optimal smart grid settings have been studied in [14, 64].

A strategy for minimizing energy losses in the system by integration of energy storage systems has been presented in [65], where the particular case of battery storage has been considered and optimality has been established. Reference [66-67] discusses the idea of integrating battery storage into distribution systems with considerable photovoltaic penetration in order to overcome the problem of intermittency. The implications on distribution system operations and overcoming the voltage rise problem have also been studied. Reference [68] looks at the placement of storage systems in distribution networks for high wind penetration, and an optimal allocation strategy has been developed. The economics relating to energy storage implementations in distribution systems with a comparative analysis of different storage mechanisms has also been presented [69].

Multiobjective Optimization

The application of multiobjective optimization [70-71] tools and methods has been made in literature in various scientific disciplines and interdisciplinary research initiatives. A multiobjective optimization problem (MOP) is the quantitative assessment of a control variable X in simultaneous view of p objective functions. The p objective functions can be united into a single objective vector f as follows

$$f(\Re^n \to \Re^p) \equiv \left\{X \ \alpha \quad f(X) = (f_1(X), f_2(X) \ldots f_p(X))^T\right\}. \tag{1.1}$$

The arrow notation shown in (1.1) represents the mapping of a function $f(X)$ where X is a vector and f is also a vector. Since an individual function could contradict another and be incommensurable, it is necessary to formulate f in a meaningful form, accommodating all functions in f. This necessitates the need for an appropriate optimality criterion called Pareto optimality [73-74], and the references indicated provide a detailed formulation of it. A derivation of the necessary conditions for the Pareto optimality criterion has been shown in reference [74]. MOPs are also traditionally applied to continuous dynamical systems, where it is transformed to an optimal control problem. In the case of discrete systems, the corresponding class of optimization problems is called discrete-time optimal control. The energy demand and cumulative costs incurred in a feeder are discrete time-variant functions. The application of MOPs in the approach shown in this work for optimizing the energy demand on a feeder is one example of the same.

Applications of Pareto optimality and MOPs in power engineering can be seen in the optimal reconfiguration of distribution feeders [75] and transmission congestion management [76]. Several efforts to resolve some of the issues relating to managing the energy needs of distribution systems with distributed assets have been proposed and implemented. Lasseter in [77-78] discusses autonomous control strategies for the micro grid systems using active power versus frequency droop characteristics. Lehtonen *et al.*, in [79] present a distribution energy management system in view of power system markets. The distribution energy management problem is one of managing multiple objectives some of which may be inherently conflicting. It can be viewed as an optimal utilization of DERs and dis-

tributed energy storage devices (DESDs) in the power distribution system to minimize several objective functions, and subject to energy balance and load balance constraints. Large system solutions introduce high dimensionality and there is the added possibility of issues relating to non-convergence. In addition, generating a Pareto optimal solution can prove to be difficult for non-convex problems. Solution methods for MOPs have been discussed in references [80-81], including evolutionary approaches and mathematically robust algorithms.

1.4 Organization of this Dissertation

The review of traditional transmission level locational marginal prices and a formulation of distribution locational marginal prices using a sensitivity based approach are presented in Chapter 2. Chapter 3 presents the control problem viewed as a multiobjective optimization problem. The optimization of the point of end use, with the presence of distributed resources and storage devices has been dealt with. The principle of Pareto optimality has been discussed and a suitable solution algorithm for the problem is developed, based on the normal boundary intersection method. Chapter 4 describes all the example test cases and the test-bed systems used for analysis. The corresponding results obtained for each example have also been described. In Chapter 5, conclusions drawn from the study, a list of recommendations and future work are listed. Appendix A presents the test data used in all the cases shown in this work. In Appendix B, an illustrative example is shown that depicts in detail, the different algorithms used in this work in solving non-linear multiobjective problems. MATLAB based computer programs used in the simulation of the test cases have been presented in Appendix C.

Chapter 2

MODELING POWER SYSTEM PRICING AND AC CIRCUIT RESPONSE

2.1 Locational Marginal Prices

Locational marginal prices in transmission engineering were first conceptualized as ‘spot prices’ for the electricity market by Schweppe [39]. As discussed earlier, LMPs indicate the direction of the expected movement of the market prices, and depict the change in optimal economic dispatch objective function when its constraints are perturbed marginally. Therefore, they depict the cost of satisfying the next increment (or decrement) in energy demand at a system node. For this reason LMPs are also referred to as a ‘shadow’ price. The perturbation can be two-sided (i.e., positive or negative), hence LMPs actually denote the cost of delivering the next marginal change in the demand at a bus. For a practical application, LMPs can be said to be the cost of delivering the next MWh of energy at the bus under study (though anomalies in LMP computation due to the decrement in demand have been observed). The mathematical basis of the LMP and the formulation of a distribution class LMP are presented in this chapter.

In a modern deregulated energy market, LMPs play a crucial role as energy economics is closely tied with the time and location of energy delivery. Though there are no exact models in public domain that specify the LMP formulations used in energy market operations, the AC optimal power flow (OPF) model or the approximate DC OPF model could be used to formulate the LMP. In case of computing LMPs as dual variables from an OPF solution, the LMPs are disintegrated into an energy, marginal loss and marginal congestion components.

In this case, it has been observed that the selection of the reference bus for computing the dispatch will affect the LMP calculation. While the dispatch remains the same, changes in the reference bus will cause changes in the LMPs computed.

A general AC OPF problem can be depicted as follows,

$$\min \; C = \sum_{i \in H} G_i^c (P_i^g) \tag{2.1}$$

such that

$$F(\Theta, V, P^b, Q^b) = 0 \tag{2.2}$$

$$\begin{bmatrix} P_{\min}^g \\ Q_{\min}^g \end{bmatrix} \le \begin{bmatrix} P^g \\ Q^g \end{bmatrix} \le \begin{bmatrix} P_{\max}^g \\ Q_{\max}^g \end{bmatrix}, \tag{2.3}$$

$$\begin{aligned} S_{\min}^l \le S^l \le S_{\max}^l, \\ V_{\min} \le V \le V_{\max}, \end{aligned} \tag{2.4}$$

where H is the set of all generator units; G^c is the fuel cost function, and P^g and Q^g are vectors of generator active and reactive power outputs. The term F corresponds to the power flow (or active and reactive power balance) equations; Θ and V are the vectors of system states – bus voltage angles and magnitudes, and P^b and Q^b are vectors of active and reactive power bus injections. The optimization is also constrained by the limits on active and reactive power output of all generating units and the system operational limits (e.g., limits on line flows (S^l) and bus voltage magnitudes) which are inequality constraints (shown in (2.4)). In practice, a security constrained OPF is used to calculate the LMPs in energy market operations. The security constrained OPF is an OPF that takes into account the 'N - 1'

contingency criteria, as constraints in the optimization. The security constrained OPF has not been considered in this work.

The rate of change of the optimal solution of the OPF with respect to change in active power load at a bus *k* would represent the LMP at bus *k*, denoted by λ_k. Theoretically this is possible if the solution C^* is a differentiable function of the perturbation in active power bus injection P_k^b at an optimal operating point x^*. Thus the LMP is found to be the Lagrange multiplier corresponding to the active power balance equation for bus *k* in the AC OPF (in (2.2)),

$$\lambda_k = \left.\frac{\partial C^*}{\partial P_k^b}\right|_{x^*} . \tag{2.5}$$

Owing to high dimensionality, it can be time intensive for a large power system to be optimally dispatched using an AC OPF. Convergence of the solution can also be an issue in case of bigger systems. The DC OPF is a linearized form of the AC OPF and has traditionally been used more often in energy market applications owing to its computational ease and mathematical simplicity [47]. The following are often the assumptions made in formulating the DC OPF problem for transmission systems:

i. Resistance of lines (R_l) is considered insignificant compared to its reactance (X_l).

ii. Bus voltage magnitudes are assumed to be flat (i.e., very close to 1.00 p.u.), and bus voltage angle deviations (compared to a reference bus) are assumed to be small.

iii. It follows from the previous two assumptions that the active power balance constraints can be neglected from the OPF formulation (i.e., in (2.2)).

From the third assumption, it can be seen that the losses in the system are not modeled inherently in the OPF. Therefore, while using the DC OPF, marginal costs of congestion and loss are also included along with the energy component in the LMP at bus k (λ_k) (see Figure 2.1). The cost of energy component ($\lambda_{k,e}$) is the cost of energy delivered at the reference bus (or *slack* bus) selected in the OPF formulation. Hence, it can be observed that for different selections of the reference bus, the energy component of the costs are different. The marginal loss component ($\lambda_{k,l}$) is used to represent the incremental cost of losses incurred to optimally dispatch the system. This term is therefore calculated as the partial derivative of the total power losses in the system with respect to active power load at k. The losses are a non-linear function of bus power injections; therefore the marginal cost of losses is calculated using a linear approximation for the losses as a function of the P_k^b quantities. The marginal congestion component ($\lambda_{k,c}$) is calculated as the cost to re-dispatch the system as a direct result of line limits being constrained, due to an incremental change in P_k^b. This term is computed using generator shift factors (GSFs) or using the system power transfer distribution factors (PTDFs). The LMPs at a bus k, from the DC optimal dispatch [47] can thus be calculated as,

$$\lambda_k = \lambda_{k,e} + \lambda_{k.l} + \lambda_{k,c} \tag{2.6}$$

$$\lambda_k = \lambda_{k,e} + \frac{\partial \sum P_{loss,l}}{\partial P_k^b} + \sum GSF_{lk}\,\mu_l \tag{2.7}$$

where μ_l is the Lagrange multiplier in the optimal dispatch corresponding to the line active power flow constraint at line l, and $P_{loss,l}$ represents the active power loss in line l calculated at the optimal operating point. This calculation process has been depicted in Figure 2.1.

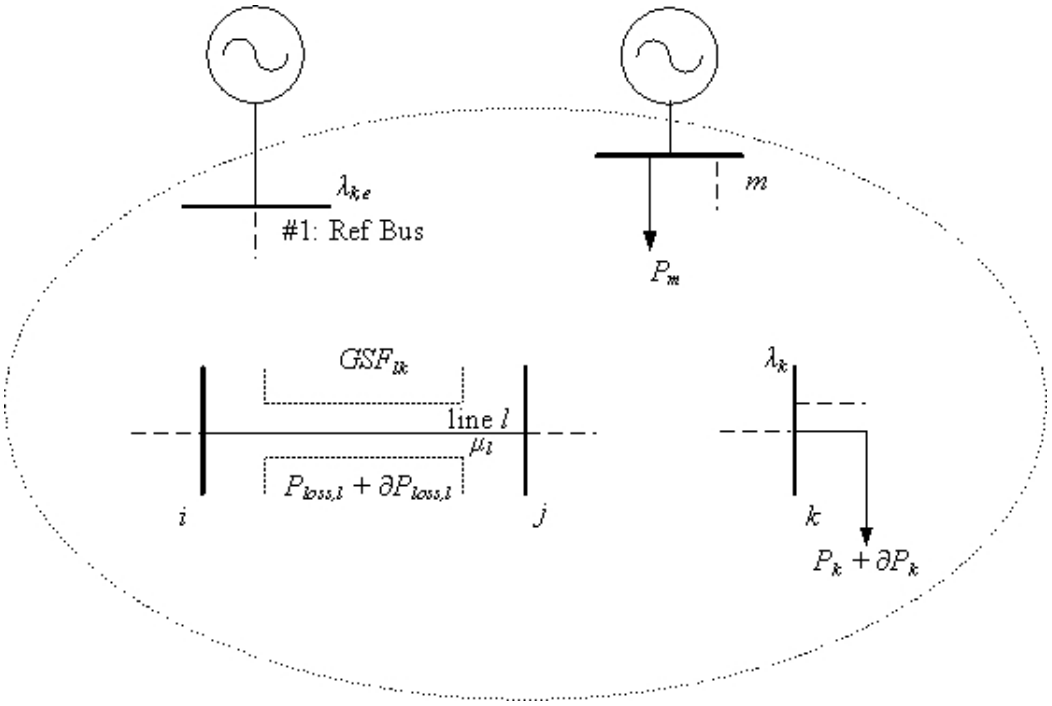

Figure 2.1 Generalized LMP calculation for bus k in a transmission network

2.2 Mathematical Formulation of DLMP

LMPs can be said to capture the *true cost* of energy delivery. The DLMP formulation for distribution systems can be derived following a similar methodology as in the case of transmission systems, but some key factors need to be considered. Distribution systems have higher resistance to reactance ratios of the lines, as compared to transmission systems; and are predominantly radial in na-

ture. Also, the appearance of single phase loads and laterals may result in three phase unbalance in the distribution system.

Another criterion to be considered is the fact that most distribution circuits are designed and rated to twice or thrice the expected loading on the lines. Transmission system states are monitored and controlled in operational real time i.e., ranging from a few seconds to a few minutes; unlike in the case of most existing distribution circuits. With the advent of 'Smart Grid' technology though, this is likely to change and a DLMP based control solution can be implemented to optimize system operation. The extension of the LMP concept to distribution systems would be beneficial in developing advanced controls in distribution systems with available dispersed distributed resource infrastructure. The main elements of the DLMP (denoted by δ_k) at a bus k, in the distribution system are:

i. cost of energy over the next hour at the several points of delivery from the transmission (or subtransmission) system to the distribution system at the distribution substation, denoted by $\delta_{k,e}$,
ii. cost of losses in the distribution system attributed to incremental loading at the selected bus, denoted as $\delta_{k,l}$,
iii. cost of congestion, loading, and other factors related to networked distribution system loading denoted as $\delta_{k,c}$, and
iv. value of utilization of renewable resources, a signal opposite in sign to $\delta_{k,e}$, denoted as v.

Mathematically,

$$\delta_k = C_e \delta_{k,e} + C_\lambda \delta_{k,\lambda} + C_g \delta_{k,c} - \nu \tag{2.8}$$

where C_e, C_ℓ, C_g are empirical constants that convert the cost components to a consistent measure. A general concept of DLMPs and the computation of the energy components of DLMP are depicted in Figure 2.2. The feeders (F_a – F_f) shown can be networked along the feeder lengths, as shown.

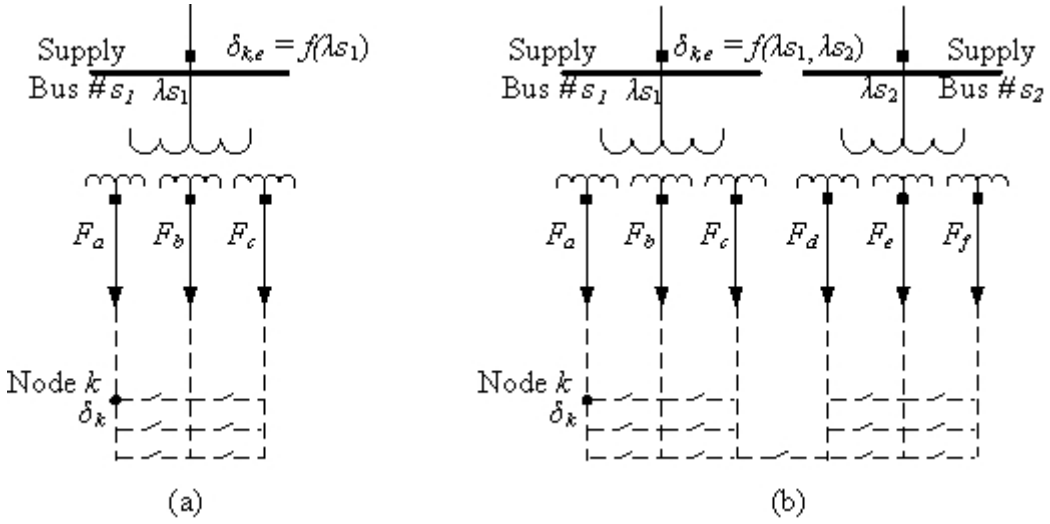

Figure 2.2 DLMP computation shown with (a) single supply, (b) multiple supplies

The several components of the proposed DLMP are formulated as follows,

$$\delta_{k,e} = \sum_{i=1}^{d_n} \pi_i \lambda_i \tag{2.9}$$

$$\delta_{k,l} = \sum_{l=1}^{n_l} \frac{\partial P_{loss,l}}{\partial P_k^b} \tag{2.10}$$

$$\delta_{k,c} = \sum_{l=1}^{n_l} \frac{\partial P_l^l}{\partial P_k^b} \tag{2.11}$$

where d_n is the number of all subtransmission and transmission supply points to the distribution system, λ_i is the LMP at substation I; π_i is the participation factor of the substation i; n_l is the number of lines in the distribution system; $P_{loss,l}$ is the

active power loss in the line l; P_k^b is the active power bus injection at bus k; and P_l^l is the active power flow on line l. All the quantities depicted in (2.9) – (2.11) are real and scalar.

The energy component is computed for a single supply-end, by using the LMP computed from the optimal dispatch of the transmission network. In case of multiple supply-ends, it is computed by applying participation factors for the supply-ends. This has been depicted in Figure 2.2. The participation factors are assigned based on a power flow algorithm. This has been discussed later in this chapter.

The loss component of the DLMP is computed as shown below. Consider the active power losses in a line l and the active power delivered at bus k as

$$P_{loss,l} = (I_l^l)^2 R_l \tag{2.12}$$

$$P_k^b = V_k I_k^b \varphi_k \tag{2.13}$$

where I_l^l is the current magnitude in line l (note: the magnitude notation $|I_l^l|$ is dropped for convenience); R_l is the resistance of line l; V_k is the voltage magnitude at bus k; φ_k is the power factor in the line at bus k; I_k^b is the load current magnitude at bus k. Assuming the bus voltage magnitude at k remains constant with very small perturbation in the loading, it follows that the derivate of line losses in l with loading at bus k can be computed as

$$\frac{\partial P_{loss,l}}{\partial P_k^b} = \frac{\partial P_{loss,l}}{\partial I_l^l}\frac{\partial I_l^l}{\partial P_k^b} = \frac{\partial((I_l^l)^2 R_l)}{\partial I_l^l}\frac{\partial I_l^l}{\partial (V_k I_k \varphi_k)},$$

$$\frac{\partial P_{loss,l}}{\partial P_k^b} = \frac{2I_l^l R_l}{V_k \varphi_k} \frac{\partial I_l^l}{\partial I_k^b}. \tag{2.14}$$

The current derivative term in (2.14) can be approximated using the power transfer distribution factors for the system as follows,

$$\frac{\partial I_l^l}{\partial I_k^b} \approx \left| (\rho_{ij,k}) \right| \tag{2.15}$$

$$\rho_{ij,k} = \left(\frac{(Z_{bus})_{ik} - (Z_{bus})_{jk}}{Z_{ij}} \right)^* \tag{2.16}$$

where $\rho_{ij,k}$ is the PTDF relating the loading in line l (from bus i to bus j) with loading in bus k. The notation $(Z_{bus})_{ik}$ is the element on the i^{th} row and k^{th} column of the bus impedance (Z_{bus}) matrix, and Z_{ij} is the primitive impedance of line l. The approximation in (2.15) is valid for feeders that exhibit near unity bus voltage magnitudes [82]. Note that the partial derivative term in (2.15) is real with the absolute value of the PTDF being considered. Hence, derivatives are taken of real quantities with respect to real quantities, and therefore the Cauchy-Riemann conditions are not involved.

In case of the congestion components, the partial derivative of active power flow in line l with load at bus k is computed through the reduced-form DC power flow model, as shown below

$$\frac{\partial P_l^l}{\partial P_k^b} = \chi_{l,k} \tag{2.17}$$

where $\chi_{l,k}$ is the rate of change of active power flow in line l with active power load at bus k, calculated from the reduced-form model. The term χ, can be derived in matrix form as follows,

$$\chi = H_b A \begin{bmatrix} B'^{-1} & 0 \\ 0 & 0 \end{bmatrix} \tag{2.18}$$

where H_b is the primitive line admittance matrix, and A is the non-directed bus-line incidence matrix. The notation B' corresponds to the modified bus susceptance matrix which is calculated by removing the row and column corresponding to the swing bus from the susceptance matrix, where B is the bus susceptance matrix referenced to ground. If n_l denotes the total number of lines in the distribution system, and n_b the total number of buses; the H_b matrix (size: n_l rows and n_l columns) is diagonal with the line admittance of line l as the diagonal element of row l. The A matrix (size: n_l rows and n_b columns) is 1 at the l,i and l,j entries, where i denotes the 'from-bus' number and j denotes the 'to-bus' number for line l. The B matrix (size: n_b-1 rows and n_b-1 columns) has a similar structure as the bus admittance matrix of the system (Y_{bus}) and considers only the line susceptances, with the row and column corresponding to the swing bus deleted.

The foregoing is an example of the DLMP formulation. It is possible with a similar approach to include other objectives and phenomena. For example it is possible to include different values of renewable generation, e.g., generation that does not produce green house gases, more complex models of distribution network congestion, peak demand reduction, energy use during the peak demand pe-

riod, and load power factor. The generalized DLMP formulation for bus *k* in a distribution system is shown in Figure 2.3.

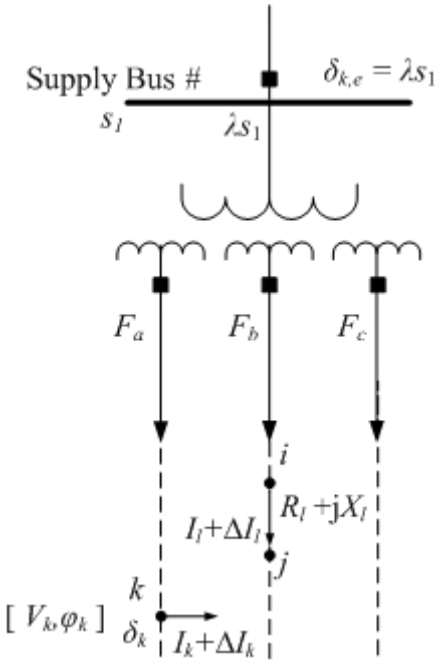

Figure 2.3 Generalized DLMP formulation for bus *k* in a distribution system

It is important to note that the power transfer distribution factors used to approximate the network model in (2.15) and (2.17) are based on approximations that are close to the exact power flow sensitivities for a transmission network. But in the case of distribution systems, for greater accuracy a closer look at distribution factors is warranted. The DC network assumptions do not provide a great deal of accuracy in most cases while modeling the system at the primary distribution level. Since the ratios of resistance to reactance of the distribution circuits are higher than in transmission networks, the active and reactive components of power flow are essentially coupled. Additionally, since the voltage levels at the downstream end of a distribution feeder can be considerably lower than the volt-

age at the distribution substation, the assumptions of voltage magnitudes being closer to 1 p.u. also could be overridden. The following sections develop a full AC model of distribution factors calculated at a specific system operating condition, using the Jacobian matrix of a Newton-based power flow program. An AC model for power transfer distribution factors has been studied and presented in literature [83-85] that is based on the Jacobian matrix of a Newton-Raphson power flow algorithm. The approach taken in this dissertation is based on the idea developed in the aforementioned references, but takes into account an additional correctional factor.

2.3 AC Sensitivity Analysis of a Power System

For a power system with n_b buses and n_l lines, the power flow solution by Newton's method [82] is obtained by solving the following linear system of equations iteratively

$$\begin{bmatrix} \Delta P \\ \Delta Q \end{bmatrix} = J \begin{bmatrix} \Delta \Theta \\ \Delta V \end{bmatrix}, \tag{2.19}$$

where ΔP and ΔQ are vectors (length: n_b-1) representing the active and reactive power mismatches at each bus (excluding the swing bus). The matrix J represents the Jacobian matrix of first order partial derivative terms with respect to the voltage angle and magnitude at each bus; and $\Delta \Theta$ and ΔV are vectors (length: n_b-1) representing the change in the bus voltage angle (Θ) and magnitude (V) at each bus (excluding the swing bus), calculated in each step of the iteration in Newton's method.

The Jacobian matrix, J (dimensions: $2n_b$-2 rows and $2n_b$-2 columns) has the form shown below,

$$J = \begin{bmatrix} J_1 & J_2 \\ J_3 & J_4 \end{bmatrix}. \tag{2.20}$$

Each differential term J_1, J_2, J_3 and J_4 within the Jacobian matrix is a submatrix (dimensions: n_b-1 rows and n_b-1 columns) with entries constituting the corresponding partial differential calculated for all non-swing buses. The above equations are shown as an example for a system with no PV buses. For a system with n_{pv} PV buses, the rows corresponding to the PV bus are removed from the ΔQ and ΔV vectors and corresponding rows and columns from the Jacobian matrix are also removed. The dimensions of $[\Delta\Theta\ \Delta V]^T$, J and $[\Delta P\ \Delta Q]^T$ are further modified to accommodate tap changing transformers, phase shifters, and PV buses that reach their reactive power limit (Q-limit) [82].

The active power and reactive power flows P_l^l and Q_l^l respectively, in a line l (from bus i to bus j) can be computed as,

$$P_l^l = V_i^2 g_{ij} - V_i V_j [g_{ij} \cos(\theta_i - \theta_j) + b_{ij} \sin(\theta_i - \theta_j)], \tag{2.21}$$

$$Q_l^l = V_i V_j [b_{ij} \cos(\theta_i - \theta_j) - g_{ij} \sin(\theta_i - \theta_j)] - V_i^2 (b_{ij} + b_{ij}^{sh} / 2), \tag{2.22}$$

where V_i, V_j are bus voltages magnitudes and θ_i, θ_j are bus voltage angles at buses i and j respectively; g_{ij} and b_{ij} are the primitive line conductance and susceptance, and b_{ij}^{sh} is the total line charging susceptance in the line between buses i and j.

Using a Taylor series approximation and neglecting second and higher order terms, the changes in active and reactive power flows in the lines can be obtained as a function of changes in bus voltage magnitudes and angles as,

$$\Delta P_l^l = \Delta\theta_i \frac{\partial P_l^l}{\partial \theta_i} + \Delta\theta_j \frac{\partial P_l^l}{\partial \theta_j} + \Delta V_i \frac{\partial P_l^l}{\partial V_i} + \Delta V_j \frac{\partial P_l^l}{\partial V_j}, \tag{2.23}$$

$$\Delta P_l^l = \Delta\theta_i \frac{\partial Q_l^l}{\partial \theta_i} + \Delta\theta_j \frac{\partial Q_l^l}{\partial \theta_j} + \Delta V_i \frac{\partial Q_l^l}{\partial V_i} + \Delta V_j \frac{\partial Q_l^l}{\partial V_j}. \tag{2.24}$$

The partial derivatives of P_l^l and Q_l^l with respect to the bus voltage parameters (V_i, V_j, θ_i and θ_j) can be obtained from (2.21) and (2.22) as follows,

$$\frac{\partial P_l^l}{\partial \theta_i} = V_i V_j [g_{ij} \sin(\theta_i - \theta_j) - b_{ij} \cos(\theta_i - \theta_j)], \tag{2.25}$$

$$\frac{\partial P_l^l}{\partial \theta_j} = -V_i V_j [g_{ij} \sin(\theta_i - \theta_j) - b_{ij} \cos(\theta_i - \theta_j)], \tag{2.26}$$

$$\frac{\partial P_l^l}{\partial V_i} = 2V_i g_{ij} - V_j [g_{ij} \cos(\theta_i - \theta_j) + b_{ij} \sin(\theta_i - \theta_j)], \tag{2.27}$$

$$\frac{\partial P_l^l}{\partial V_j} = -V_i [g_{ij} \cos(\theta_i - \theta_j) + b_{ij} \sin(\theta_i - \theta_j)], \tag{2.28}$$

$$\frac{\partial Q_l^l}{\partial \theta_i} = -V_i V_j [b_{ij} \sin(\theta_i - \theta_j) + g_{ij} \cos(\theta_i - \theta_j)], \tag{2.29}$$

$$\frac{\partial Q_l^l}{\partial \theta_j} = V_i V_j [b_{ij} \sin(\theta_i - \theta_j) + g_{ij} \cos(\theta_i - \theta_j)], \tag{2.30}$$

$$\frac{\partial P_l^l}{\partial V_i} = -V_j [g_{ij} \sin(\theta_i - \theta_j) + b_{ij} \cos(\theta_i - \theta_j)] - 2V_i (b_{ij} + \frac{b_{ij}^{sh}}{2}), \tag{2.31}$$

$$\frac{\partial P_l^l}{\partial V_j} = -V_i[g_{ij}\sin(\theta_i - \theta_j) + b_{ij}\cos(\theta_i - \theta_j)]. \tag{2.32}$$

Equations (2.23) and (2.24) can be represented in matrix form as,

$$\begin{bmatrix} \Delta P^l \\ \Delta Q^l \end{bmatrix} = S \begin{bmatrix} \Delta\Theta \\ \Delta V \end{bmatrix}, \tag{2.33}$$

where ΔP^l and ΔQ^l are vectors (length: n_l) representing the change in active and reactive power line flows for the entire system; and S is defined as the line flow sensitivity matrix consisting of active and reactive power line flow sensitivities with respect to bus voltage angles and magnitudes. The line flow sensitivity matrix, S (dimensions: $2n_l$ rows, and $2n_b - 2$ columns) has the form shown below,

$$S = \begin{bmatrix} S_1 & S_2 \\ S_3 & S_4 \end{bmatrix}. \tag{2.34}$$

Each submatrix S_1, S_2, S_3 and S_4 (size: n_l row, and n_b–1 columns) is made up of the corresponding differential terms that can be calculated as shown in (2.25) - (2.32). Using the Jacobian matrix J from the Newton-based power flow algorithm and the line flow sensitivity matrix S derived in this section, a formulation of an AC distribution factors for application in distribution system analysis is developed in the forthcoming section.

2.4 Jacobian-based AC Distribution Factors

The bus mismatch equations (2.19) of the power flow algorithm constitute the mismatch in the active and reactive powers measured at each bus at each step of the power flow solution and can be represented as follows,

$$\begin{bmatrix} \Delta P \\ \Delta Q \end{bmatrix} = \begin{bmatrix} \Delta P^b \\ \Delta Q^b \end{bmatrix} + \begin{bmatrix} \sum \Delta P^l \\ \sum \Delta Q^l \end{bmatrix}, \tag{2.35}$$

where ΔP^b and ΔQ^b are vectors (length: n_b–1) that represent the changes in injected bus active and reactive powers at each bus, and $\sum \Delta P^l$ and $\sum \Delta Q^l$ are vectors (length: n_b–1) that represent the sum total of the changes in the injected active and reactive powers at each bus through the lines connected at each bus.

A bus-line directed incidence matrix ℓ (dimensions: n_b-1 rows and n_l columns) for the system is defined as follows: ℓ_{ij} is zero everywhere except if line j starts at bus i (ℓ_{ij} = -1) or ends at bus i (ℓ_{ij} = +1). Note that $|\ell| = A$, where $|.|$ represents term by term absolute value.

Using the incidence matrix ℓ, (2.35) can be represented as follows,

$$\begin{bmatrix} \Delta P \\ \Delta Q \end{bmatrix} = \begin{bmatrix} \Delta P^b \\ \Delta Q^b \end{bmatrix} + \begin{bmatrix} \lambda & 0 \\ 0 & \lambda \end{bmatrix} \begin{bmatrix} \Delta P^l \\ \Delta Q^l \end{bmatrix} \tag{2.36}$$

where ΔP^l and ΔQ^l are the vectors representing the change in active and reactive power line flows P_l^l and Q_l^l for the entire system. Substituting (2.19) in (2.36) and pre-multiplying by the inverse of the power flow Jacobian matrix J, the following expression is obtained,

$$\begin{bmatrix} \Delta \delta \\ \Delta V \end{bmatrix} = J^{-1} \begin{bmatrix} \Delta P^b \\ \Delta Q^b \end{bmatrix} + J^{-1} \begin{bmatrix} \lambda & 0 \\ 0 & \lambda \end{bmatrix} \begin{bmatrix} \Delta P^l \\ \Delta Q^l \end{bmatrix}. \tag{2.37}$$

Pre-multiplying (2.37) by the line flow sensitivity matrix S, and substituting in the expression from (2.33), the following expression is obtained,

$$\begin{bmatrix} \Delta P^l \\ \Delta Q^l \end{bmatrix} = SJ^{-1} \begin{bmatrix} \Delta P^b \\ \Delta Q^b \end{bmatrix} + SJ^{-1} \begin{bmatrix} \lambda & 0 \\ 0 & \lambda \end{bmatrix} \begin{bmatrix} \Delta P^l \\ \Delta Q^l \end{bmatrix}. \tag{2.38}$$

Equation (2.38) can be simplified using a matrix L defined as follows,

$$L = \begin{bmatrix} \lambda & 0 \\ 0 & \lambda \end{bmatrix}, \tag{2.39}$$

$$(I - SJ^{-1}L)\begin{bmatrix} \Delta P^{l} \\ \Delta Q^{l} \end{bmatrix} = SJ^{-1}\begin{bmatrix} \Delta P^{b} \\ \Delta Q^{b} \end{bmatrix}. \tag{2.40}$$

Therefore, the AC distribution factors can be represented in matrix form as,

$$\begin{bmatrix} \Delta P^{l} \\ \Delta Q^{l} \end{bmatrix} = \rho_{AC}\begin{bmatrix} \Delta P^{b} \\ \Delta Q^{b} \end{bmatrix}, \tag{2.41}$$

where,

$$\rho_{AC} = (I - SJ^{-1}L)^{-1}SJ^{-1}. \tag{2.42}$$

The detailed equations describing the components of J and S matrices are consistent with all system notations used in the dissertation. The dimensions of various matrices depicted in the above formulation are listed in Table XX for simplicity. The Jacobian-based AC distribution factors ρ_{AC} developed in this section can be applied to the primary distribution system model for analysis and calculation of the DLMPs.

Table 2.1 Dimensions of various terms used in the Jacobian-based formulation

TERM	DIMENSIONS	TERM	DIMENSIONS
J	$(2n_b - 2)$ x $(2n_b - 2)$	ΔP, ΔQ	$(n_b - 1)$ x 1
S	$2n_l$ x $(2n_b - 2)$	$\Delta\Theta$, ΔV	$(n_b - 1)$ x 1
ℓ	$(n_b - 1)$ x n_l	ΔP^b, ΔQ^b	$(n_b - 1)$ x 1
J_1 - J_4	$(2n_b - 2)$ x $(2n_b - 2)$	ΔP^l, ΔQ^l	n_l x 1
S_1 - S_4	$2n_l$ x $(2n_b - 2)$	L	$(2n_b - 2)$ x $2n_l$

2.5 Salient Features of DLMPs

DLMP as a Control Signal

In this section, the key aspects of the DLMP formulation and its proposed usage are discussed. An important component of the United States Department of Energy is the use of sensory signals for 'smart' control of the entire power system. In distribution engineering, this Smart Grid objective implies that measurements should be used to develop a control signal (or signals), and the DLMP signal described above is an example of this control strategy.

In essence, the DLMP is a feedback control signal as depicted in Figure 2.4. With reference to Figure 2.4, the transmission system and power marketing considerations are the input to the transmission LMP calculation. It is clear that the calculation of DLMPs will require additional sensory signals from the distribution system as compared to legacy systems. Some of these signals are attainable from direct measurement, but other may have to be estimated. It is proposed that synchronized measurements and time stamped state estimated data be used for this purpose.

In this formulation for DLMPs, several key constants (C_e, C_ℓ, C_g) need to be selected in (2.8). These constants are multifaceted in nature in that they should reflect the dollar value of the phenomena captured, they are penalty (or bonus) factors to discourage (or encourage) certain modes of operation, and they should give an appropriate proportionate percentage of the DLMP for the given component. A sample selection of constants is shown in the test cases described. If the DLMPs are used for pricing power and energy at ultimate points of delivery in the

distribution system, the scaling of these constants is particularly important. Examination of Figure 2.4 also indicates that the proposed DLMP formulation has a feedback configuration. The stability of the loop is found to be highly damped for typical values of the *C* terms in (2.8). The response of the control loop is illustrated in the test cases in Chapter 4.

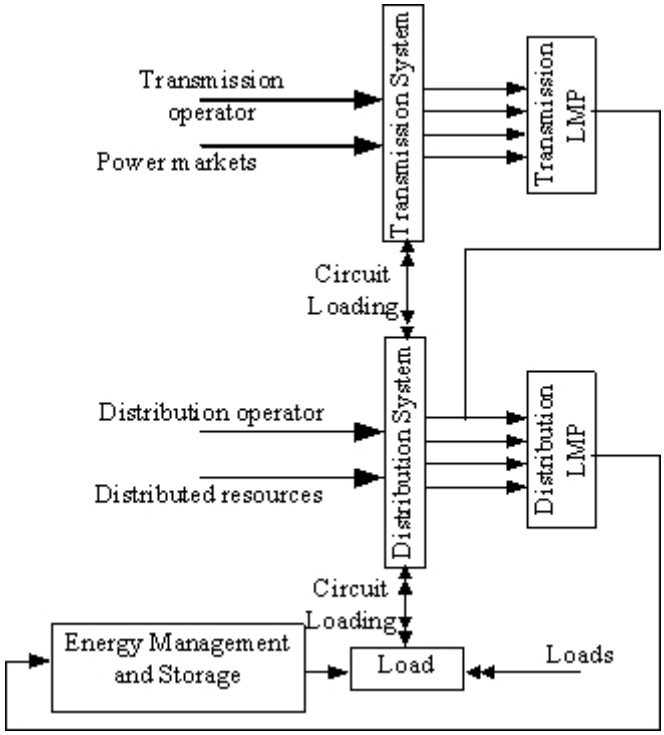

Figure 2.4 Distribution control using a DLMP signal: a feedback depiction [25]

Selection of Reference Bus

The selection of reference bus can affect the DLMPs calculated, as in the case of the LMP formulation. Farther we go from the supply, it can be observed that the DLMP will accrue additional losses along the entire length of the feeder and hence will be higher. This phenomenon can be accommodated for, using a suitable derating term that varies with the distance of the bus from supply. This

issue has not been studied in the current formulation. This is also likely in the case of the congestion component of the DLMP. The location of a constrained segment in a feeder will significantly affect the DLMPs calculated for the system. A parallel can be drawn for the case of congestion, with the transmission network. Hence, the knowledge of DLMP based real-time prices in distribution systems would also aid in the event of system evaluation for expansion planning.

Unbalance in Distribution Circuits

Unbalance in the loads in a distribution system also has to be considered within the framework of the DLMP formulation. IEEE 519 [86] defines the point of common coupling (PCC) as 'the interface between source and loads in a power system'. Extending the idea to a distribution system with distributed assets (i.e., DERs and DESDs) for purposes of this dissertation the PCC can be assumed the point of interface of loads, sources, *and the distributed assets* in the system. In the work developed in this dissertation, DLMPs have been formulated for the point of common coupling assumed to be balanced in the aggregate three-phase sense. Hence, the DLMPs are computed at a distribution feeder bus *k* that has a combination of unbalanced, balanced and single phase. This is depicted in Figure 2.5.

If V^- and V^+ can be said to denote the magnitude of the negative and positive sequence voltages respectively for an unbalanced system, and V^-/V^+ is the unbalance factor of a representative system bus, then if V^-/V^+ is small, it is recommended to use V^+ in calculations described in this chapter.

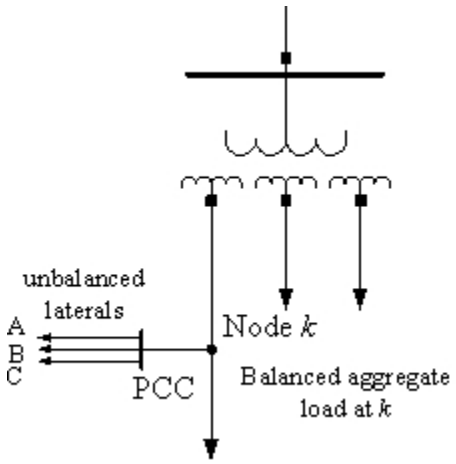

Figure 2.5 Point of common coupling for DLMP calculation purposes

Summary

The DLMP formulation shown in this chapter is derived primarily from the LMP idea, but as an extension to distribution systems. It is assumed that the LMP at the transmission level is made available through an optimal dispatch algorithm. Incremental costs due to additional loss and possible congestion in distribution circuits are numerically added to the energy component of the DLMP. In case of a networked distribution system or a case with multiple points of supply, the LMPs at different supply sides are considered using participation factors. A power flow algorithm for the distribution system can be performed using forecasts of load and distributed resource output. Based on the power flow solution, participation factors can be assigned to a supply end depending on the participation of the multiple supply ends in managing the forecast load.

Chapter 3

DISTRIBUTION ENERGY MANAGEMENT

3.1 Energy Management in Distribution Systems

Traditional distribution systems are radial systems that feed the end use customers through three phase primary feeders and single phase laterals. In a conventional understanding, load management [87] refers to the management of the end use load shape to satisfy a number of objectives including: reduced demand during peak system load periods; acceptable system reliability; acceptable customer convenience and incentives; and compatibility with existing system designs. With the presence of DERs and DESDs in the distribution system, the optimal management will need to be performed on the basis of several diverse objectives, hence resulting in a multiobjective optimization problem. The control of the energy demand over a predefined time horizon *T*, on a bus *k* on the distribution feeder has been dealt with in this chapter. DERs in the distribution level are intermittent and hence do not offer any possibility of control. But the presence of DESDs makes it possible to schedule the DESDs in an optimal fashion to serve several objectives.

3.2 Problem Statement

In general, the energy management control objective for a bus *k* in the distribution feeder, can be represented as an aggregate J_{agg},

$$J_{agg}(\Re^n \rightarrow \Re^p) \equiv \left\{ X_d \ \alpha \ \ J_{agg}(X_d) = (f_1(X_d), f_2(X_d) \ldots f_p(X_d))^T \right\} \qquad (3.1)$$

such that

$$A_{eq}X_d = b_{eq} \tag{3.2}$$

$$A_{in-eq}X_d \leq b \tag{3.3}$$

where $p \geq 2$, J_{agg} is an aggregate objective used to simultaneously represent all objective functions f_1, f_2 … f_p in the objective space, and X_d is a vector representing active power delivered at bus k at each time interval in the optimization horizon. Equations (3.2) and (3.3) represent the equality and inequality constraints including the lower and upper bounds on the control variable X_d. The control objective J_{agg} is to be optimized at the PCC at bus k, as shown in Figure 3.1.

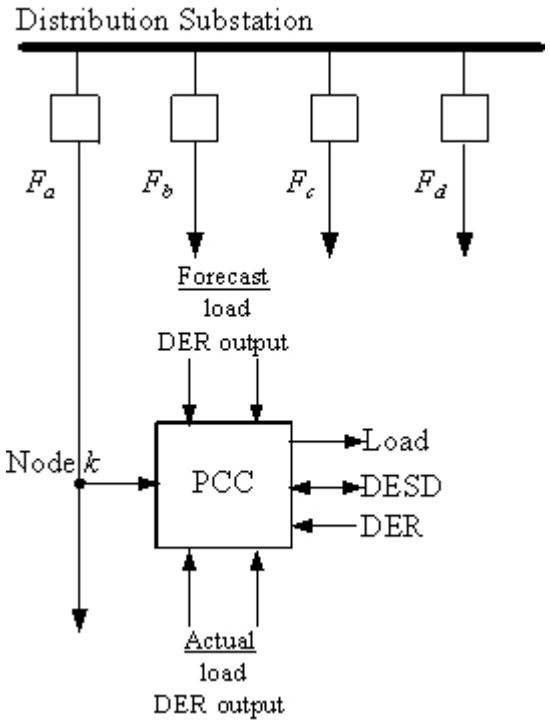

Figure 3.1 Depiction of the location of control calculation

3.3 Multiobjectives of System Operation

The objectives used to represent the optimization of the energy demand at a bus k, can be represented empirically as functions of the instantaneous active

power demand from the distribution feeder. Therefore, the control vector X_d is chosen to be the active power demand from the utility grid. The voltage fluctuations at the load end for variations in the active power load at the PCC has not been taken into account in any computations, as it is a reasonable assumption in view of the nature of the study undertaken.

Consider p objective functions labeled f_i. For the formulation shown below, the case of $p = 4$ is illustrated. The objectives chosen in this formulation, for optimal control of the energy demand on a bus k are:

i. Minimize the peak demand (kW) from the distribution network over the time horizon T.

ii. Minimize the energy demand from the distribution network (kWh) during a predefined '*peak load period*' denoted by *PK*.

iii. Minimize the total cost of energy delivered from the distribution network for the time horizon T ($).

iv. Minimize the energy lost in the DESD converter and battery implementation of storage (kWh). The energy loss is calculated over the study time horizon T.

The cited four objectives are captured in the form of the f_i functions. Vector X_d represents power levels supplied by the distribution system at time $t = i\Delta t$ time intervals. The elements of X_d are $x_{d,i}$. The entire time horizon over which the optimization is carried out is split into n equally spaced time intervals of duration Δt. Also note that several of the cited $f_i(X_d)$ functions could be interrelated (and mutually inclusive or correlated). The four f_i considered here are:

i. The objective relating to peak power demand from the distribution system is captured by f_1 as shown below,

$$f_1(X_d) = \max_{i \in T}(x_{d,i}). \tag{3.4}$$

ii. The peak period energy supplied from the distribution network is,

$$f_2(X_d) = \sum_{i \in PK} x_{d,i}\Delta t. \tag{3.5}$$

iii. The total cost of energy taken from the distribution supply for the entire duration of the time horizon is expressed as,

$$f_3(X_d) = \sum_{i \in T} \delta_k x_{d,i}\Delta t. \tag{3.6}$$

iv. The total energy loss in the converters for the DESD over $n\Delta t$ is a function of the square of the current. Assuming the voltage at the DC interface terminals to be a constant, f_4 can be approximated by,

$$f_4(X) = \sum_{i \in T} \varepsilon \left| x_{s,i} \right| \Delta t. \tag{3.7}$$

The term $x_{s,i}$ represents the storage charging rate at time interval i; and ε represents the percentage of power loss in the interface converters.

Function f_1 is nonlinear and cannot be represented in a conventional linear programming algorithm for the solution of the multiobjective optimization. The function f_1 is hence linearized by augmenting the control vector with an additional control variable z such that,

$$z = f_1(X_d) \tag{3.8}$$

$$z \geq x_{d,i} (\forall i = 1,2,...,n) \tag{3.9}$$

Equations (3.8) and (3.9) relax the requirements of f_1 into constraints. Since this optimization formulation is a minimization problem, it is permissible to include (3.9) in the set of all inequality constraints represented by (3.3) as n additional constraints. The vector X_d is augmented with the addition of z as a control variable and is represented by,

$$X_d = \begin{bmatrix} x_{d,1} & x_{d,2} & \dots & x_{d,n} & z \end{bmatrix}^T . \tag{3.10}$$

A detailed description of the solution method for the control problem has been presented progressively in the forthcoming sections. The optimal solution seeks to utilize the distributed resource infrastructure and the installed storage capacity to minimize the several objectives. The DLMP based control of energy demand on a bus in the distribution feeder can hence be viewed as not distant from the much more traditional *unit commitment* problem which seeks to optimally schedule power generation units to minimize the costs associated with power generation. The time horizon of solving unit commitment algorithms is one day ahead or one week ahead, typically. Distribution energy management has been studied along similar lines as an algorithm for optimal deployment of the distributed storage capacity in a day-ahead approach.

3.4 Constraints

The optimization is constrained by the power ratings of the electronic controllers, energy storage medium, and other system components. The load balance equation has been shown as follows,

$$\begin{bmatrix} x_{d,1} & x_{d,2} & \dots & x_{d,n} \end{bmatrix}^T = X_{load} - X_{DG} + X_S \tag{3.11}$$

where X_{load}, is a vector representing the load at bus k for every time interval in the optimization (kW); X_{DG} is a vector representing power output of the DER at bus k for every time interval (kW); and X_S is the vector of rates of charging of the DESD for every time interval (kW). Thus, the terms X_{load}, X_{DG}, X_S are vectors representing the load, power output of the renewable resource, and the storage charging rates, respectively for each time interval in the optimization time window.

Note that (3.11) is an instantaneous balance of power. Since X_{load} and X_{DG} are determinate, the control variable for the multiobjective optimization is changed from X_d to X_S. Please note that for the sake of simplicity, in the remainder of this report the control vector in the multiobjective optimization formulation is the rate at which the storage element is charged. Substituting (3.11) in (3.4) - (3.7), the objective functions can be represented in the appropriate form. The balance of energy within the distributed storage device (e.g., a battery) introduces additional constraints on the optimization. To maintain the state of charge of battery device within its permissible limits,

$$x_{s,i}\Delta t = sE_{s,\max} \qquad (3.12)$$

$$(0 \le s \le 1),$$

where s is the state of charge (SOC); and $E_{s,max}$ is the maximum installed storage capacity (kWh).

The rate of charging of the DESD at the i^{th} time interval depends on the available state of charge on the battery element. Therefore, $x_{s,i}$ is dependent on the rate of charging (or discharging) of the battery in all previous time intervals from

the beginning of the study period. Therefore, since $x_{s,i}$ depends on the states corresponding to the previous time intervals, (3.12) results in formulating a portion of the inequality constraints that is represented by (3.2). The remainder portion of (3.3) is constituted by the *n* equations depicted in (3.9). The maximum power rating of the converters P_{max}, introduces the lower and upper bounds on control variable $x_{s,i}$ (see (3.3)).

3.5 Mathematical Representation of the Control Problem

The generalized objectives of the distribution energy management formulation and the constraints of optimization have been discussed in the previous sections. The final mathematical depiction of the problem is shown in this section. The control vector X_S is represented as,

$$X_S = \begin{bmatrix} x_{s,1} & x_{s,2} & \dots & x_{s,n} & z \end{bmatrix}^T. \tag{3.13}$$

The objective functions of the problem are given by,

$$f_1(X_S) = z \tag{3.14}$$

$$f_2(X_S) = \sum_{i \in PK} (x_{s,i} + x_{load,i} - x_{DG,i})\Delta t \tag{3.15}$$

$$f_3(X_S) = \sum_{i \in T} \delta_k (x_{s,i} + x_{load,i} - x_{DG,i})\Delta t \tag{3.16}$$

$$f_4(X_S) = \sum_{i \in T} \varepsilon \left| x_{s,i} \right| \Delta t \tag{3.17}$$

where $x_{load,i}$ represents the load demand at the i^{th} time interval (kW); and $x_{DG,i}$ represents the DER power output at the i^{th} time interval (kW).

The constraints of the resulting multiobjective optimization problem $(\forall i = 1...n)$ are,

$$\sum_{i=1}^{i} x_{s,i}\Delta t \le (1-s_0)E_{s,\max} \tag{3.18}$$

$$\sum_{i=1}^{i} -x_{s,i}\Delta t \le s_0 E_{s,\max} \tag{3.19}$$

$$x_{DG,i} - x_{load,i} \ge x_{s,i} - z \tag{3.20}$$

$$-P_{\max} \le x_{s,i} \le P_{\max}. \tag{3.21}$$

Equations (3.18) – (3.20) represent the set of 3*n* inequality constraints and (3.21) represents the lower and upper bounds on the control variables $x_{s,1}\ldots x_{s,n}$, and s_0 represents the initial condition on the state of charge at the beginning of the study period. The lower and upper bounds on *z* are unknown and hence can set to infinity for simulation purposes. The total number of inequality constraints is 5*n*.

3.6 Normal Boundary Intersection Method

The solution for traditional linear optimization problems is easily facilitated through the use of linear programming tools which make use of the *simplex* method. In the case of multiple objectives to be optimized simultaneously, with the functions themselves not linear, the use of superior techniques are necessitated. In the optimization of multiobjectives, the global optima of a function f_i might not coincide with that of f_j. Functions can also be incommensurable and completely conflicting, necessitating the use of the *Pareto optimality criterion* [74]. A control solution X_S^* is a Pareto optimum if there does not exist another solution X in the solution space such that $f_i(X_S) \le f_i(X_S^*)$ for $i = 1, 2 \ldots p$, and $f_j(X_S) < f_j(X_S^*)$ for at least one j (i.e., if there does not exist another solution which improves on at least one objective without deteriorating any of the others)

[72]. A Pareto optimal front is the locus of Pareto optimal points in the solution space, for multiple combinations of weighting the objectives. The normal boundary intersection (NBI) method has been applied to this effect in this report, for the problem at hand [80]. Mathematically, a *convex hull* of a vector space can be defined as the set of all convex combinations of the points in the vector space. A convex hull of individual minima, Ψ is constructed in the NBI method, which spans all possible Pareto optima of the MOP and will be a *p*-dimensional hyperplane. The convex hull can be represented in matrix form as,

$$\Psi = \left\{ \Phi W \mid W \in \Re^4, \sum_{i=1}^{4} w_i = 1, (w_i \geq 0) \right\} \tag{3.22}$$

$$\Phi = \begin{bmatrix} f_1(X^*_{S,1}) & f_1(X^*_{S,2}) & f_1(X^*_{S,3}) & f_1(X^*_{S,4}) \\ f_2(X^*_{S,1}) & f_2(X^*_{S,2}) & f_2(X^*_{S,3}) & f_2(X^*_{S,4}) \\ f_3(X^*_{S,1}) & f_3(X^*_{S,2}) & f_3(X^*_{S,3}) & f_3(X^*_{S,4}) \\ f_4(X^*_{S,1}) & f_4(X^*_{S,2}) & f_4(X^*_{S,3}) & f_4(X^*_{S,4}) \end{bmatrix} - \begin{bmatrix} 1 \\ 1 \\ 1 \\ 1 \end{bmatrix} \begin{bmatrix} f_1(X^*_{S,1}) & f_2(X^*_{S,2}) & f_3(X^*_{S,3}) & f_4(X^*_{S,4}) \end{bmatrix}. \tag{3.23}$$

Solution $X_{S,i}^*$ denotes the global optimum for function $f_i(X_S)$, and W denotes a vector of weights w_i for the functions f_i, (note that weights w_i are convex, i.e., $\Sigma w_i = 1$). If u represents a unit normal to Ψ, then $\Phi W + ud$ would represent the coordinates of a point on the normal, a distance d away from the convex hull. The point of intersection between the normal and the objective vector J_{agg} will be a Pareto optimum when the solution lies on the boundary of J_{agg} closest to the origin. Hence, the NBI formulation for the MOP can be represented as,

$$\max_{X_S, d} d \tag{3.24}$$

such that

$$\Phi W + ud = J_{agg}(X_S) \tag{3.25}$$

$$A_{in-eq} X_S \leq b \tag{3.26}$$

$$A_{eq} X_S = b_{eq}. \tag{3.27}$$

A geometric representation is shown in Figure 3.2, for p = 2 and sample weighting combinations W_i, W_j, W_k, and W_l. Graphs for greater values of p would lie in multidimensional space, and therefore are hard to visualize.

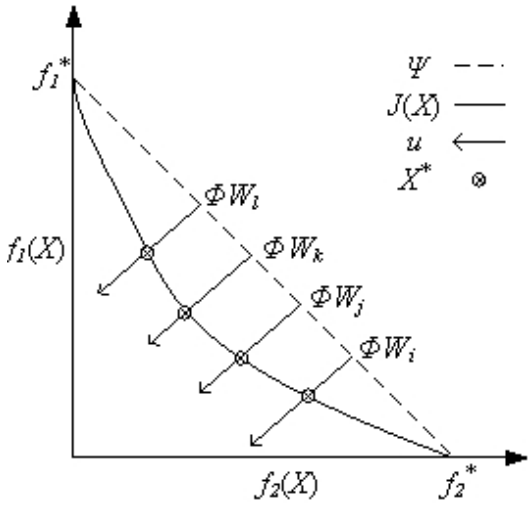

Figure 3.2 A graphical representation of NBI based Pareto solutions for a bi-dimensional problem (p = 2)

3.7 Separable Programming

A multi-variable function (of n_s independent variables) is a separable function, if it can be written as a sum of n_s single variable functions. When separable functions are applied in linear programming problems the resulting

class of optimization problems are classified in literature as *separable programming* (SP) problems [88]. Their application in the current control problem lies in the following property of separable functions. In case a multi-variable separable function is nonlinear, it can be written by an approximate form in SP by separating the function into single variable functions such that each function (of each of the individual variables) is approximated in a linear form.

Mathematically,

$$f_4(X_S) = \sum_{i \in T} f_{4,i}(x_{s,i}) \tag{3.28}$$

where each $f_{4,i}$ has an SP approximation given by,

$$f_{4,i}(x_{s,i}) \approx \sum_{j=1}^{p_b} f_{4,i}(x_{s,i}^j)\alpha_{i,j} \tag{3.29}$$

such that,

$$x_{s,i} = \sum_{j=1}^{p_b} x_{s,i}^j \alpha_{i,j} \tag{3.30}$$

$$\sum_{j=1}^{p_b} \alpha_{i,j} = 1, \tag{3.31}$$

where $x^j_{s,i}$ is a point (called *the breakaway point*) in the range of $x_{s,i}$, and $f_{4,i}$ is an evaluation of the function at the point $x^j_{s,i}$, with $\alpha_{i,j}$ as a weight assigned to $x^j_{s,i}$, and p_b breakaway points chosen in the range of $x_{s,i}$ (see Figure 3.3). This approximation is valid for convex functions that are continuous and differentiable in its range. Three breakway points (p_b = 3) are chosen for each x_i as follows,

$$\left[x^1_{s,i} \quad x^2_{s,i} \quad x^3_{s,i}\right] = \left[-P_{\max} \quad 0 \quad P_{\max}\right]. \tag{3.32}$$

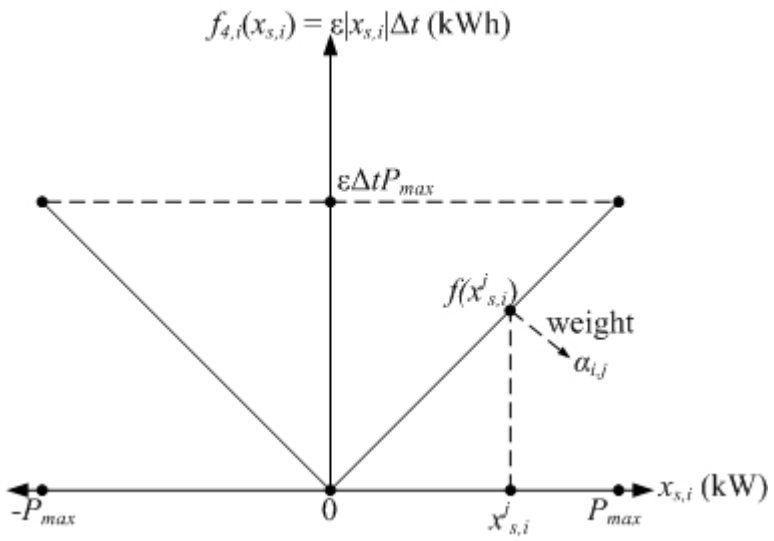

Figure 3.3 Generalized SP breakaway points for function f_4

All other objective functions of the MOP also need to be represented in the SP form, with variable transformation from $x_{s,i}$ to $\alpha_{i,j}$. Functions f_2, f_3, and f_4 are functions of $x_{s,1} - x_{s,n}$; and f_1 is a function of z. Hence, to obtain the Pareto optimal solution using SP, f_2, f_3, and f_4 will need to be represented as a function of the $\alpha_{i,j}$. Table 3.1 shows the value of objective functions computed at the breakaway points. Table 3.2 describes the dimensions of various terms in the multiobjective optimization depicted in this chapter.

3.8 Solution Algorithm

Separable programming introduces a transformation of the control variables from the x-domain to the α-domain. The final form of the optimization that is solved to obtain the solution to the control problem, is shown in the following equations,

$$\max_{X_S} \; d \tag{3.32}$$

such that

$$A_{in-eq} X_S \leq b, \tag{3.33}$$

$$A_{eq} X_S = b_{eq}. \tag{3.34}$$

Table 3.1 Objective functions evaluated at breakaway points

	TIME INTERVAL	$j = 1$	$j = 2$	$j = 3$
$x^j_{s,i}$	T	$-P_{max}$	0	P_{max}
$f_2(x^j_{s,i})$	PK	$-\Delta t P_{max}$	0	$\Delta t P_{max}$
	T-PK	0	0	0
$f_3(x^j_{s,i})$	T	$-\delta_k \Delta t P_{max}$	0	$\delta_k \Delta t P_{max}$
$f_4(x^j_{s,i})$	T	$\varepsilon \Delta t P_{max}$	0	$\varepsilon \Delta t P_{max}$

Table 3.2 Dimension of various terms in the multiobjective optimization

TERM	DIMENSIONS	TERM	DIMENSIONS
X_S	$(np_b + 2)$ x 1	U	p x 1
Φ	p x p	J_{agg}	p x 1
ψ	p x 1	b	$5n$ x 1
X_{DG}	n x 1	b_{eq}	$(4 + n)$ x 1
X_{load}	n x 1	A_{in-eq}	$5n$ x $(np_b + 2)$
X_d	n x 1	A_{eq}	$(4 + n)$ x $(np_b + 2)$

The control vector X_S (length: $np_b + 2$) is defined as,

$$X_S = \left[\alpha_{1,1} \ldots \alpha_{1,p_b} \quad \alpha_{2,1} \ldots \alpha_{2,p_b} \quad \ldots \quad \alpha_{n,1} \ldots \alpha_{n,p_b} \quad z \quad d\right]^T. \tag{3.35}$$

The inequality constraints are defined as follows (for $i = 1, 2 \ldots n$),

$$\sum_{j=1}^{p_b} x^j_{s,i} \alpha_{i,j} \leq P_{\max} \tag{3.36}$$

$$\sum_{j=1}^{p_b} -x^j_{s,i} \alpha_{i,j} \leq P_{\max} \tag{3.37}$$

$$\sum_{i=1}^{i}\sum_{j=1}^{p_b} x_{s,i}^{j}\alpha_{i,j} \le (1-s_0)E_{s,\max} \tag{3.38}$$

$$\sum_{i=1}^{i}\sum_{j=1}^{p_b} -x_{s,i}^{j}\alpha_{i,j} \le s_0 E_{s,\max} \tag{3.39}$$

$$\sum_{j=1}^{p_b} (x_{s,i}^{j}\alpha_{i,j} - z) \le x_{DG,i} - x_{load,i}. \tag{3.40}$$

The equality constraints are defined as,

$$\begin{bmatrix} f_1(X_S) & f_2(X_S) & f_3(X_S) & f_4(X_S) \end{bmatrix}^T - \begin{bmatrix} u_1 & u_2 & u_3 & u_4 \end{bmatrix}^T d = \psi \tag{3.41}$$

$$\sum_{j=1}^{p_b} \alpha_{i,j} = 1. \tag{3.42}$$

A flowchart describing the use of NBI to develop Pareto solutions, with SP adjustments is shown in Figure 3.4. The process is described briefly in the following steps:

i. Obtain the system data for bus *k*, and setup the NBI problem. Choose weights for the objectives in the optimization. This is one subproblem in the MOP.

ii. Transform the optimization problem by changing control domain from *x* to α. Solve the separable program to obtain the Pareto solution.

iii. Go to step (i). Perturb the weights for the objective functions. Repeat steps (i) and (ii) until a set of Pareto solutions are obtained for equidistant weight selections.

iv. Select a solution from the Pareto front, that best describes system needs, and operational requirements. This solution represents the optimal control of DESD storage rates, for the study interval.

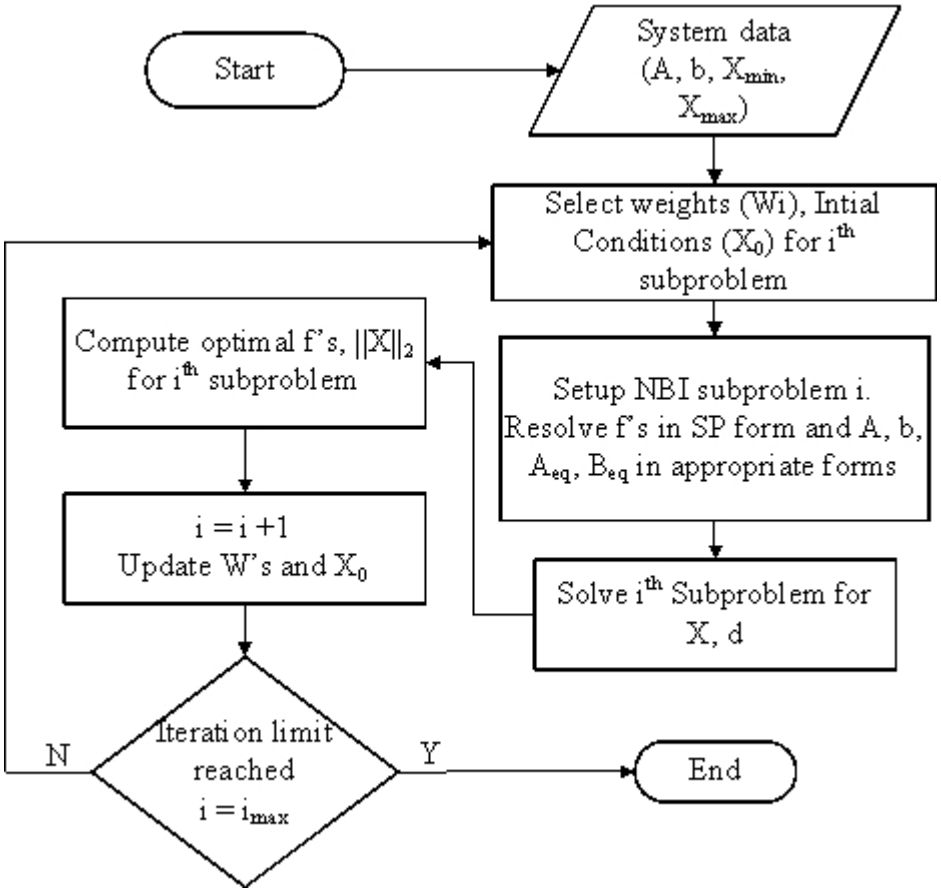

Figure 3.4 Calculating Pareto solutions using NBI with SP adjustements

3.9 Additional Considerations

Selection of Objectives

In the foregoing section, the several multiobjectives have been defined in terms of a control variable *X*. The control variable selected is the charging power for the energy storage device. However, the concept indicated is general enough to accommodate other objectives and other control variables. For example, there

may be cases in which some elements of the demand are controllable; there may be communication between one load and another, and there could be exchange of power in some way at the secondary level; if reactive power were incorporated into the model, an additional control variable might be the reactive power injected into the primary distribution supply. It is believed that the multiobjective approach taken would accommodate most of these formulations. The MOP structure described in this chapter can also be modified to represent any value of p. Some test cases in the following chapter describe and make use of such a modified formulation.

Solution Criteria

There are several aspects that are important in evaluating the validity of NBI based solutions in being Pareto solutions. Normal boundary intersection is based on the idea that the normal to the convex hull of minima for a MOP will intersect the boundary of the objective functions at a Pareto optimal point. This is valid if the boundary of the objective functions is a convex region (which is true for practically every known application in literature [80]). This point of intersection is of interest and it is obtained by maximizing the distance on any normal from a point on the convex hull. Each of the points on the convex hull is obtained for a specific weighting combination of the objectives. Even if the boundary is not a convex region, the solution of the NBI will not be a Pareto optimal point, but will still be an 'efficient' solution [80]. Hence, the NBI method has been shown to be efficient and mathematically robust in solving multiobjective optimization problems in literature (see Figure 3.2). For the problem at hand, it is extremely

difficult to visualize the solution or the tradeoff boundary in the objective functions, as the problem is 4-dimensional and the length of the true control solution is *n*, where *n* is the number of time steps in the time horizon *T*.

Separable programming is also a topic well documented in literature [88] and lends itself to applications where a function is non-linear and multi-variable, as described earlier. The necessary conditions for a multi-variable function to be separable are: it should be variable-independent (i.e., can be written as a sum of single variable functions); it should be convex in the range where the non-linearity is approximated; and it should be continuous and differentiable in the range of approximation. All these conditions hold true in the problem at hand. Hence, the validity of the application is implicit. An illustrative example has been solved in Appendix B to describe the steps in the application of separable programming and NBI in solving non-linear multiobjective problems.

Selection of Weights

For the problem at hand, weights are essentially coordinates of the points on a 4 dimensional hyperplane. Weight selection for the optimal control problem at a bus *k* is done to obtain an equidistant trace of Pareto optimal points. For the test cases illustrated in the following chapter, the individual weight for an objective function is allowed to jump between fixed states, in the range of zero and one. The NBI method also requires the weights to be convex (i.e., they sum to one). The other consideration in weight selection is to choose weights for subsequent subproblems of NBI that are close to within a tolerance limit. Hence, the Pareto optimal solution for subsequent subproblems would also be geometrically

close. As a result, the solution for one subproblem could be used as a starting point (or initial condition) for the next subproblem, ensuring faster convergence rates of the computer program.

Storage Utilization

The resolution of time steps used for DLMP computation and the control algorithm is fixed at a value denoted by Δt, and could be set anywhere in the range of 1 minute to 1 hour. Storage device life times are directly proportional to the number of charge-discharge cycles. Since it is impractical for the storage device to be controlled or operated (on a long term basis) at time steps lower than 15 minutes – 30 minutes, an additional limiting constraint is included in the formulation such that the minimum time steps in storage operations are greater than a preset limit. An additional consideration in storage device utilization is 'deep discharge'. This can also be accommodated in the formulation discussed in this chapter, by varying the right hand side of the inequality constraints in (3.38) and (3.39). This modification has not been applied to the current formulation and in the results shown in this report.

3.10 Control Algorithm Implementation

The application of the DLMP based real-time prices in distribution systems for developing a control algorithm is shown in this section. The suggested approach makes use of a sliding-mode structure. The system dynamic behavior (in loads and DER output) is forecast for a day-ahead operation. Control of the system at nodes in the distribution system is effectuated for the day-ahead operation.

After a time ΔT hours has elapsed, the system dynamics are forecast for another day-ahead operation and the optimal control variables are re-calculated.

The following are the proposed stages in implementing the DLMP based control strategy (see Figure 3.5):

i. Transmission level LMPs are computed (as day-ahead forecasts) over a time horizon of 1 day, i.e. $T = 24$ h.

ii. Day-ahead forecasts of the DLMP are computed at load locations in Bus #3, over time horizon T. This operation can be performed at the substation using DMS software capabilities.

iii. Energy management control objective, J is optimized at each control location over time horizon T. This operation has to be performed in a distributed fashion at each control location. Steps (i)-(iii) are repeated every 1 h, with updated day-ahead forecasts for load and renewable power output (i.e., $\Delta T = 1$ h).

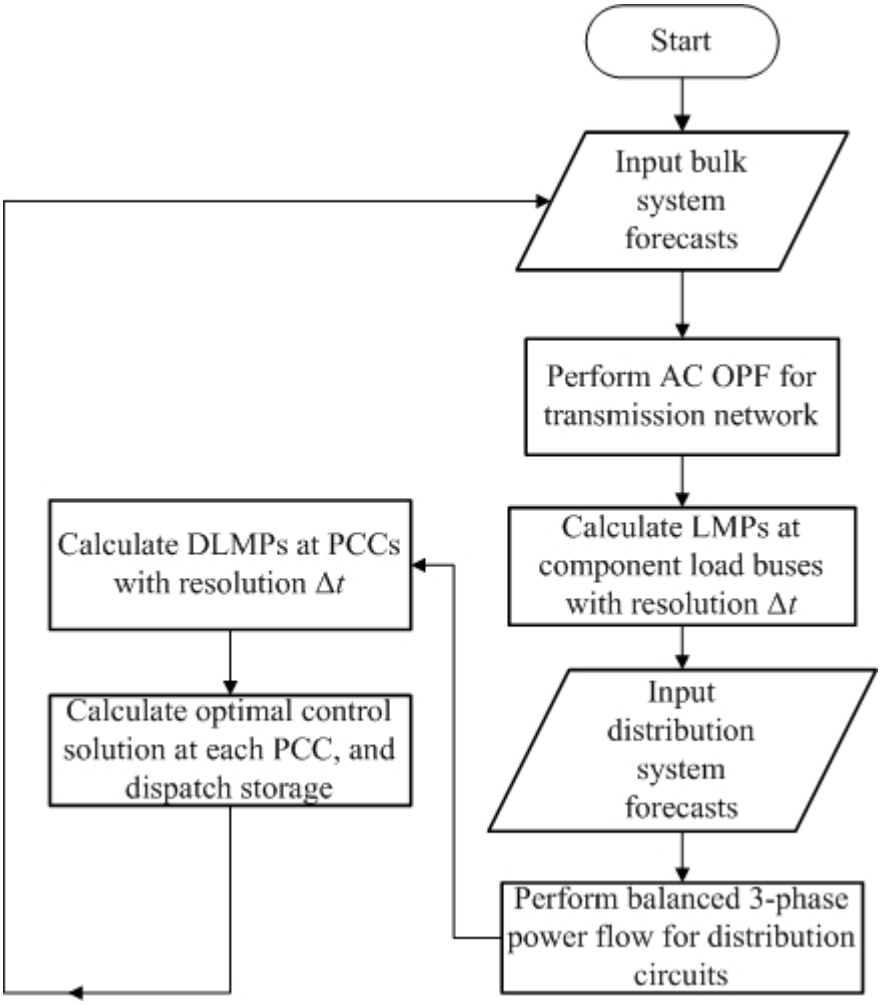

Figure 3.5 Suggested approach for implementing DLMP based control strategy

Chapter 4

APPLICATIONS AND NUMERICAL RESULTS

4.1 Description of Test Systems

Several test beds are used to test and illustrate the calculation and control concepts proposed. Each test bed was chosen to correspond to the objectives of what is being illustrated. A detailed description of a finite number of test cases and the results obtained are shown in this chapter. The test beds used are:

i. The “green hub” test system taken from the FREEDM project
ii. A well publicized and used test bed known as the Roy Billinton Test System
iii. The “Large Scale System Simulation” test bed from the FREEDM project.

Figure 4.1 shows the green hub test bed system. The one line diagrams for the RBTS transmission network and the distribution system at component Bus #3 are shown in Figures 4.2 and 4.3. Figure 4.4 describes the Large Scale System Simulation (LSSS) test system used for the FREEDM system demonstrations. The LSSS test system is a modified version of the distribution system at Bus #3, which has been developed for the FREEDM project to study the effect of solid state transformers in a large scale distribution system. Since the distribution system at Bus #3 represents the loads as aggregate load points, the level of three phase detail is not available to study transients introduced due to the presence of solid state devices in the distribution system. Therefore, the feeder F5 of the RBTS has been replaced by the IEEE 34 bus test feeder to obtain the LSSS test

feeder – to obtain a model of a large scale distribution system with a certain portion of the system providing three phase details of the feeders and laterals. The IEEE 34 bus test feeder is a test system developed by the IEE PES Distribution Systems Analysis Subcommittee that is based on a real feeder in Arizona [95]. Table 4.1 provides details of the several test cases investigated in this report.

Table 4.1 Description of test cases

SYSTEM	CASE	TASKS OUTLINED
GREEN HUB TEST SYSTEM	I	i. Assume an optimally pre-dispatched subtransmission system, and assign unequal LMPs for the two supply connections. ii. Calculate DLMPs and perform control operation at nodes 2, 5, 9 and 12. (Nodes 3, 6, 8 and 11 are laterals serving bulk loads with no control implementation.)
RBTS	II	i. Optimally dispatch the transmission network. Calculate LMPs at Bus #3. ii. Calculate DLMPs at different representative nodes in the Bus #3 distribution system. iii. Implement control strategy at the representative nodes. Compare operations with no control strategy implemented.
	III	i. Compare the bulk system LMPs at Bus #3 with and without control implementation. ii. Compare the base load at Bus #3 with the actual load at Bus #3 after control implementation. iii. Define renewable penetration indices. Compare the cost savings with different levels of renewable penetration.
	IV	i. Study the operation of the system in an islanded mode (considering a bus fault at source-end of feeder F1). ii. Compare DLMPs and control solution for pre-fault, faulted and post-fault scenarios.
LSSS	V	i. Repeat steps shown in test case II.

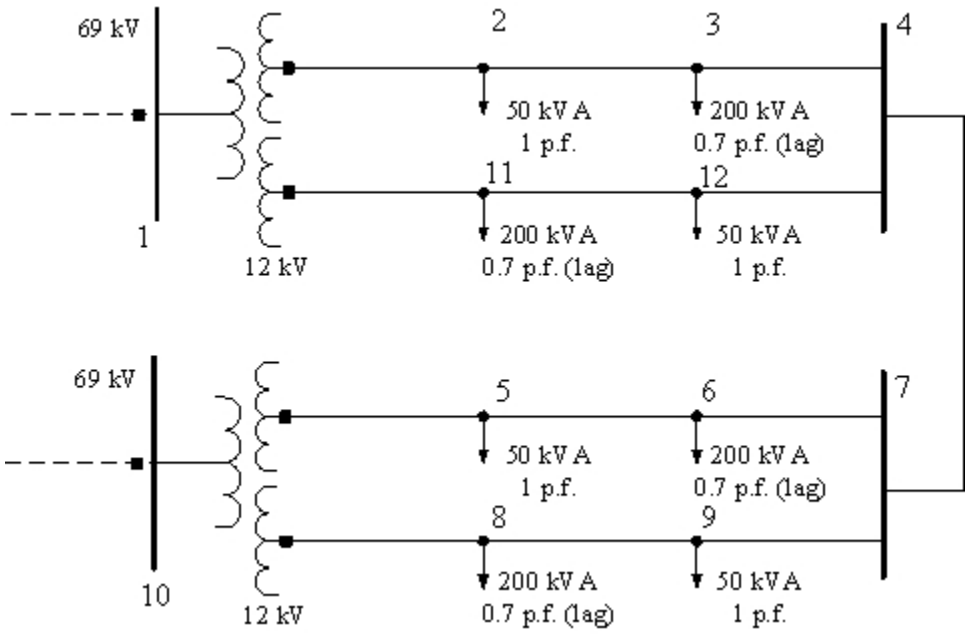

Figure 4.1 One line diagram of the green hub test system

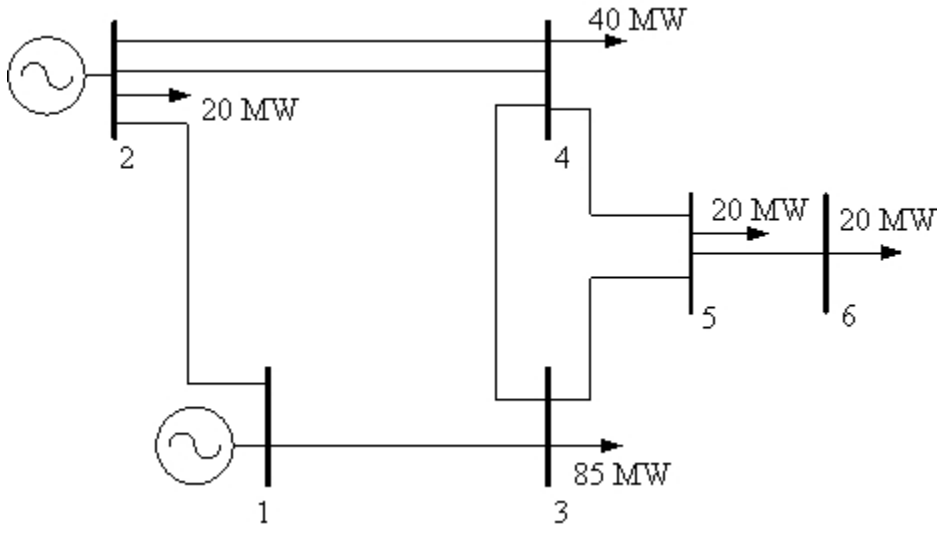

Figure 4.2 One line diagram of the RBTS transmission network

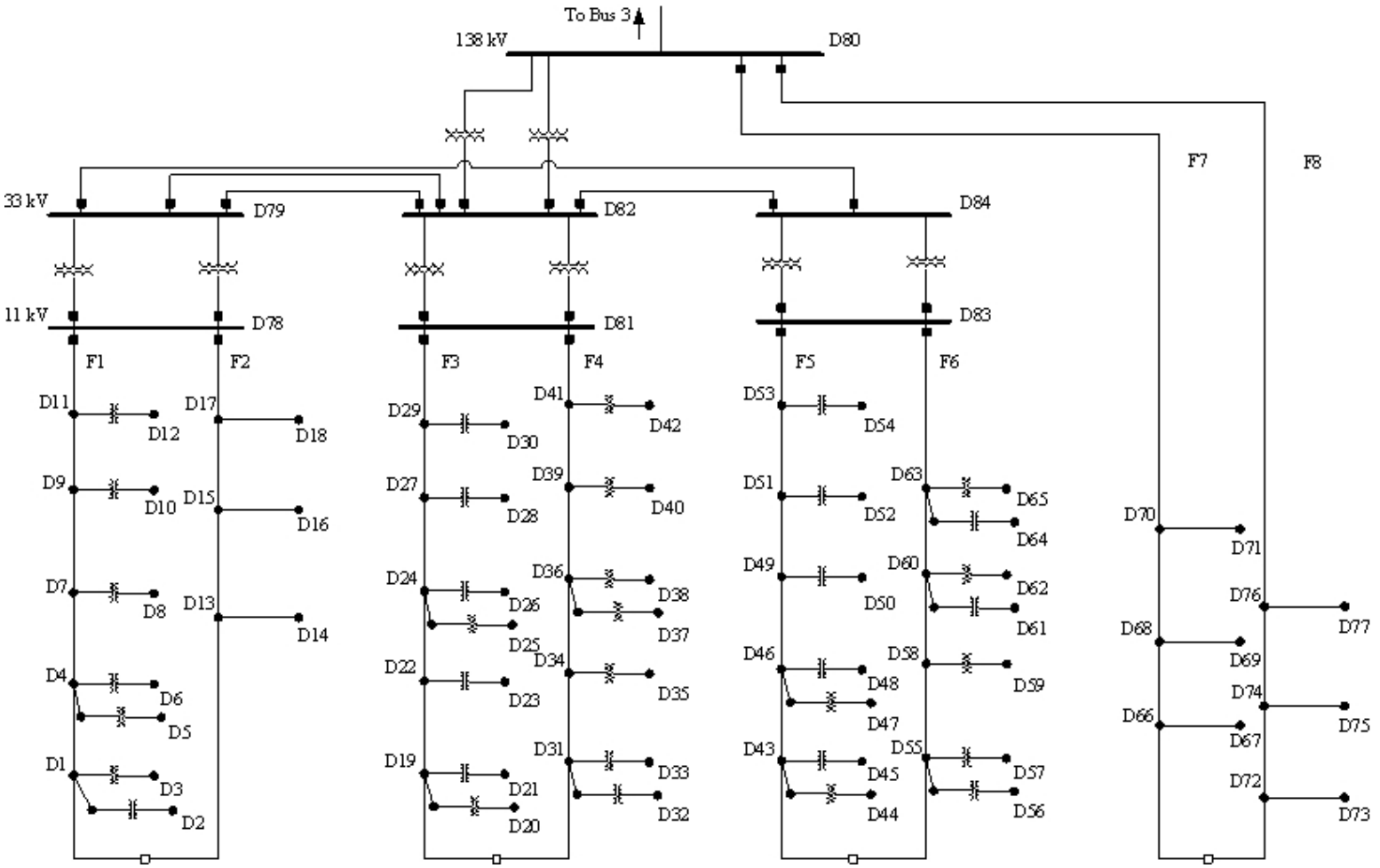

Figure 4.3 One line diagram of the RBTS distribution system at component Bus #3

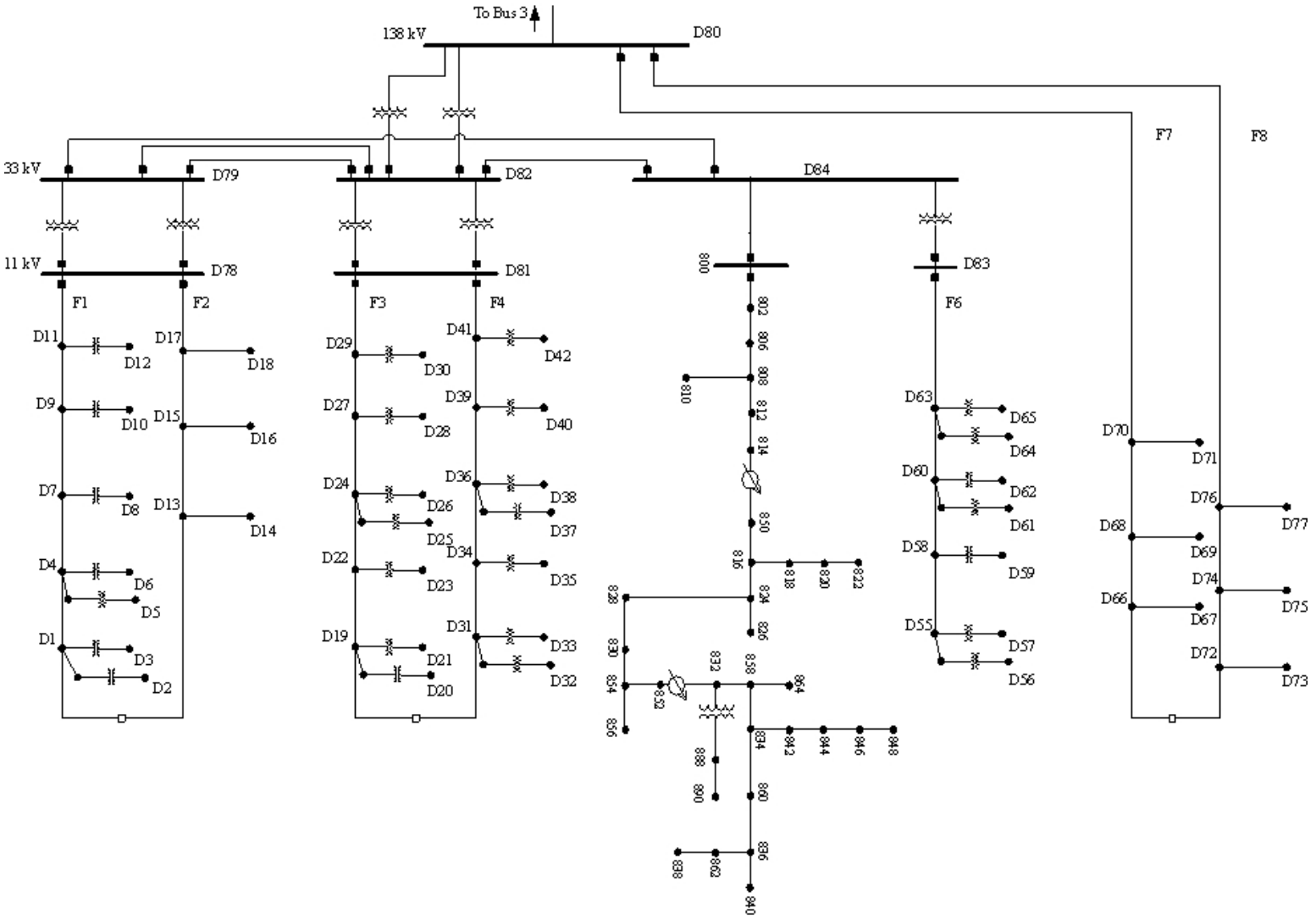

Figure 4.4 Large Scale System Simulation (LSSS) test-bed

The MATLAB R2010 platform was used in simulating all the test cases in this report. The MATPOWER (version 4.0b4) package has been used in performing the AC OPFs on the RBTS transmission network and Newton-Raphson power flow for the distribution systems in all test cases [89]. All simulations were carried out on a 2.50 GHz Intel i5-2520M processor with 8.00 GB of RAM on a 64-bit operating system.

The green hub test feeder is part of FREEDM systems center's ongoing research in implementation of solid state controlled devices in power delivery and energy management. The green hub test feeder has two supply ends, and the impact of the selection of the reference bus has been studied. The green hub system has been used to show the preliminary results of the application of the methods developed in this dissertation. The RBTS is a test system that was primarily developed to perform reliability studies [90-91]. The RBTS provides detailed models of the component distribution circuits at the component load buses in its transmission network. The Bus #3 distribution system along with the transmission network is used to study practical applications of the proposed strategy in this report, on large-scale distribution circuits. The LSSS test system has been used to study off-normal operating conditions, namely: an islanded operation of the distribution system with a substation level outage, and a networked operation of the distribution system with the normally-open switches being closed at the downstream end of the feeders.

4.2 Test System Data

The test cases depicted in Table 4.1 make use of the three test systems described earlier. Renewable resources and storage devices are integrated at different points of common coupling identified in the test systems for implementing the DLMP based control of the energy demand at the PCC. In all the test systems used, a major portion of the system is maintained as a legacy or traditional distribution circuit. Table 4.2 provides a list of all the PCCs chosen for each test system. The level of penetration of the DERs and the total energy capacity of the DESDs in each of the test systems has been shown in the following sections. Typical wind and solar power output data used for the test cases is shown in Fig. 4.5.

Table 4.2 Nodes selected for control implementation

TEST SYSTEM	NODES CHOSEN FOR CONTROL APPLICATION
Green hub test system	#2, #5, #9 and #12
RBTS Bus #3 distribution system	All load points in feeders F1-F6
LSSS test system	All load points in feeders F1-F4 and F6

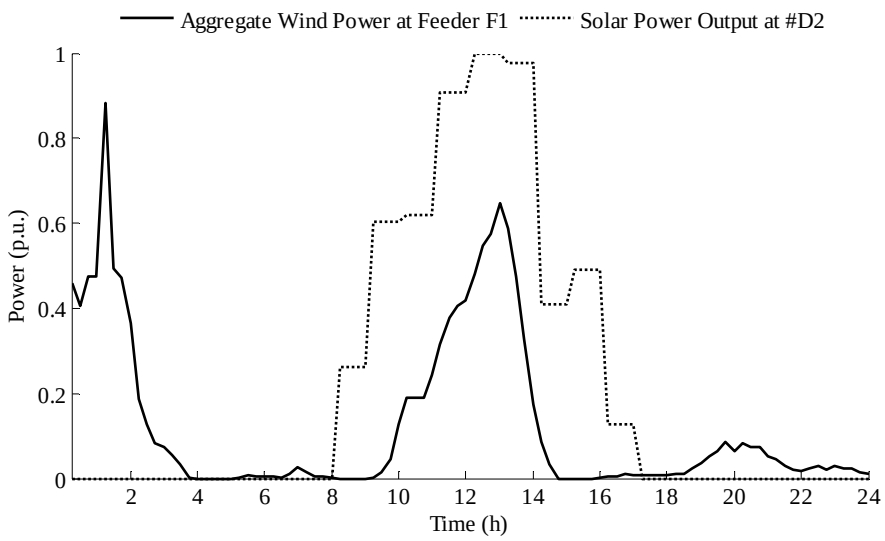

Figure 4.5 Typical wind and solar power output used in test cases II-V

The renewable resources' (e.g., wind and solar) power output data used for the test cases in this report, have been obtained from the National Renewable Energy Laboratory's (NREL) energy data repository [92]. The LMP data assigned to supply connections in test case I were obtained from the ISO New England (ISO-NE) historical market information [93]. The several daily load data (forecasts and actual) used for all test cases were obtained from the Electric Reliability Council of Texas's (ERCOT) backcasted and historical system data [94]. All of the data from the above resources were obtained for a typical summer weekday in the month of June. All relevant test data and system information are provided wherever necessary; and other supplementary test data are provided in appendix sections of this report, as indicated for each test case.

4.3 Test Case I: Green Hub Test System

In this test case, the impact of unequal supply LMPs at the two supply connections at node 1 and node 10 are seen. The test system data (i.e., load data,

renewable power output, and line impedance) are shown in Appendix A. LMPs at nodes 1 and 10 are pre-assigned as shown in Figures 4.6 and 4.7; with significantly lower LMPs pre-assigned at node 10. The test parameters used in test case I are shown in Table 4.3.

The DLMPs computed at the different controlled load points (namely, #2, #5, #9 and #12) are shown in Figures 4.6 and 4.7; and the reference buses chosen in these figures for the calculation of the energy component of the DLMP are #1 and #10, respectively. The controlled load at nodes 2 and 12 after the application of the energy management control algorithm are also shown in Figures 4.8 and 4.9 (note: the term 'controlled load' in these figures refers to the load seen at SST primaries with the optimal utilization of DESDs and DERs).

Table 4.3 Test data for test case I

DESD energy loss percentage (ε)	5%	Time steps in optimization (Δt)	15 min
Weights of NBI algorithm (w_i)	Equidistant with resolution of 0.25	Renewable incentive term (υ)	0 $/MWh
Peak power rating of energy storage (P_{max})	12.5 kW	Energy storage capacity (E_{max})	10 kWh
Peak wind power output	0.25*(Peak load)	Peak solar power output	0.25*(Peak load)

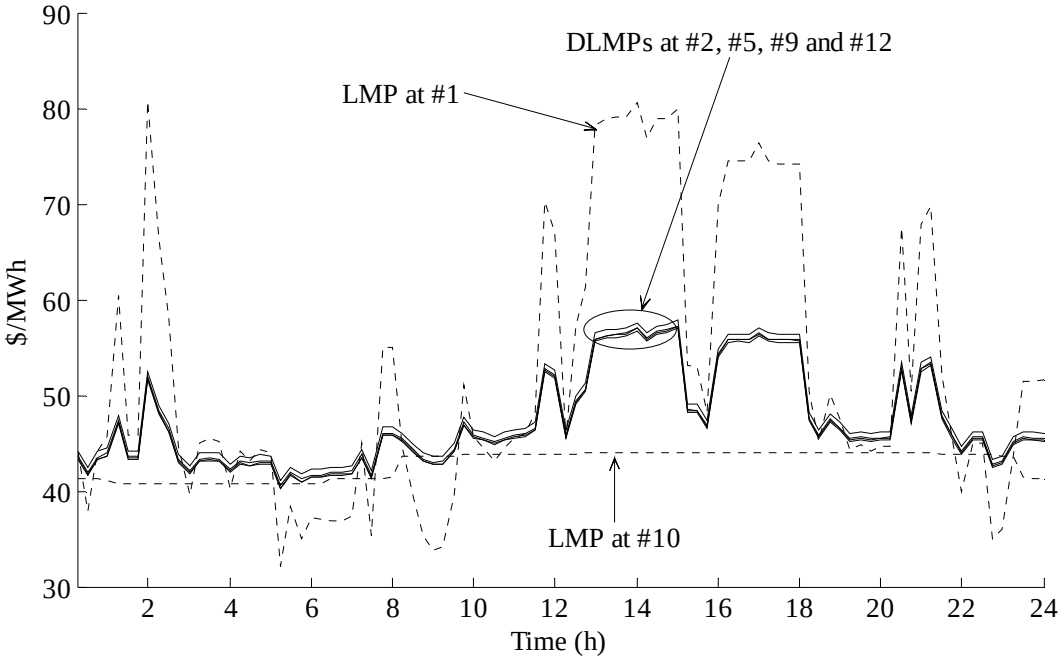

Figure 4.6 Comparison of LMPs and DLMPs with #1 chosen as reference bus in test case I

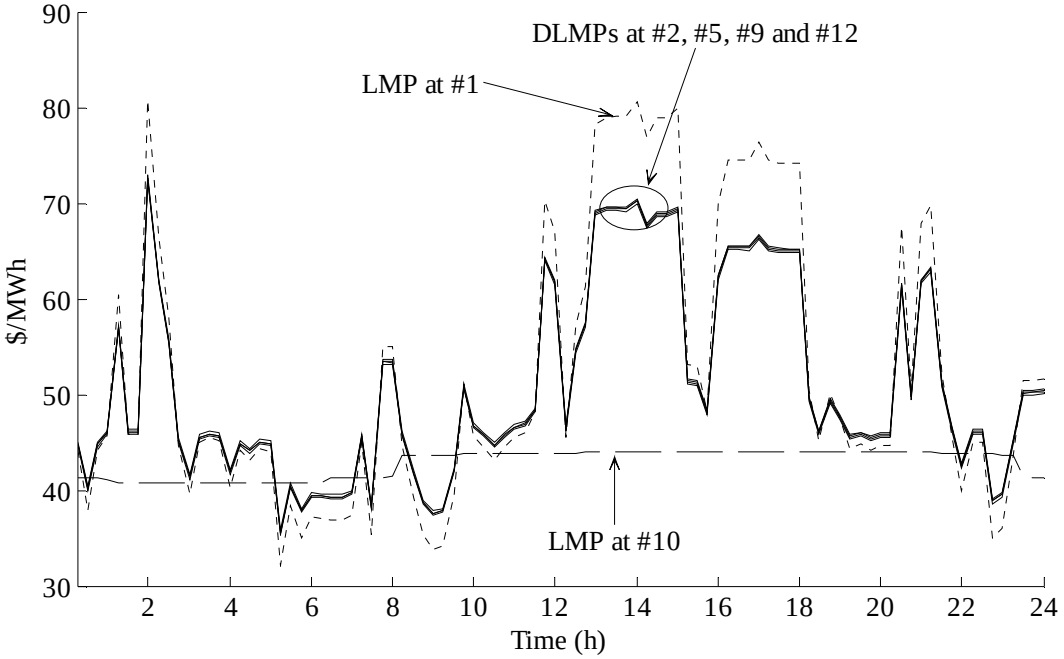

Figure 4.7 Comparison of LMP and DLMPs with #10 chosen as reference in test case I

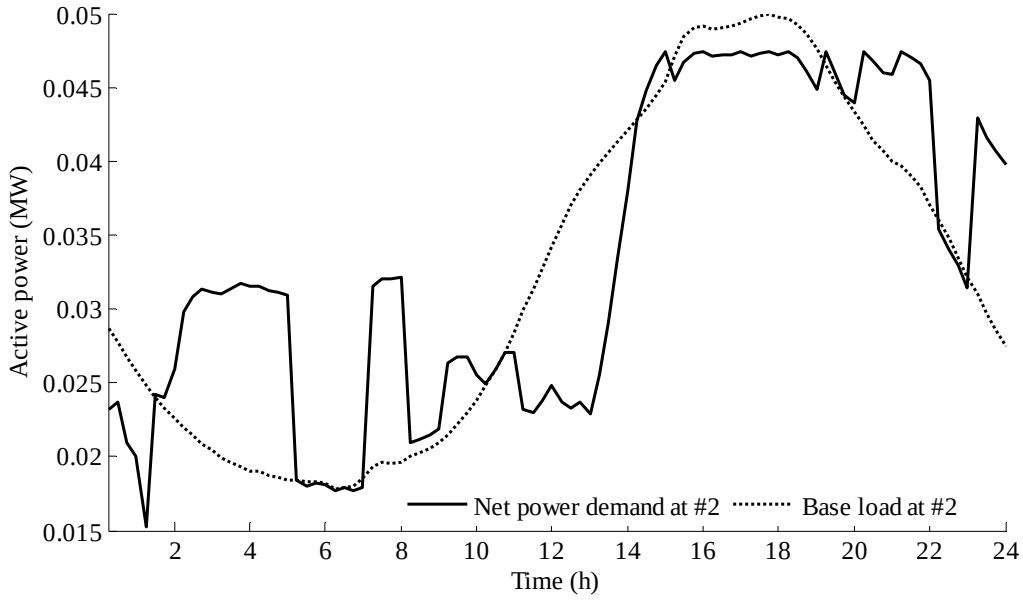

Figure 4.8 Comparison of controlled load and base load at #2 in test case I

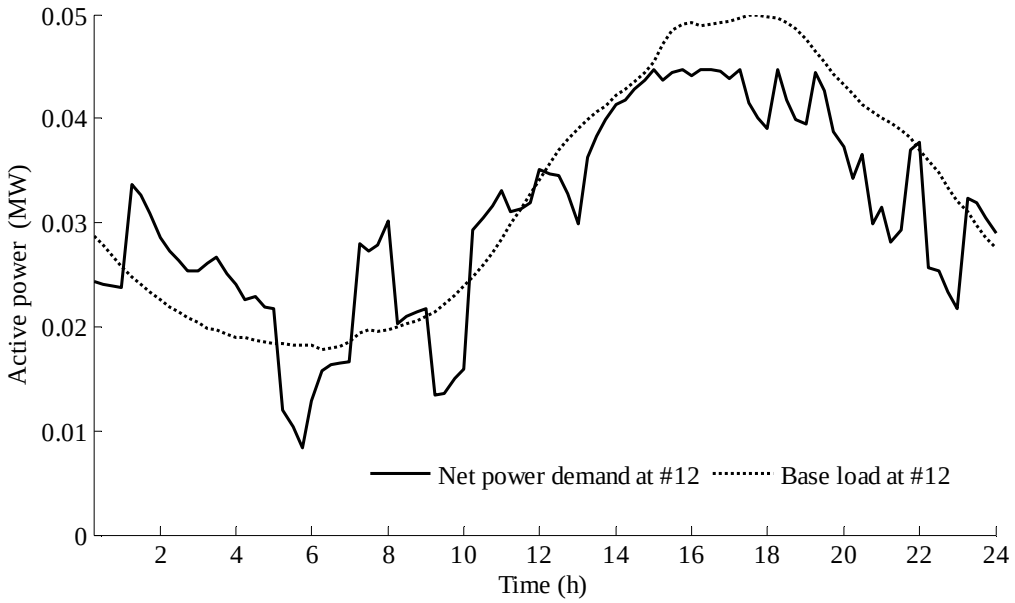

Figure 4.9 Comparison of controlled load and base load at #12 in test case I

As discussed earlier, the disparity in the calculated DLMPs for the system with different reference buses that have unequal transmission LMP component

can be seen from this test case. In a practical field scenario, the transmission-level LMP at nearby substations will be unequal but close to each other. In this test case though, a vast difference in the LMPs at the two supply connections has been used to highlight the differences in DLMPs seen with different selections for the reference bus.

In the case of multiple supply connections, the energy component of the DLMP is computed using participation factors. The participation factors are calculated in the formulation through a distribution power flow algorithm. In a power flow algorithm the generator that is set as a reference bus, is used to dispatch the losses in the system, and the other generating units participate in maintaining the energy balance. Hence, based on this reasoning, the participation factor for the supply end that is the reference bus should be lower than the combined participation factor for other supply ends. Therefore, the LMP at the reference bus would have a lower influence on the energy component of the DLMPs in the system. This reasoning is backed by what is observed in Figures 4.6 and 4.7.

4.4 Test Case II: Roy Billinton Test System

The Roy Billinton Test System consists of a 230 kV transmission superstructure and a 138 kV subtransmission system (Figure 4.2). Typical load shapes for the RBTS transmission network used in this study are shown in Figure 4.10. Table 4.4 shows the generator cost functions used for 11 generating units on the RBTS transmission system. Linear cost functions are assumed for all generating units and the polynomial coefficients C_0 and C_1 corresponding to the zeroth order and first order terms are shown. Important test case parameters are shown in Ta-

ble 4.5. All other test parameters are the same as in the previous test case (Table 4.3). In this test case, using the day-ahead forecast and actual load for the transmission network along with the generator cost functions, the RBTS transmission network is optimally dispatched to compute the LMPs at the respective load buses. The distribution feeders on component Bus #3 have loads classified as residential, commercial or industrial (Figure 4.3). Table 4.6 shows the load type classification at load points in Bus #3 along with the peak load and the total number of customers at each load point. For the implementation of the optimal control strategy, all load points in feeders F1-F6 are chosen. The remaining load points (i.e., those on feeders F7, F8) are medium and large 3-phase industrial loads rated at 138 kV and controls are not implemented. Therefore 34.71% of the total load at Bus #3 is deemed as controllable. Distributed resources and storage devices are dispersed over Bus #3 at all control points. The aggregate load at each control location averaged over all the laterals can be assumed to be balanced in the three phase sense.

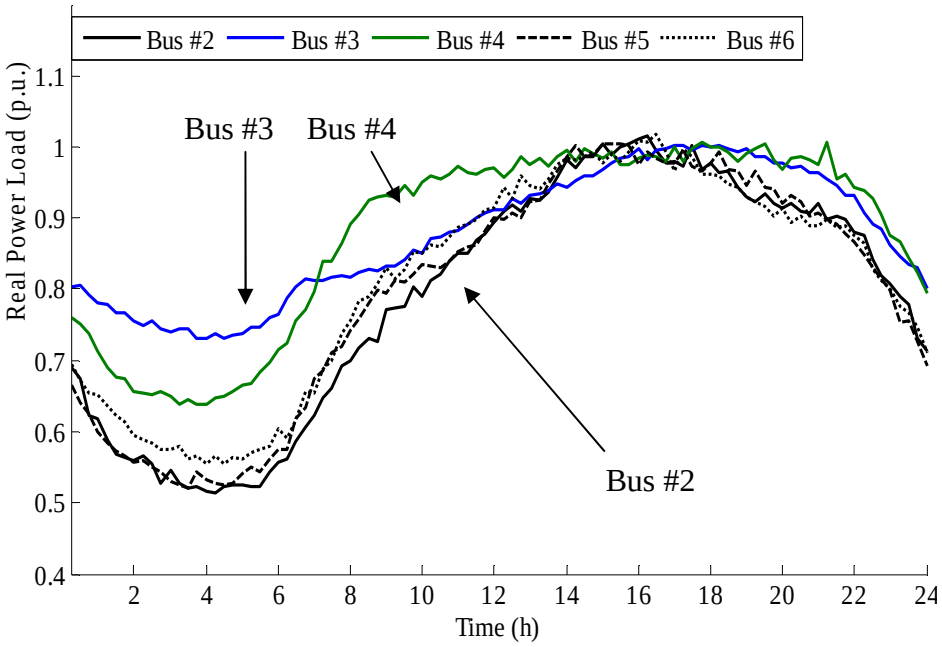

Figure 4.10 Typical daily load characteristics in the RBTS transmission network

Table 4.4 Generation cost functions used for test cases II-V

BUS #	CAPACITY, P^G_{MAX} (MW)	COST FUNCTION, $G^C(P^G)$ ($/h) (POLYNOMIAL COEFFICIENTS: C_0, C_1)
1	40	34.00, 90.18
	40	32.00, 90.18
	10	36.50, 68.49
	20	32.25, 77.63
2	5	30.50, 71.43
	5	30.50, 11.43
	40	30.50, 81.42
	20	35.50, 55.71
	20	30.50, 75.71
	20	35.50, 85.71
	20	30.50, 105.71

Table 4.5 Test data for test cases II-V

Peak power rating of energy storage (P_{max})	0.25 MW	Energy storage capacity ($E_{s,max}$)	0.5 MWh
Peak wind power Output	0.30*(Peak load)	Peak solar power output	0.30*(Peak load)

Table 4.6 Load type classification for load points in Bus #3 for test cases II-V

	SMALL	MEDIUM	LARGE
RESIDENTIAL	D3, D26, D45, D52 (0.7750†, 190††)	D2, D6, D8, D10, D12, D35, D37, D38, D40, D42, D56, D57, D59, D61, D62 (0.8367, 250)	D20, D21, D23, D32, D44 (0.8500, 230)
COMMERCIAL	D5, D28, D30, D33, D48, D50, D54, D64, D65 (0.5222, 15)	-	D25, D47 (0.9250, 1)
INDUSTRIAL	D14, D16, D18 (1.0167, 1)	D67, D69, D77 (6.9167, 1)	D71, D73, D75 (11.5833, 1)

†Peak load (MW) for each node, ††Number of individual customers at each node

The optimal energy storage operations for all load points in the distribution system are shown in Figure 4.11. The DLMPs at load points D2 (with medium residential type loads), D5 (with small commercial type loads) and D18 (with small industrial type loads) are depicted in Figure 4.12. A three dimensional

representation of DLMPs in F1 and F2 are depicted in Figure 4.13. The control of the energy demand at nodes D2, D18 and D25 in the Bus #3 distribution are shown in Figures 4.14, 4.15 and 4.16.

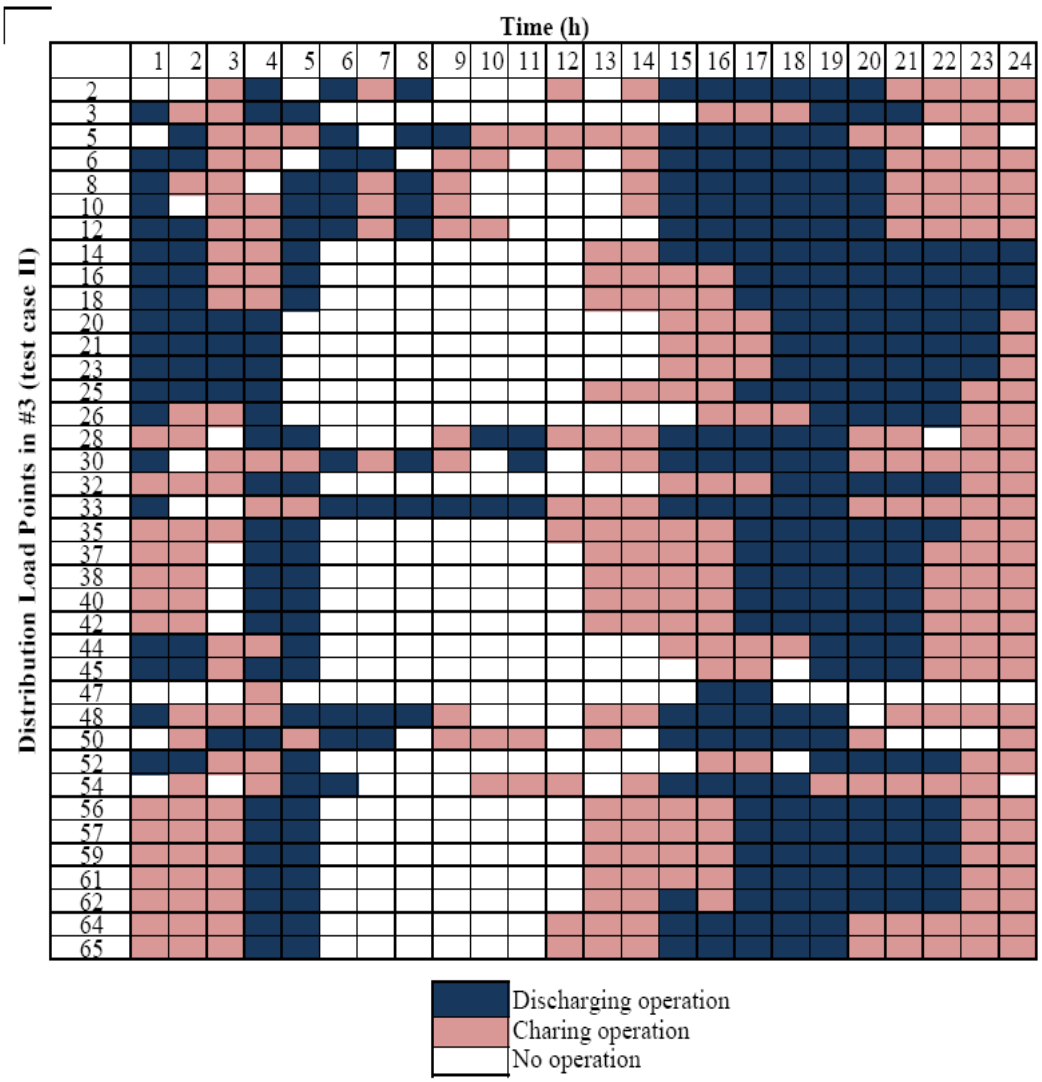

Figure 4.11 Graphical representation of energy storage operation for test case II

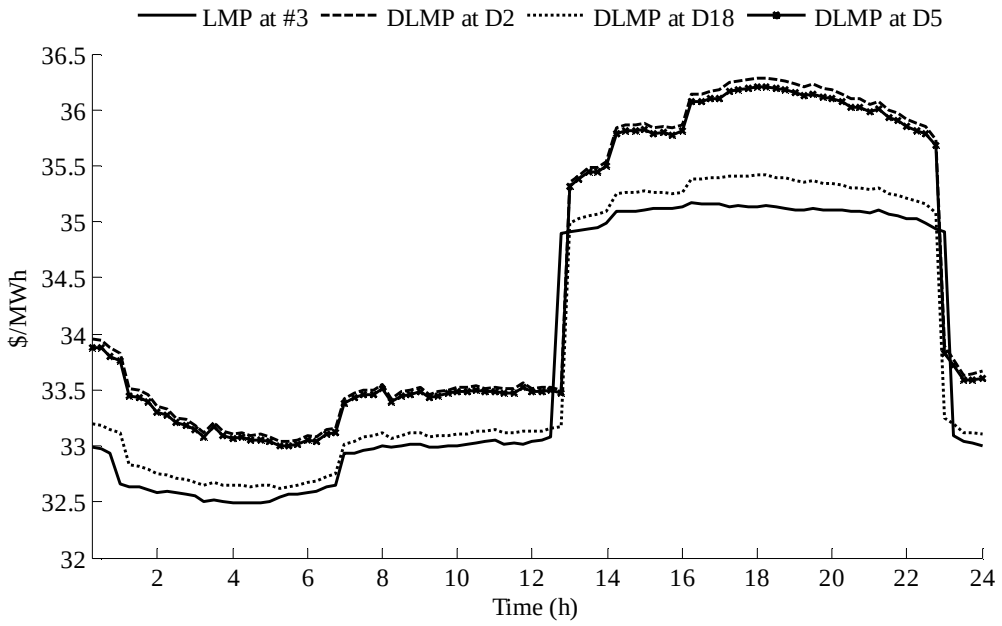

Figure 4.12 Comparison of LMP at #3 and the DLMPs at D2, D5, and D18 in test case II

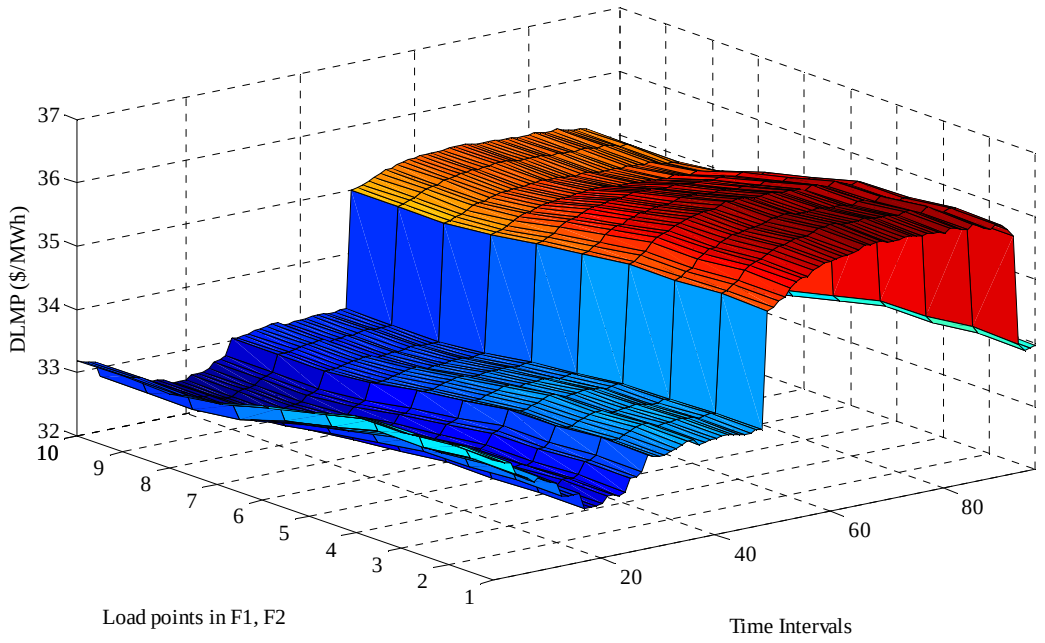

Figure 4.13 Graphical representation DLMPs in feeders F1 and F2

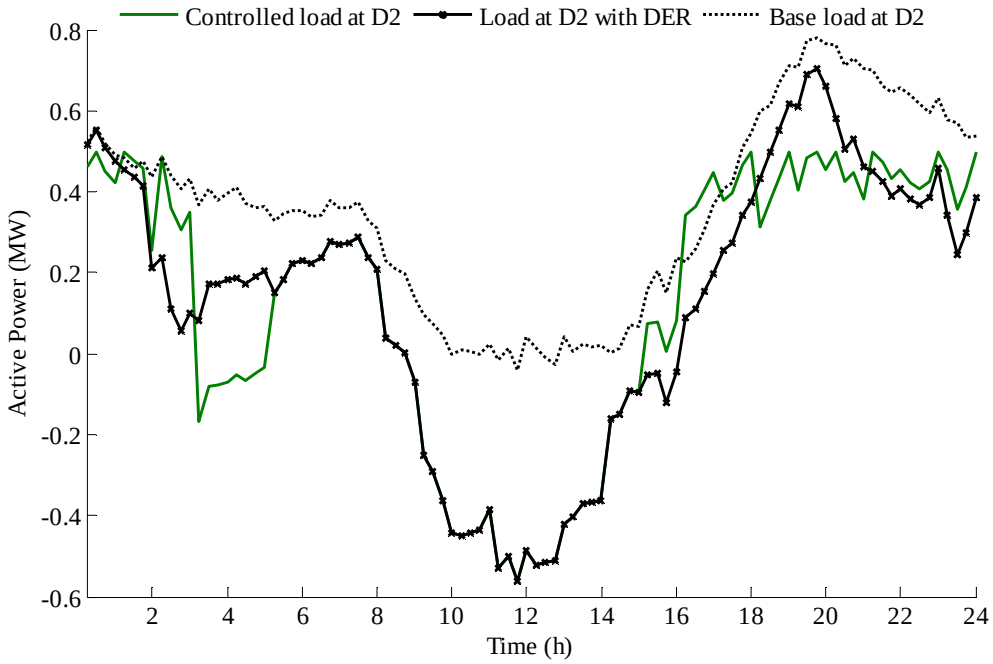

Figure 4.14 Base load, load with DER and controlled load at D2 in test case II

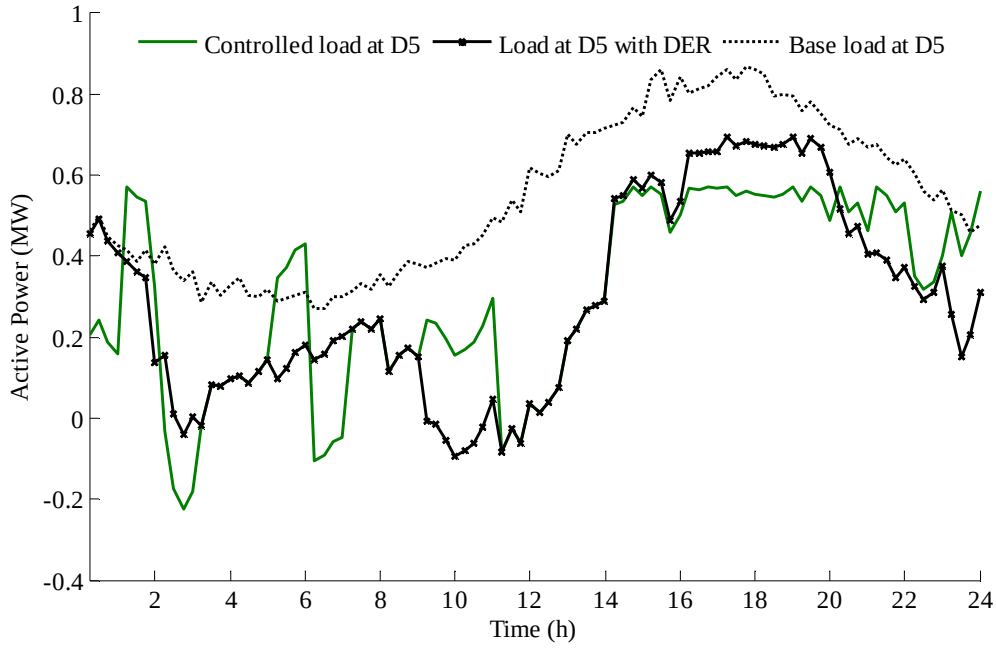

Figure 4.15 Base load, load with DER and controlled load at D5 in test case II

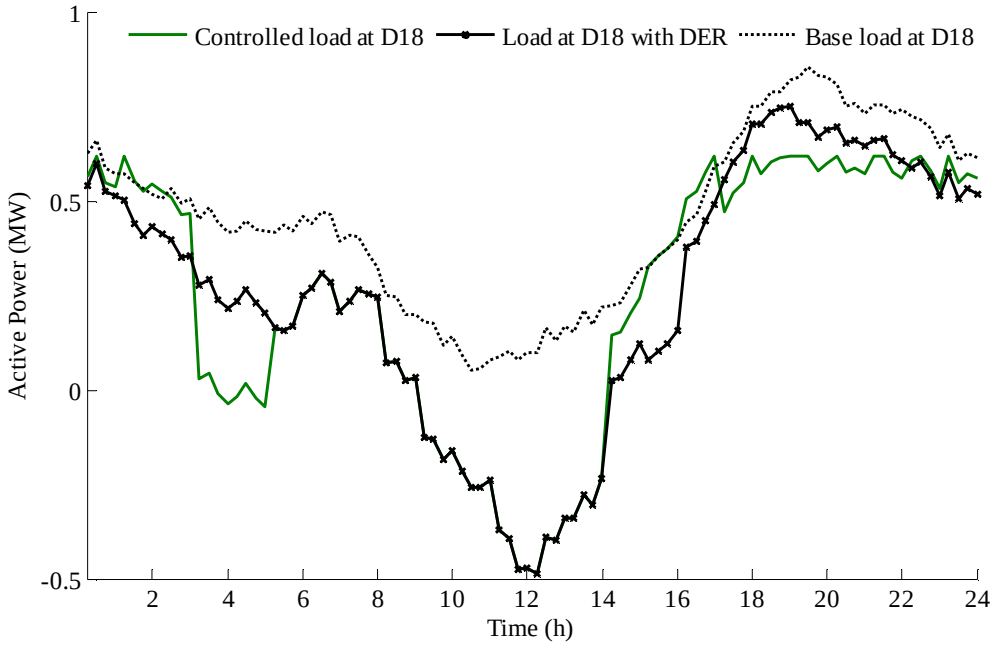

Figure 4.16 Base load, load with DER and controlled load at D18 in test case II

4.5 Test Case III: Comparison of Control Scenarios

In test cases III, the interaction of the DLMP based control algorithm for energy management, on the bulk power system prices has been analyzed. The application of the optimal control algorithm has been considered in test case III as two different scenarios, namely: sub-case III (A), with the control implementation on the base load without the presence of DERs; and sub-case III (B), with the control implementation on the base load in the presence of DERs. Figures 4.17 and 4.18 describe the two scenarios and the system-wide active power demand observed with the implementation of the control algorithm. In each of the two subcases in this section, the loads represented are the portion of the total instantaneous active power demand in Bus #3 where the control algorithm has been implemented.

The comparisons of the LMP of Bus #3 are shown for cases III (A) and (B) in Figure 4.19. The cumulative costs of energy delivery (denoted by CCE) can be calculated by integrating the product of the instantaneous LMP and the MW load over time, throughout the time horizon *T*. This calculation was made using the LMPs observed at Bus #3 and have been compared in Figure 4.20, for cases III (A) and (B).

In each of the sub-cases, the improvement in the load shapes can be observed in Figures 4.17 and 4.18. The control algorithm performs adequately to optimize the utilization of energy storage devices based on the multiobjectives specified.

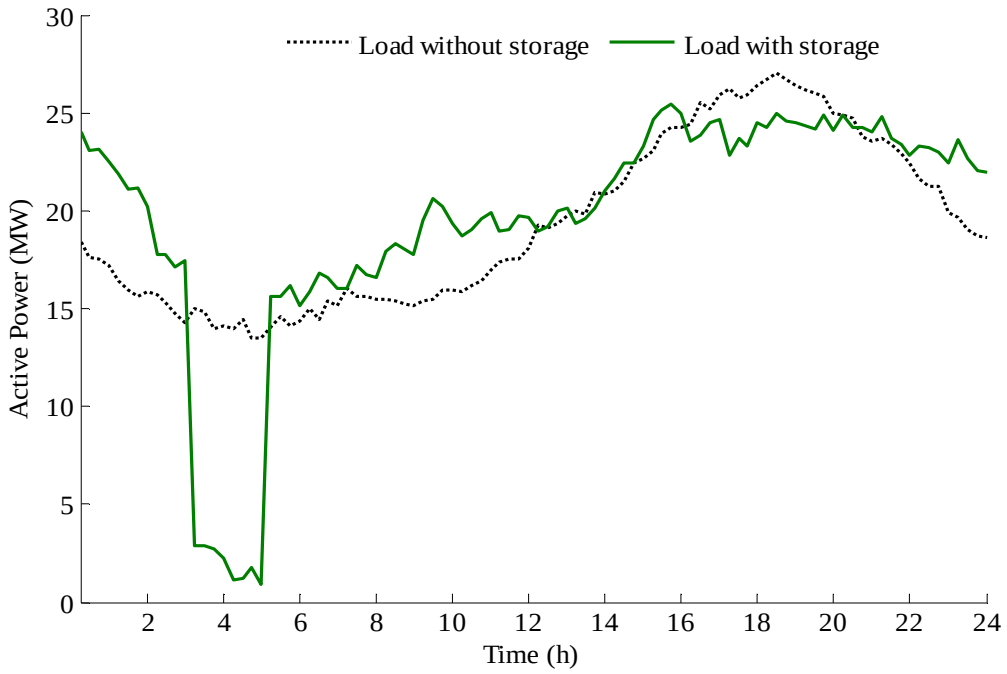

Figure 4.17 Total active power demand over time *T* in test case III (A)

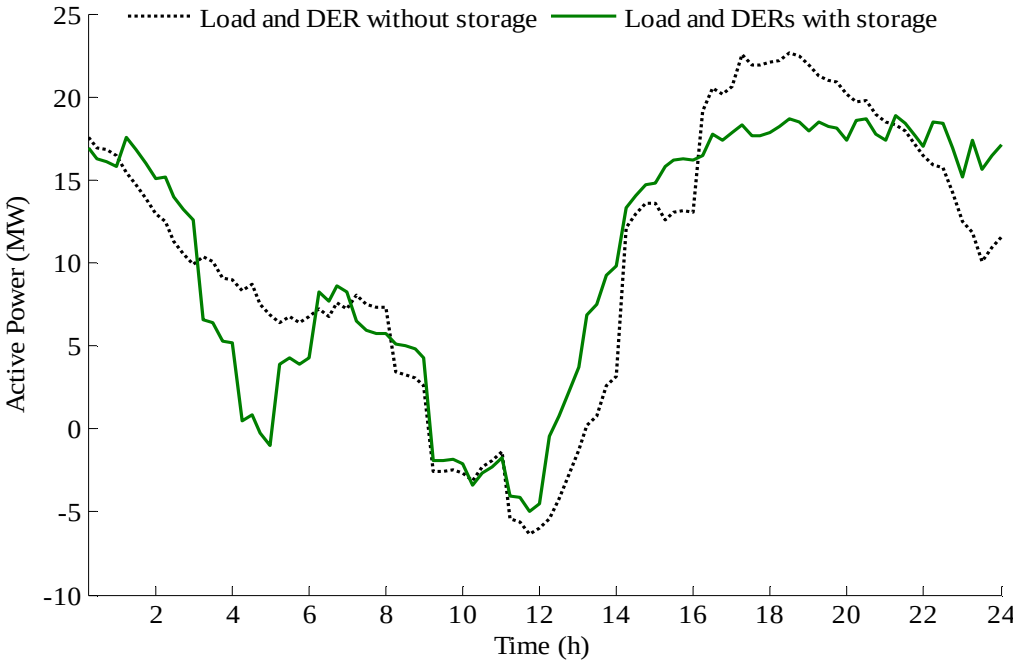

Figure 4.18 Total active power demand over time *T* in test case III (B)

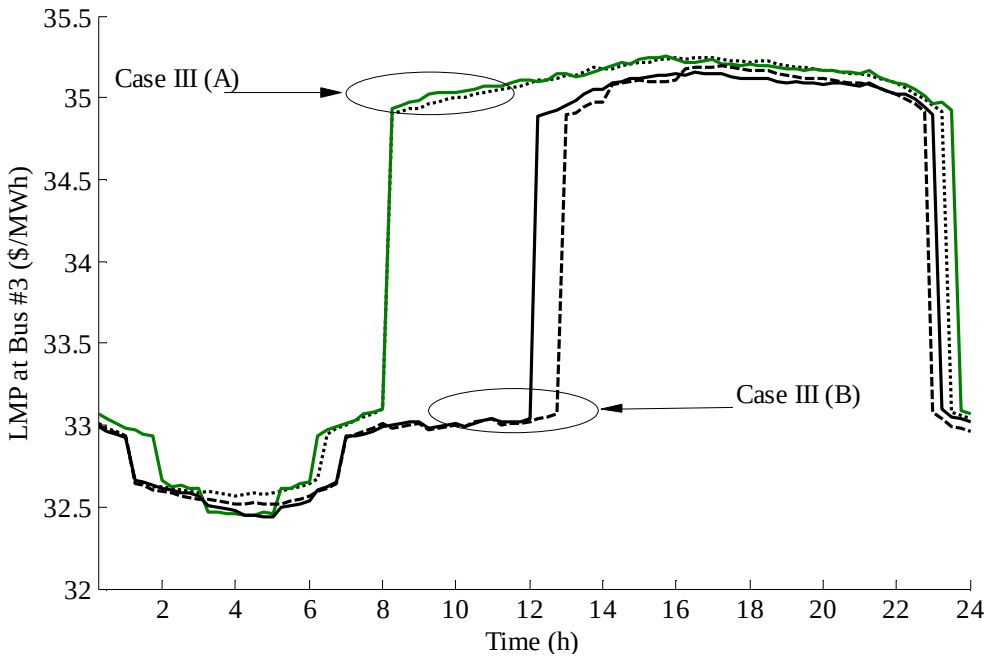

Figure 4.19 Comparison of LMP at Bus #3 for cases III (A) and (B)

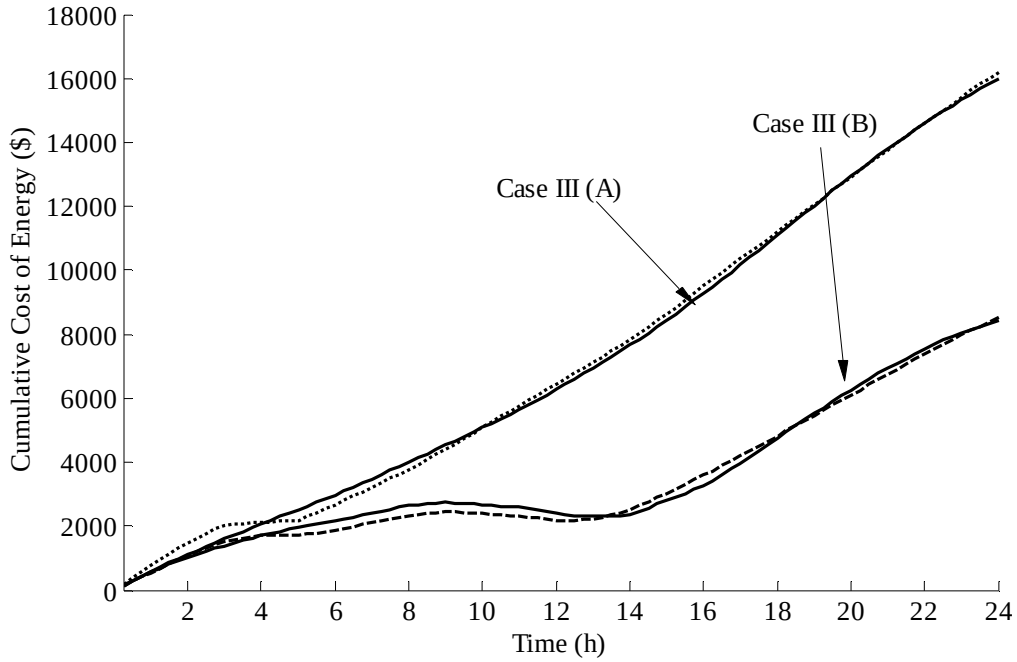

Figure 4.20 Comparison of cumulative cost of energy at Bus #3 for cases III (A) and (B)

It can be observed from Figure 4.18 that the improvement in the LMP of Bus #3 with control implementation is minimal. It can be observed from Figure 4.20 that the CCE is much lower for case III (B) compared to III (A). However, in each case the differences observed between the CCE curves with and without the energy management control algorithm are insignificant. Therefore, the savings in cumulative cost of energy over a time horizon *T* can be attributed to the reduction in net active power demand due to the inclusion of DERs in the distribution system.

4.6 Test Case IV: Islanded Case

The operation of the distribution system in an islanded mode is shown in test case IV. A line outage scenario has been considered: the line serving feeder

F1 (line D11-D78 in Figure 4.3) is tripped at 1800 h, and full service is restored at 1900 h, by closing the normally open switch at the downstream end of feeders F1 and F2. This time interval is chosen in this test case, as it best represents the peak loading period in the system. The feeder segment connecting D1 and D13 is normally open, but is closed to restore service to feeder F1. Figure 4.21 shows a contour map of the percentage of unserved load at each load point in feeder F1 during the outage considered. A graphical depiction of the state of charge of energy storage devices in feeder F1 is also shown as a contour map in Figure. 4.22. It can be seen between the intervals of the outage, that the state of charge at the load points decreases continuously till the energy storage depletes itself to meet the demand. In Figures 4.21 and 4.22, the seven load points in F1 are number serially in the decreasing order of distance from bus D78; and the time intervals are numbered such that each interval represents a duration of Δt h.

The depiction of system DLMPs in F1, F2 are shown as contour maps in Figures 4.23 and 4.24 for pre-fault and post-fault durations. It can be observed from the pre-fault duration that DLMPs are lower for the loads are closer to the source end of the feeder, as compared to loads farther away from the source. In the post-fault duration, feeder F2 is additionally serving the load of feeder F1. It can be observed in the post-fault duration that DLMPs in F1 and F2 are higher compared to DLMPs in the pre-fault duration due to the increase in the congestion component of the DLMP, as a consequence of higher feeder loading.

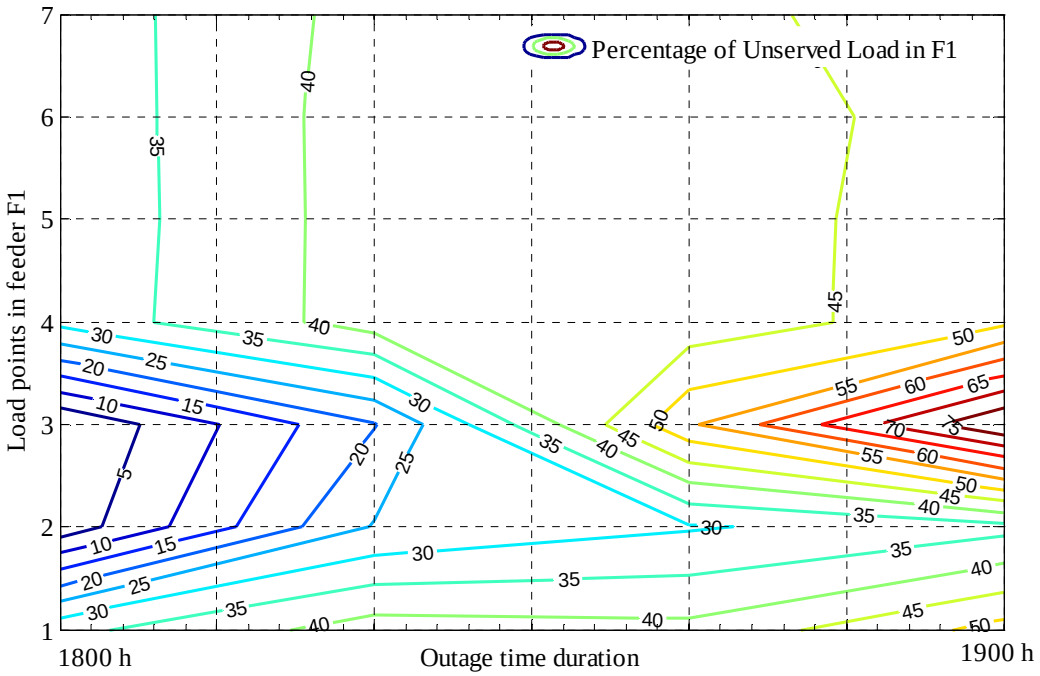

Figure 4.21 Representation of percentage of unserved load in F1 for test case IV

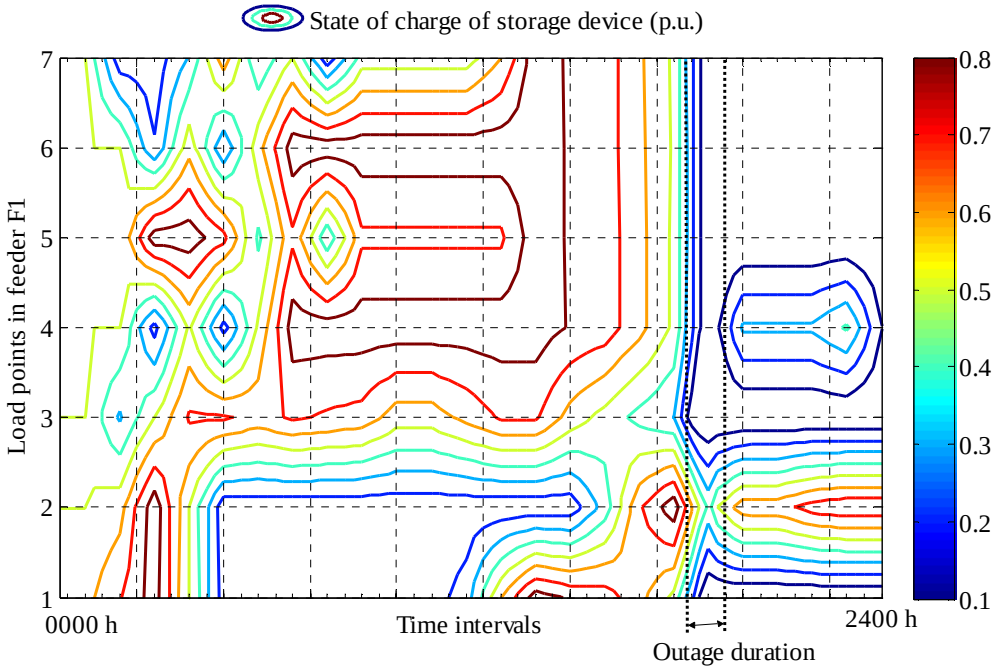

Figure 4.22 Representation of DESD state of charge at load points for test case IV

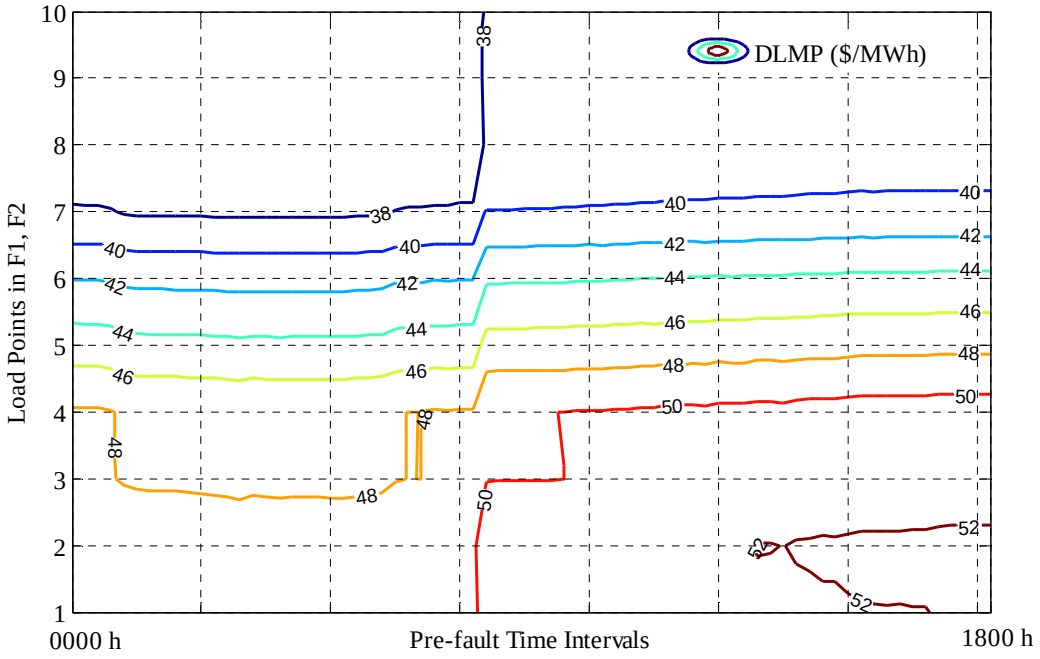

Figure 4.23 Graphical representation of DLMPs in feeders F1 and F2 for pre-fault duration in test case IV

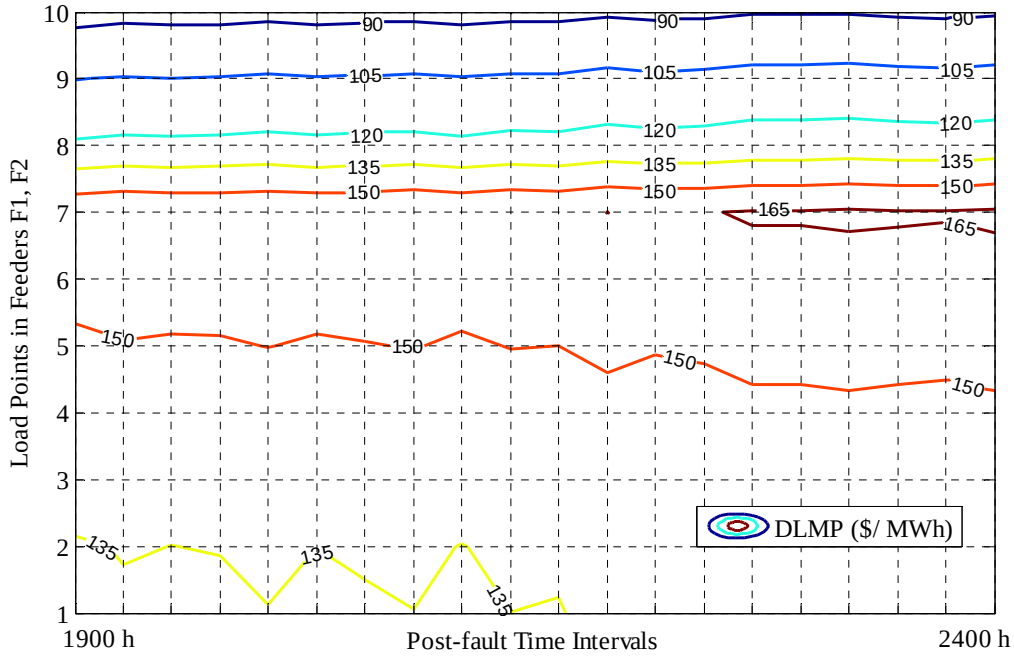

Figure 4.24 Graphical representation of DLMPs in feeders F1 and F2 for post-fault duration in test case IV

4.7 Test Case V: Large Scale System Simulations

The implementation of the DLMP method and the control algorithm on the LSSS test system is addressed in this section. The LSSS test system is part of ongoing research under the FREEDM systems research center. As part of this dissertation, the control algorithm was implemented on the conventional feeders (F1, F2, F3, F4 and F6) on the LSSS. The control algorithm was integrated with a model of the LSSS in a PSCAD environment, which is being researched at North Carolina State University to study solid state transformer switching transients and operation. Figure 4.25 portrays the control implementation at a load point D5 in the distribution system. A sampling of pertinent results of this study is presented here. A graphical representation of the storage operations in the LSSS test system is depicted in Figure 4.26.

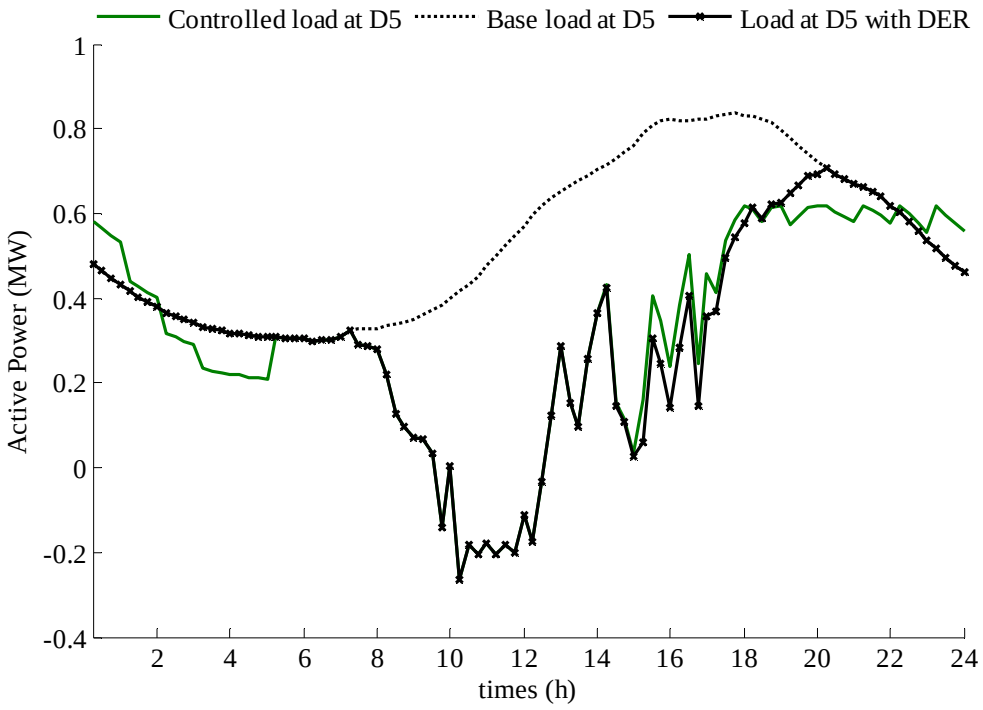

Figure 4.25 Base load, load with DER and controlled load at D5 in test case V

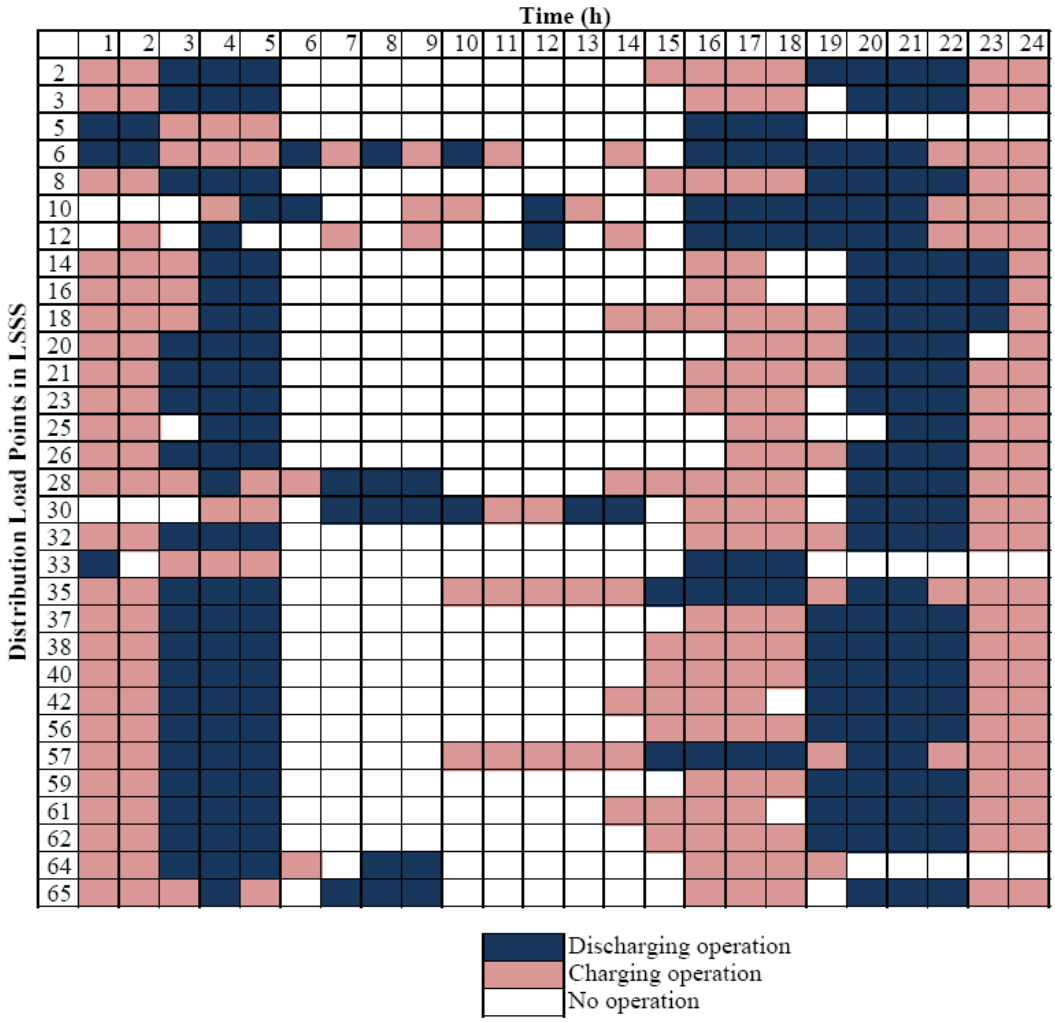

Figure 4.26 Graphical representation for energy storage operation in test case V

4.8 Computational Efficiency

The simulation studies performed in this work makes use of the parallel processing capability of the High Performance Computing (HPC) facility at the Arizona State University Advanced Computing Center (A2C2) [96]. The A2C2 cluster, also known as the Saguaro system, comprises of over 5000 processor cores, with an available memory of 11 TB of RAM and 1.5 GB of L2 cache

memory. The Saguaro cluster is representative of a modest sized supercomputer. The computation of various tasks in the Saguaro system can be performed using secure shell scripts that can be transmitted from a remote host. Parallel tasks can be executed if they are functionally independent, and can be done remotely using a single script file. The A2C2 facility was used to implement a portion of the controls indicated in this dissertation and results are taken to be representative of what a parallel processing computer can accomplish in the simulation of distribution system controls. It is emphasized that the use of the parallel processor is only as a simulator for the distributed controls which are microprocessor implemented and distributed across a power distribution system. The Pareto optimal control solutions calculated for the different points of common coupling in the distribution system are computed at parallel nodes on the supercomputer, to simulate a parallel processing environment.

The control calculation involves a linear programming (LP) routine that is solved using the simplex method. Since the control algorithm calculates a uniform Pareto optimal front corresponding to w equidistant weighting options for the objectives, this corresponds to w LP problems solved at each parallel node. The size of the control vectors and constraint matrices of the LP are a function of the number and resolution of time steps Δt chosen in time horizon T. The computation times are found to be dependent on the size of the control vector and the constraint matrices. The resolution of the time steps and the mean computer processing times are shown in Figure 4.27. Table 4.7 details the parameters of the LP

problem and the corresponding matrix dimensions for time horizon T = 24 h and weights w = 35.

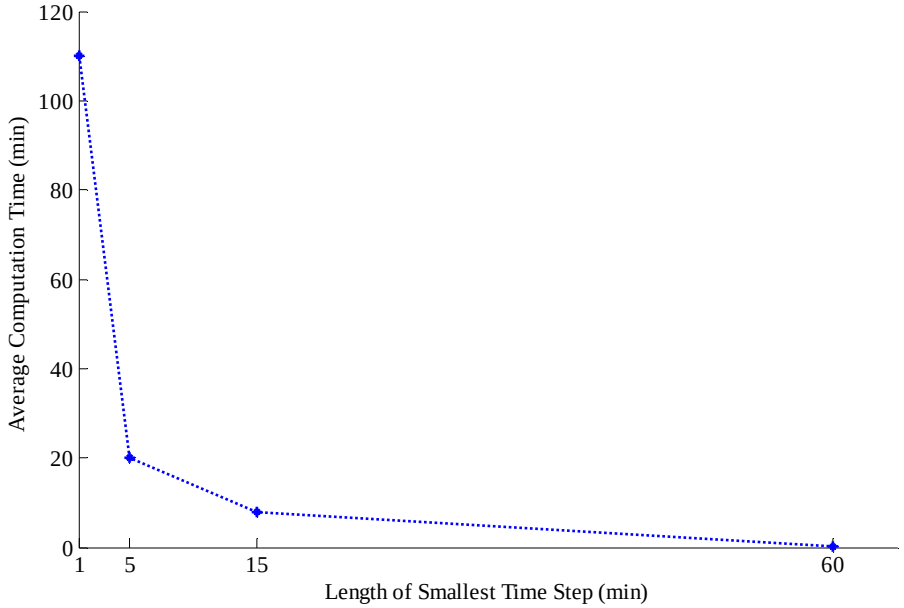

Figure 4.27 Comparison of computation time with length of the control time step

Table 4.7 Comparison of linear programming parameters for different time steps (Test cases II-IV)

Δt (mins)	Size of control vector X	Size of $A_{in\text{-}eq}$ (in $A_{in\text{-}eq}X \leq b$)	Size of A_{eq} (in $A_{eq}X = b_{eq}$)
1	4322	7200† x 4322††	1444† x 4322††
5	866	1440 x 866	292 x 866
15	290	480 x 290	100 x 290
60	74	120 x 74	28 x 74

†Number of rows, †† Number of columns

4.9 Summary of Test Cases

The test cases described in this chapter detail the applications of the DLMP formulation and the multiobjective control algorithm for storage device utilization. An implementation framework has also been portrayed which fits closely with other existing operations in distribution management systems. The

formulations have been validated in test case I with the effect of multiple supplies in the primary distribution being studied.

The test cases using the RBTS and the LSSS test-bed (cases II-V) depict the application of the proposed strategy in a large-scale distribution system. These studies present the DLMPs calculated at representative residential, commercial and industrial load locations on the feeders in the distribution system at component Bus #3. The DLMPs and respective controlled loads are depicted for these locations. It can be seen that the base loads are reduced considerably and an improvement in the load factors is also seen. The cumulative costs of energy are compared in case III for different scenarios. It is seen that system-wide control implementation improves the load shapes and load factor with or without the presence of DERs. It is also found that the interactions with the bulk power system prices are predominantly due to the deployment of DERs dispersed in the system, and the reduction in the bulk system LMPs can be attributed to reduction in active power demand due to DER deployment. The application of the formulations in an islanded operation of the distribution feeders has been studied in case IV. The operation of the distributed energy storage devices in meeting the unserved load during an outage scenario is also evident. Test case V describes the results of integrating the control algorithm on the LSSS test system modeled in a PSCAD.

Chapter 5

CONCLUSIONS, RECOMMENDATIONS AND FUTURE WORK

5.1 Conclusions

Several electricity market operators have in recent times been working on the issue of integration of energy storage to provide regulation of their ancillary service markets [21]. Increased deployment of distributed assets in distribution systems is an expected phenomenon in the near future. The work done in this dissertation seeks to solve some of the existing and potential problems encountered in distribution system operations with distributed assets. The work shown here also develops a model for extending time-of-day pricing to distribution circuits. A distribution locational marginal pricing formulation has been developed using an AC sensitivity-based approach. The potential import of real-time prices in distribution feeders and DLMP aided control for distribution management systems can be evaluated using the techniques and test cases implemented in this work. The Jacobian-based sensitivity analysis developed in this dissertation provides for a correction factor over other similar approaches developed in literature, and is seen to provide better results in the computation of the DLMP signal.

A multiobjective optimization algorithm has also been developed that optimizes the use of distributed energy storage in power distribution systems. The MOP based control loop developed in this report is found to be robust in computing Pareto optimal solutions that reflect the best possible system operating point for given system conditions. The results show the applicability of the NBI method for the control algorithm under consideration. The control formulation is also

flexible enough to feature extrinsic objectives that need to be accommodated, while computing the optimal operating point for a given node in the distribution system. Based on the need for simplicity in terms of implementation, and also in view of system operating conditions, the MOP objectives can be varied and prioritized. Based on the computational rigor, it is recommended to use a time step of 15 min on the control formulation, while choosing a higher resolution for the LMP and DLMP calculation.

Table 5.1 Major contributions of this research work

PRIMARY CONTRIBUTIONS	SECONDARY CONTRIBUTIONS
• A new approach to power distribution system pricing, via the distribution locational marginal pricing formulation.	• A novel method for Jacobian-based sensitivity analysis, for calculation of AC sensitivity factors in primary distribution systems.
• Formulation of energy storage utilization as a multiobjective optimization problem.	• Use of novel systems theoretic concepts in developing a mathematical robust solution algorithm for the multiobjective optimization problem.
• Demonstration of applications of the proposed methods in large scale distribution systems and a suggested framework for implementation in distribution system operations.	• Demonstration of the application of parallel computing in simulating distributed operations in power systems.

5.2 Recommendations

The suggested approach for implementation of the energy management control algorithm has already been presented in Figure 3.5. Optimal power flow and LMP calculations are standard operations in a market environment and EMS. The extension of the LMPs to distribution system will necessitate the need for performing a power flow algorithm of the distribution circuit to compute DLMPs. This operation is generally performed at the distribution substation, and is part of the DMS operational structure. The control of the system-wide distributed storage assets though, need to be implemented in a distributed fashion at each controlled load point. To facilitate decentralized (or distributed) control the need for added communication capability arises. Dedicated software capability at each controlled load point is another requirement. This can be implemented via microprocessors and distributed across the power system. These are potential areas for improvement over current operational practices observed in contemporary distribution engineering.

In all the above mentioned aspects, the recommended approach for implementation ties in with some of the objectives of the Smart Grid initiative. The work presented in this dissertation also provides systems theoretic tools and techniques for practical application of solid state controlled devices (e.g., SSTs) in distribution systems, as being researched under the aegis of the FREEDM systems center. The major contributions of this research work are listed in Table 5.1.

5.3 Future Work

The work presented in this dissertation provides a formulation for DLMPs in distribution systems and a multiobjective control algorithm for utilization of distributed assets. Some of the issues that can be tackled in future research work in this area include the following:

i. Expansion of the DLMP formulation to three-phase detail, with the computational ability to compute DLMPs on single phase and three phase laterals.

ii. Develop three phase sensitivity analysis for power distribution systems to compute the distribution factors used in the DLMP formulation.

iii. Improvement of the problem statement in the multiobjective optimization to include additional objectives, system conditions and constraints.

iv. Improvement of the solution algorithm to an operator selective procedure.

v. Demonstrate the application of the formulations in a DMS and SCADA environment.

vi. Implement the formulations on the FREEDM green hub test system.

REFERENCES

[1] E. Sims, "Distribution-system operation and maintenance," *Electronics and Power*, v. 12, No. 2, 1966, pp. 51-54.

[2] I. Roytelman, B. Wee, R. Lugtu, "Volt / VAr control algorithm for modern distribution management system," *IEEE Trans. on Power Systems*, v. 10, No. 3, 1995, pp. 1454-1460.

[3] P. Vovos, A. Kiprakis, A. Wallace, G. Harrison, "Centralized and distributed voltage control: Impact on distributed generation penetration," *IEEE Trans. on Power Systems*, v. 22, No. 1, 2007, pp. 476-483.

[4] P. Mahat, Z. Chen, B. Bak-Jensen, C. Bak, "A simple adaptive overcurrent protection of distribution systems with distributed generation," *IEEE Trans. on Smart Grid*, v. 2, No. 3, 2011, pp. 428-437.

[5] L. Comassetto, D. Bernardon, L. Canha, A. Abaide, "Software for automatic coordination of protection devices in distribution system," *IEEE Trans. on Power Delivery*, v. 23, No. 4, 2008, pp. 2241-2246.

[6] J. Meeuwsen, W. Kling, W. Ploem, "The influence of protection system failures and preventive maintenance on protection systems in distribution systems," *IEEE Trans. on Power Delivery*, v.12, No.1, 1997, pp. 125-133.

[7] R. Gupta, A. Ghosh, A. Joshi, "Performance comparison of VSC-based shunt and series compensators used for load voltage control in distribution systems," *IEEE Trans. on Power Delivery*, v. 26, No. 1, 2011, pp. 268-278.

[8] S. Choi, B. Li, D. Vilathgamuwa, "Dynamic voltage restoration with minimum energy injection," *IEEE Trans. on Power Systems*, v. 15, No. 1, 2000, pp. 51-57.

[9] J. Paserba, D. Leonard, N. Miller, S. Naumann, M. Lauby, F. Sener, "Coordination of a distribution level continuously controlled compensation device with existing substation equipment for long term VAr management," *IEEE Trans. on Power Delivery*, v. 9, No. 2, 1994, pp. 1034-1040.

[10] J. Allmeling, "A control structure for fast harmonics compensation in active filters," *IEEE Trans. on Power Electronics*, v. 19, No. 2, 2004, pp. 508- 514.

[11] W. Cassel, “Distribution management systems: functions and payback,” *IEEE Trans. on Power Systems*, v. 8, No. 3, 1993, pp. 796-801.

[12] I. Roytelman, V. Ganesan, "Coordinated local and centralized control in distribution management systems," *IEEE Trans. on Power Delivery*, v. 15, No. 2, 2000, pp. 718-724.

[13] N. Singh, E. Koliokys, H. Feldmann, R. Kussel, R. Chrustowski, C. Jaborowski, " Power system modeling and analysis in a mixed energy management and distribution management system," *IEEE Trans. on Power Systems*, v. 13, No. 3, 1998, pp. 1143-1149.

[14] L. Ochoa, G. Harrison, "Minimizing energy losses: optimal accommodation and smart operation of renewable distributed generation," *IEEE Trans. on Power Systems*, v. 26, No. 1, 2011, pp. 198-205.

[15] C. Su, D. Kirschen, "Quantifying the effect of demand response on electricity markets," *IEEE Trans. on Power Systems*, v. 24, No. 3, 2009, pp. 1199-1207.

[16] B. Daryanian, R. Bohn, R. Tabors, "Optimal demand-side response to electricity spot prices for storage-type customers," *IEEE Trans. on Power Systems*, v. 4, No. 3, 1989, 897-903.

[17] J. Short, D. Infield, L. Freris, "Stabilization of grid frequency through dynamic demand control," *IEEE Trans. on Power Systems*, v. 22, No. 3, 2007, 1284-1293.

[18] A. Botterud, M. Ilic, I. Wangensteen, "Optimal investments in power generation under centralized and decentralized decision making," *IEEE Trans. on Power Systems*, v. 20, No. 1, 2005, 254-263.

[19] C. Gellings *et al.*, "Integrating demand-side management into utility planning," *IEEE Trans. on Power Systems*, v. 1, No. 3, 1986, pp. 81-87.

[20] J. Thalman, J. Carruthers, "Interconnecting and integrating DG into the distribution system," *CEC IEPR Committee Workshop*, 2011, available at: http://www.energy.ca.gov/2011_energypolicy/documents/2011-06-22_workshop/presentations/02_PGandE_0622_CEC_DG_Presentation_pge.pdf

[21] California Independent System Operator, "Integration of energy storage technology white paper – identification of issues and proposed solutions," 2008, available at: http://www.caiso.com/1fd5/1fd56f931140.pdf

[22] A. Ter-Gazarian, N. Kagan, "Design model for electrical distribution systems considering renewable, conventional and energy storage units," *IEE*

Proc. on Generation, Transmission, and Distribution, v. 139, No. 6, 1992, pp. 499-504.

[23] United States Department of Energy, "Smart Grid: an introduction," Office of Electricity Delivery and Energy Reliability, Washington DC, 2008.

[24] S. Bhattacharya *et al.*, "Design and development of generation-I silicon based solid state transformer," *Proc. 25th Annual IEEE Applied Power Electronics Conference and Exposition*, 2010, pp. 1666 -1673.

[25] G. Heydt *et al.*, "Pricing and control in the next generation power distribution system," (*Submitted*) *IEEE Trans. on Smart Grid*, 2011.

[26] N. Okada, "Verification of control methods for a loop distribution system using loop power flow controller," *Proc. IEEE PES Power Systems Conference and Exposition,* 2006, pp. 2116-2123.

[27] A. Bracale, R. Angelino, G. Carpinelli, D. Lauria, M. Mangione, D. Proto, "Centralized control of dispersed generators providing ancillary services in distribution networks," *Proc. 44th Universities Power Engineering Conference*, 2009, pp. 1-5.

[28] M. Lind, A. Saleem, "Reasoning about control situations in power systems," *Proc. Conference on Intelligent Systems Applications to Power Systems,* 2009, pp. 1-6.

[29] F. Viawan, "Steady state operation and control of power distribution systems in the presence of distributed generation," Ph.D. Thesis, Chalmers University of Technology, Göteborg, Sweden, 2006.

[30] K. Schneider, D. Chassin, Y. Chen, J. Fuller, "Distribution power flow for smart grid technologies," *Proc. Power Systems Conference and Exposition*, 2009, pp. 1-7.

[31] R. Brown, "Impact of Smart Grid on distribution system design," *Proc. IEEE Power and Energy Society General Meeting*, 2008, pp. 1-4.

[32] X. Mamo, M. McGranaghan, R. Dugan, J. Maire, O. Devaux, "A roadmap for developing real time distribution system simulation tools for the smart grid," *Proc. IET Conference on Smart Grid for Distribution,* 2008, pp. 1-7.

[33] A. McEachern, W. Grady, W. Moncrief, G. Heydt, M. McGranaghan, "Revenue and harmonics: an evaluation of some proposed rate structures," *IEEE Trans. On Power Systems*, v. 10, No. 1, 1995, pp. 474-482.

[34] Q. Gao, J. Yu, P. Chong, P. So, E. Gunawan, "Solutions for the “silent node” problem in an automatic meter reading system using power-line communications," *IEEE. Trans. On Power Delivery*, v. 23, No. 1, 2008, pp. 150-156.

[35] A. Mazer, *The California Experience: Electric Power Planning for Regulated and Deregulated Markets*, IEEE book chapter, pp. 278-290, 2007.

[36] R. Ferrero, S. Shahidehpour, “Short-term power purchases considering uncertain prices,” *IEE Procs. On Generation, Transmission and Distribution*, v. 144, No. 5, 1997, pp. 423-428.

[37] R. Christie, B. Wollenberg, I. Wangensteen, “Transmission management in the deregulated environment,” *Procs. of the IEEE*, v. 88, No. 2, 2000, pp. 170-195.

[38] D. Sun, “Application of OPF in deregulated electricity market, *IEEE Trans. on Power Systems*, v. 12, No. 1, 1997, pp. 448-449.

[39] F. Schweppe, B. Daryanian, R. Tabors, “Algorithms for a spot price responding residential load controller,” *IEEE Trans. on Power Systems*, v. 4, No. 2, 1989, pp. 507-516.

[40] California Independent System Operator, Open Access Same-Time Information System, available at:
http://oasis.caiso.com

[41] F. Li, R. Bo, “Congestion and price prediction under load variation,” *IEEE Trans. on Power Systems*, v. 24, No. 2, 2009, pp. 911-922.

[42] T. Orfanogianni, G. Gross, “A general formulation for LMP evaluation,” *IEEE Trans. on Power Systems*, v. 22, No. 3, 2007, 1163-1173.

[43] J. Morales, A. Conejo, J. Perez-Ruiz, “Simulation of the impact of wind production on locational marginal prices,” *IEEE Trans. on Power Systems*, v. 26, No. 2, 2011, pp. 820-828.

[44] D. Cheverez-Gonzalez, C. DeMarco, “Admissible locational marginal prices via laplacian structure in network constraints,” *IEEE Trans. On Power Systems*, v. 24, No. 1, 2009, pp. 125-133.

[45] Y. Fu, Z. Li, “Different models and properties on LMP calculations,” *Proc. IEEE Power Engineering Society General Meeting*, 2006, pp. 1-8.

[46] I. Leevongwat, P. Rastgoufard, E. Kaminsky, "Status of deregulation and locational marginal pricing in power markets," *Proc. 40th Southeastern Symposium on System Theory*, 2009, pp. 193-197.

[47] T. Overbye, X. Cheng, Y. Sun, "A comparison of the AC and DC power flow models for LMP calculations," *Proc. 37th Annual Hawaii International Conference on System Sciences*, 2004, pp. 1-8.

[48] L. Murphy, R. Kaye, F. Wu, "Distributed spot pricing in radial distribution systems," *IEEE Trans. on Power Systems*, v. 9, No. 1, 1994, pp. 311-317.

[49] P. Sotkiewicz, J. Vignolo, "Towards a cost causation-based tariff for distribution networks with DG," *IEEE Trans. on Power Systems*, v. 22, No. 2, 2007, pp. 1051-1060.

[50] J. Lima, J. Noronha, H. Arango, P. Santos, "Distribution pricing based on yardstick regulation," *IEEE Trans. on Power Systems*, v. 17, No. 1, 2002, pp. 198-204.

[51] P. M. Sotkiewicz, J. M. Vignolo, "Nodal pricing for distribution networks : Efficient pricing for efficiency enhancing DG," *IEEE Trans. on Power Systems*, v. 21, No. 2, 2006, pp. 1013-1014.

[52] R. K. Singh, S. K. Goswami, "Optimum allocation of distributed generations based on nodal pricing for profit, loss reduction, and voltage improvement including voltage rise issue," *International Journal of Electrical Power Energy Systems*, v. 32, 2010, pp. 637–644.

[53] K. Shaloudegi, N. Madinehi, S. H. Hosseinian, H. A. Abyaneh, "A novel policy for locational marginal price calculation in distribution systems based on loss reduction allocation using game theory," *IEEE Trans. on Power Systems*, v. 27, No. 2, 2012, pp. 811-820.

[54] P. M. DeOliveira-DeJesus, M. T. Poncedeleao, J. M. Yusta, H. M. Khodr, A. J. Urdaneta, "Uniform marginal pricing for renumeration of distribution networks," *IEEE Trans. on Power Systems*, v. 20, No. 3, 2005, pp. 1302-1310.

[55] C. Gu, J. Wu, F. Li, "Reliability-based distribution network pricing," *IEEE Trans. on Power Systems*, v. 1, No. 99, 2012, pp. 1-8.

[56] S. Grillo, M. Marinelli, S. Massucco, F. Silvestro, "Optimal management strategy of a battery-based storage system to improve renewable energy integration in distribution networks," *IEEE Trans. on Smart Grid*, v. 3, No. 2, 2012, pp. 950-958.

[57] M. Singh, V. Khadkikar, A. Chandra, R. K. Varma, "Grid interconnection of renewable energy sources at the distribution level with power-quality improvement features," *IEEE Trans. on Power Delivery*, v. 26, No. 1, 2011, pp. 307-315.

[58] A. Pregelj, M. Begovic, A. Rohatgi, "Recloser allocation for improved reliability of DG-enhanced distribution networks," *IEEE Trans. Power Syst.*, v. 21, No. 3, 2006, pp. 1442-1449.

[59] Y. M. Atwa, E. F. El-Saadany, "Reliability evaluation for distribution system with renewable distributed generation during islanded mode of operation," *IEEE Trans. on Power Systems*, v. 24, No. 2, 2009, pp.572-581.

[60] Y. M. Atwa, E. F. El-Saadany, A. C. Guise, "Supply adequacy assessment of distribution system including wind-based DG during different modes of operation," *IEEE Trans. Power Systems*, v. 25, No. 1, 2010, pp. 78–86.

[61] Y. M. Atwa, E. F. El-Saadany, M. M. A. Salama, R. Seethapathy, M. Assam, S. Conti, "Adequacy evaluation of distribution system including wind/solar DG during different modes of operation," *IEEE Trans. on Power Systems*, v. 26, No. 4, 2011, pp.1945-1952.

[62] Y. Xu, C. Singh, "Adequacy and economy analysis of distribution systems integrated with electric energy storage and renewable energy resources," *IEEE Trans. on Power Systems*, v. 1, No. 99, 2012, pp. 1-10.

[63] Y. M. Atwa, E. F. El-Saadany, M. M. A. Salama, R. Seethapathy, "Optimal renewable resources mix for distribution system energy loss minimization," *IEEE Trans. on Power Systems*, v. 25, No. 1, 2010, pp.360-370.

[64] L. F. Ochoa, A. Keane, G. P. Harrison, "Minimizing the reactive support for distributed generation: Enhanced passive operation and smart distribution networks," *IEEE Trans. on Power Systems*, v. 26, No. 4, 2011, pp.2134-2142.

[65] A. Gabash, P. Li, "Active-reactive optimal power flow in distribution networks with embedded generation and battery storage," *IEEE Trans. on Power Systems*, v. 1, No. 99, 2012, pp. 1-10.

[66] C. A. Hill, M. C. Such, D. Chen, J. Gonzalez, W. M. Grady, "Battery energy storage for enabling integration of distributed solar power generation," *IEEE Trans. on Smart Grid*, v. 1, No. 99, 2012, pp. 1-8.

[67] X. Liu, A. Aichhorn, L. Liu, H. Li, "Coordinated control of distributed energy storage system with tap changer transformers for voltage rise mitigation under high photovoltaic penetration," *IEEE Trans. on Smart Grid*, v. 1, No. 99, 2012, pp. 1-8.

[68] Y. M. Atwa, E. F. El-Saadany, "Optimal allocation of ESS in distribution systems with a high penetration of wind energy," *IEEE Trans. on Power Systems*, v. 25, No. 4, 2010, pp.1815-1822.

[69] F. A. Chacra, P. Bastard, G. Fleury, R. Clavreul, "Impact of energy storage costs on economical performance in a distribution substation," *IEEE Trans. on Power Systems*, v. 20, No. 2, 2005, pp. 684- 691.

[70] J Branke, K. Deb, K. Miettinen, R. Slowinski, *Multiobjective Optimization: Interactive and Evolutionary Approaches*, Berlin, Germany: Springer-Verlag, 2008.

[71] K. M. Miettinen, *Nonlinear Multiobjective Optimization*, Boston, MA: Kluwer, 1999.

[72] W. Cao, M. Ying, "Similarity-based supervisory control of discrete-event systems," *IEEE Trans. on Automatic Control*, v. 51, No. 2, 2006, pp. 325-330.

[73] J. Lin, "Multiple-objective problems: Pareto-optimal solutions by the method of proper equality constraints," *IEEE Trans. on Automatic Control*, v. AC-21, No. 5, 1976, pp. 641-650.

[74] W. Schmitendorf, G. Leitmann, "A simple derivation of necessary conditions for Pareto optimality," *IEEE Trans. on Automatic Control*, v. 19, No. 5, 1974, pp. 601-602.

[75] A. Ahuja, S. Das, A. Pahwa, "An AIS-ACO hybrid approach for multi-objective distribution system reconfiguration," *IEEE Trans. on Power Systems*, v. 22, No. 3, 2007, pp. 1101-1111.

[76] J. Hazra, A. Sinha, "Congestion management using multiobjective particle swarm optimization," *IEEE Trans. on Power Systems*, v. 22, No. 4, 2007, pp. 1726-1734.

[77] R. Lasseter, "Dynamic distribution using (DER) distributed energy resources," *Proc. IEEE Power Engineering Society Transmission and Distribution Conference and Exhibition*, 2006, pp. 932-934.

[78] H. Nikkhajoei, R. Lasseter, "Microgrid protection," *Proc. IEEE Power Engineering Society General Meeting*, 2007, pp. 1-6.

[79] M. Lehtonen *et al.*, "Distribution energy management in the environment of de-regulated electricity market," *Proc. Energy Management and Power Delivery*, v. 2, 1995, pp. 516-521.

[80] I. Das, J. Dennis, "Normal-boundary intersection: an alternate method for generating Pareto optimal points in multicriteria optimization problem," *Institute for Computer Applications in Science and Engineering (ICASE) report*, 1996.

[81] J. Branke, K. Deb, K. Miettinen, R. Slowinski, *Multiobjective Optimization: Interactive and Evolutionary Approaches*, Berlin Germany: Springer Verlag, 2008.

[82] G. Heydt, *Computer Analysis Methods for Power Systems*, Scottsdale AZ: Stars in a Circle Publications, 1996.

[83] A. J. Wood, B. F. Wollenberg, *Power Generation, Operation and Control*, New York NY: John Wiley and Sons Inc., 1996.

[84] C. Y. Evrenosoglu, A. Abur, "Effects of measurement and parameter uncertainties on the power transfer distribution factors," *Procs. of International Conference on Probabilistic Methods Applied to Power Systems*, 2004, pp. 608-611.

[85] A. Kumar, S. C. Srivastava, "AC power transfer distribution factors for allocating power transactions in deregulated markets," *IEEE Power Engineering Review*, v. 22, No. 7, 2002, pp. 42-43.

[86] IEEE Std. 519-1992, "IEEE recommended practices and requirements for harmonic control in electric power systems," Piscataway, NJ, 1992.

[87] R. Delgado, "Load management - a planner's view," *IEEE Trans. on Power Apparatus and Systems*, v. PAS-102, No. 6, 1983, pp. 1812-1813.

[88] S. Stefanov, *Separable Programming: Theory and Methods*, Boston, MA: Kluwer, 2001.

[89] R. Zimmerman, C. Murillo-Sánchez, R. Thomas, "MATPOWER steady-state operations, planning and analysis tools for power systems research and education," *IEEE Trans. on Power Systems*, v. 26, No. 1, 2011, pp. 12-19.

[90] R. Billinton, S. Jonnavithula, "A test system for teaching overall power system reliability assessment," *IEEE Trans. on Power Systems*, v. 11, No. 4, 1996, pp. 1670-1676.

[91] R. Billinton *et al.*, "A reliability test system for education purposes – basic data," *IEEE Trans. on Power Systems*, v. 4, No. 3, 1989, pp. 1238-1244.

[92] National Renewable Energy Laboratory (NREL), Technology Analysis Models and Tools, available at:
http://www.nrel.gov/analysis/models_tools.html

[93] ISO New England, Markets, available at:
www.iso-ne.com/markets/index.html

[94] Electric Reliability Council of Texas (ERCOT), Load Profiling Market Information, available at:
http://www.ercot.com/mktinfo/loadprofile/

[95] Distribution Test Feeders, IEEE Distribution Systems Analysis Subcommittee, available at:
http://ewh.ieee.org/soc/pes/dsacom/testfeeders/index.html

[96] High Performance Computing (HPC) Initiative, Advanced Computing Center at Arizona State University, available at:
http://a2c2.asu.edu/

APPENDIX A

SUPPLEMENTAL TEST DATA

TABLE A.1 Feeder characteristics for test case I

Conductor characteristics	2/0 Al ACSR 6 strands Al, 1 layer, 270 A max current magnitude
Impedance	0.896 + j 0.7743 ohm/mile
Length of each feeder segment	2 miles

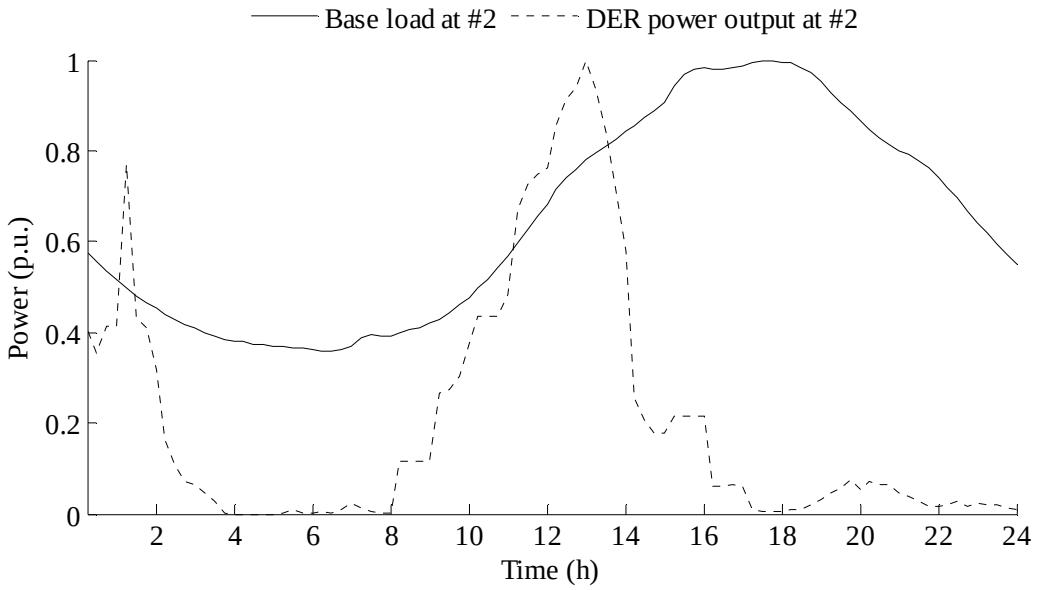

Figure A.1 Load and renewable power output data for test case I at node #2

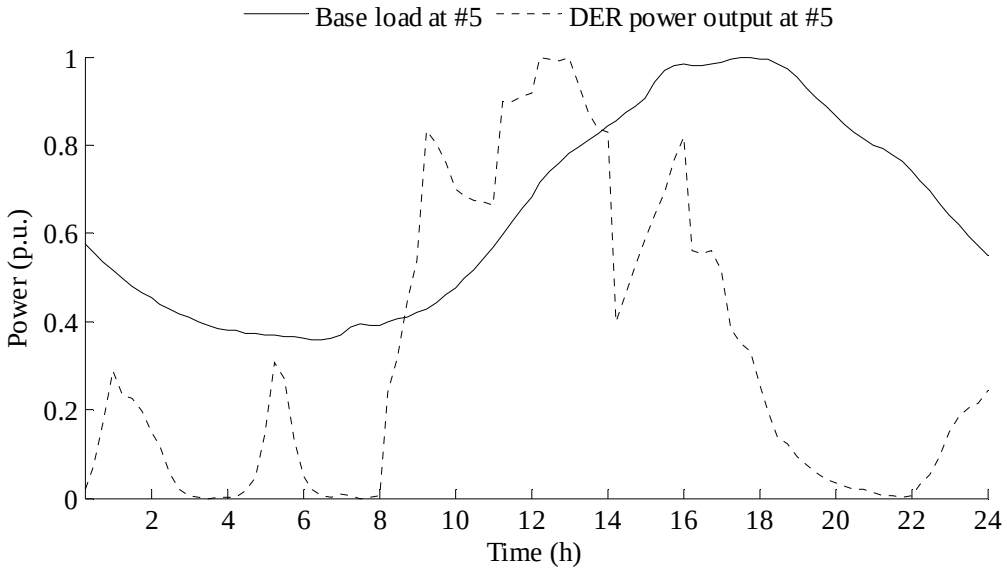

Figure A.2 Load and renewable power output data for test case I at node #5

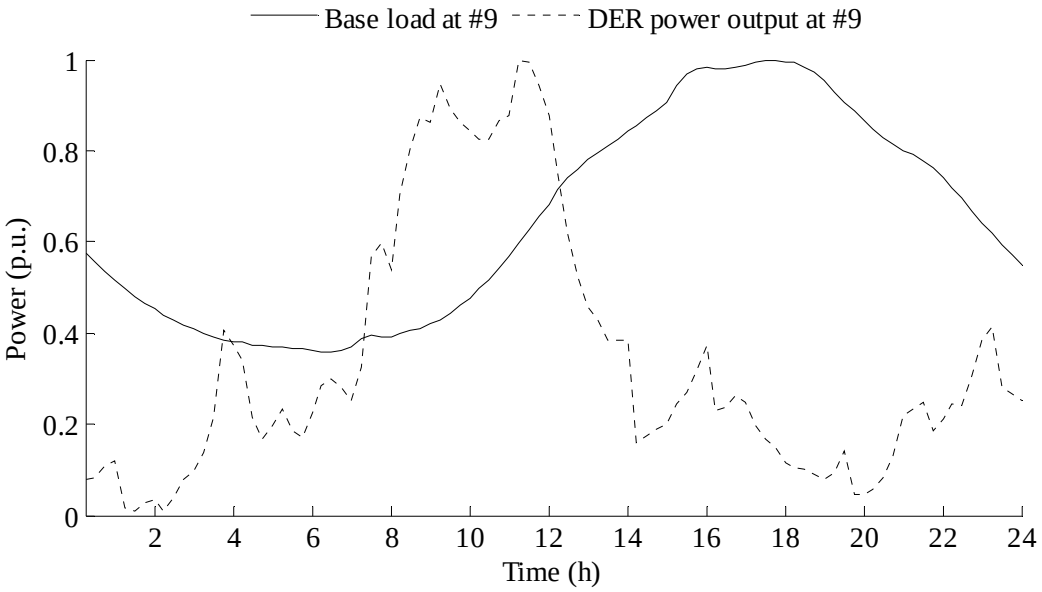

Fig. A.3 Load and renewable power output data for test case I at node #9

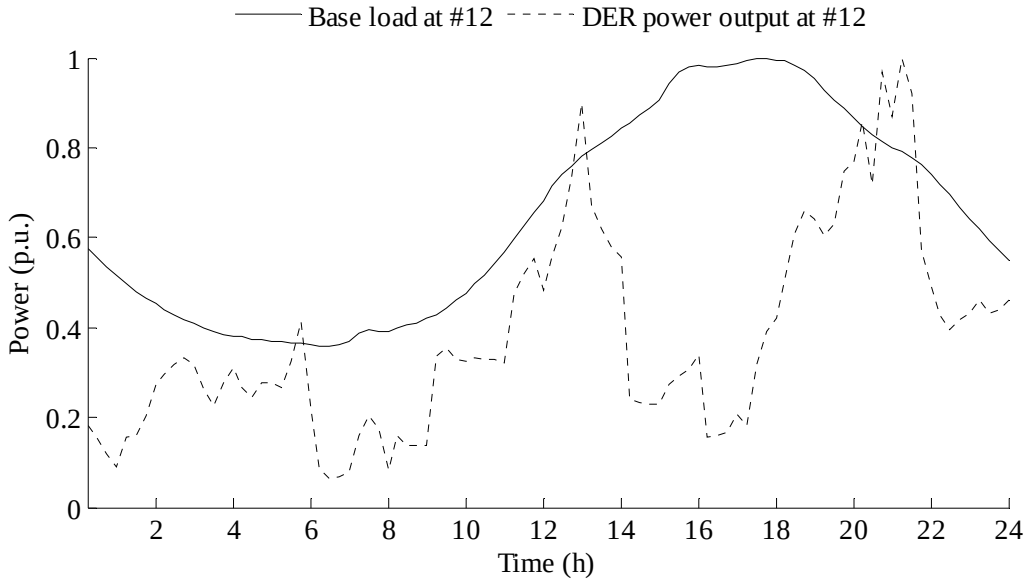

Fig. A.4 Load and renewable power output data for test case I at node #12

(all terms shown in Figures A.1-A4 are shown in p.u. on their individual ratings)

Table A.2 (a) Bus data of Bus #3 distribution system used in test cases II-V

Bus	Bus type [1:PQ 2:PV 3:RF 4:IS]	*P* demand (MW)	*Q* demand (MW)	*Gs* (ohms)	*Bs* (ohms)	Bus area	Voltage magnitude (p.u.)	Voltage angle (deg)	Base voltage (kV)	Loss zone	Vmax (p.u.)	Vmin (p.u.)
1	1	0.0000	0.0000	0.0000	0.0000	1	1	0.0000	11.0000	1	1.05	0.9700
2	1	0.0000	0.0000	0.0000	0.0000	1	1	0.0000	0.4150	1	1.05	0.9700
3	1	0.0000	0.0000	0.0000	0.0000	1	1	0.0000	0.4150	1	1.05	0.9700
4	1	0.0000	0.0000	0.0000	0.0000	1	1	0.0000	11.0000	1	1.05	0.9700
5	1	0.0000	0.0000	0.0000	0.0000	1	1	0.0000	0.4150	1	1.05	0.9700
6	1	0.0000	0.0000	0.0000	0.0000	1	1	0.0000	0.4150	1	1.05	0.9700
7	1	0.0000	0.0000	0.0000	0.0000	1	1	0.0000	11.0000	1	1.05	0.9700
8	1	0.0000	0.0000	0.0000	0.0000	1	1	0.0000	0.4150	1	1.05	0.9700
9	1	0.0000	0.0000	0.0000	0.0000	1	1	0.0000	11.0000	1	1.05	0.9700
10	1	0.0000	0.0000	0.0000	0.0000	1	1	0.0000	0.4150	1	1.05	0.9700
11	1	0.0000	0.0000	0.0000	0.0000	1	1	0.0000	11.0000	1	1.05	0.9700
12	1	0.0000	0.0000	0.0000	0.0000	1	1	0.0000	0.4150	1	1.05	0.9700
13	1	0.0000	0.0000	0.0000	0.0000	2	1	0.0000	11.0000	1	1.05	0.9700
14	1	0.0000	0.0000	0.0000	0.0000	2	1	0.0000	11.0000	1	1.05	0.9700
15	1	0.0000	0.0000	0.0000	0.0000	2	1	0.0000	11.0000	1	1.05	0.9700
16	1	0.0000	0.0000	0.0000	0.0000	2	1	0.0000	11.0000	1	1.05	0.9700
17	1	0.0000	0.0000	0.0000	0.0000	2	1	0.0000	11.0000	1	1.05	0.9700
18	1	0.0000	0.0000	0.0000	0.0000	2	1	0.0000	11.0000	1	1.05	0.9700
19	1	0.0000	0.0000	0.0000	0.0000	3	1	0.0000	11.0000	1	1.05	0.9700
20	1	0.0000	0.0000	0.0000	0.0000	3	1	0.0000	0.4150	1	1.05	0.9700
21	1	0.0000	0.0000	0.0000	0.0000	3	1	0.0000	0.4150	1	1.05	0.9700
22	1	0.0000	0.0000	0.0000	0.0000	3	1	0.0000	11.0000	1	1.05	0.9700

Table A.2 (b) Bus data of Bus #3 distribution system used in test cases II-V

Bus	Bus type [1:PQ 2:PV 3:RF 4:IS]	*P* demand (MW)	*Q* demand (MW)	*Gs* (ohms)	*Bs* (ohms)	Bus area	Voltage magnitude (p.u.)	Voltage angle (deg)	Base voltage (kV)	Loss zone	Vmax (p.u.)	Vmin (p.u.)
23	1	0.0000	0.0000	0.0000	0.0000	3	1	0.0000	0.4150	1	1.05	0.9700
24	1	0.0000	0.0000	0.0000	0.0000	3	1	0.0000	11.0000	1	1.05	0.9700
25	1	0.0000	0.0000	0.0000	0.0000	3	1	0.0000	0.4150	1	1.05	0.9700
26	1	0.0000	0.0000	0.0000	0.0000	3	1	0.0000	0.4150	1	1.05	0.9700
27	1	0.0000	0.0000	0.0000	0.0000	3	1	0.0000	11.0000	1	1.05	0.9700
28	1	0.0000	0.0000	0.0000	0.0000	3	1	0.0000	0.4150	1	1.05	0.9700
29	1	0.0000	0.0000	0.0000	0.0000	3	1	0.0000	11.0000	1	1.05	0.9700
30	1	0.0000	0.0000	0.0000	0.0000	3	1	0.0000	0.4150	1	1.05	0.9700
31	1	0.0000	0.0000	0.0000	0.0000	4	1	0.0000	11.0000	1	1.05	0.9700
32	1	0.0000	0.0000	0.0000	0.0000	4	1	0.0000	0.4150	1	1.05	0.9700
33	1	0.0000	0.0000	0.0000	0.0000	4	1	0.0000	0.4150	1	1.05	0.9700
34	1	0.0000	0.0000	0.0000	0.0000	4	1	0.0000	11.0000	1	1.05	0.9700
35	1	0.0000	0.0000	0.0000	0.0000	4	1	0.0000	0.4150	1	1.05	0.9700
36	1	0.0000	0.0000	0.0000	0.0000	4	1	0.0000	11.0000	1	1.05	0.9700
37	1	0.0000	0.0000	0.0000	0.0000	4	1	0.0000	0.4150	1	1.05	0.9700
38	1	0.0000	0.0000	0.0000	0.0000	4	1	0.0000	0.4150	1	1.05	0.9700
39	1	0.0000	0.0000	0.0000	0.0000	4	1	0.0000	11.0000	1	1.05	0.9700
40	1	0.0000	0.0000	0.0000	0.0000	4	1	0.0000	0.4150	1	1.05	0.9700
41	1	0.0000	0.0000	0.0000	0.0000	4	1	0.0000	11.0000	1	1.05	0.9700
42	1	0.0000	0.0000	0.0000	0.0000	4	1	0.0000	0.4150	1	1.05	0.9700
43	1	0.0000	0.0000	0.0000	0.0000	5	1	0.0000	11.0000	1	1.05	0.9700
44	1	0.0000	0.0000	0.0000	0.0000	5	1	0.0000	0.4150	1	1.05	0.9700

Table A.2 (c) Bus data of Bus #3 distribution system used in test cases II-V

Bus	Bus type [1:PQ 2:PV 3:RF 4:IS]	*P* demand (MW)	*Q* demand (MW)	*Gs* (ohms)	*Bs* (ohms)	Bus area	Voltage magnitude (p.u.)	Voltage angle (deg)	Base voltage (kV)	Loss zone	Vmax (p.u.)	Vmin (p.u.)
45	1	0.0000	0.0000	0.0000	0.0000	5	1	0.0000	0.4150	1	1.05	0.9700
46	1	0.0000	0.0000	0.0000	0.0000	5	1	0.0000	11.0000	1	1.05	0.9700
47	1	0.0000	0.0000	0.0000	0.0000	5	1	0.0000	0.4150	1	1.05	0.9700
48	1	0.0000	0.0000	0.0000	0.0000	5	1	0.0000	0.4150	1	1.05	0.9700
49	1	0.0000	0.0000	0.0000	0.0000	5	1	0.0000	11.0000	1	1.05	0.9700
50	1	0.0000	0.0000	0.0000	0.0000	5	1	0.0000	0.4150	1	1.05	0.9700
51	1	0.0000	0.0000	0.0000	0.0000	5	1	0.0000	11.0000	1	1.05	0.9700
52	1	0.0000	0.0000	0.0000	0.0000	5	1	0.0000	0.4150	1	1.05	0.9700
53	1	0.0000	0.0000	0.0000	0.0000	5	1	0.0000	11.0000	1	1.05	0.9700
54	1	0.0000	0.0000	0.0000	0.0000	5	1	0.0000	0.4150	1	1.05	0.9700
55	1	0.0000	0.0000	0.0000	0.0000	6	1	0.0000	11.0000	1	1.05	0.9700
56	1	0.0000	0.0000	0.0000	0.0000	6	1	0.0000	0.4150	1	1.05	0.9700
57	1	0.0000	0.0000	0.0000	0.0000	6	1	0.0000	0.4150	1	1.05	0.9700
58	1	0.0000	0.0000	0.0000	0.0000	6	1	0.0000	11.0000	1	1.05	0.9700
59	1	0.0000	0.0000	0.0000	0.0000	6	1	0.0000	0.4150	1	1.05	0.9700
60	1	0.0000	0.0000	0.0000	0.0000	6	1	0.0000	11.0000	1	1.05	0.9700
61	1	0.0000	0.0000	0.0000	0.0000	6	1	0.0000	0.4150	1	1.05	0.9700
62	1	0.0000	0.0000	0.0000	0.0000	6	1	0.0000	0.4150	1	1.05	0.9700
63	1	0.0000	0.0000	0.0000	0.0000	6	1	0.0000	11.0000	1	1.05	0.9700
64	1	0.0000	0.0000	0.0000	0.0000	6	1	0.0000	0.4150	1	1.05	0.9700
65	1	0.0000	0.0000	0.0000	0.0000	6	1	0.0000	0.4150	1	1.05	0.9700
66	1	0.0000	0.0000	0.0000	0.0000	7	1	0.0000	138.0000	1	1.05	0.9700

Table A.2 (d) Bus data of Bus #3 distribution system used in test cases II-V

Bus	Bus type [1:PQ 2:PV 3:RF 4:IS]	*P* demand (MW)	*Q* demand (MW)	*Gs* (ohms)	*Bs* (ohms)	Bus area	Voltage magnitude (p.u.)	Voltage angle (deg)	Base voltage (kV)	Loss zone	Vmax (p.u.)	Vmin (p.u.)
67	1	0.0000	0.0000	0.0000	0.0000	7	1	0.0000	138.0000	1	1.05	0.9700
68	1	0.0000	0.0000	0.0000	0.0000	7	1	0.0000	138.0000	1	1.05	0.9700
69	1	0.0000	0.0000	0.0000	0.0000	7	1	0.0000	138.0000	1	1.05	0.9700
70	1	0.0000	0.0000	0.0000	0.0000	7	1	0.0000	138.0000	1	1.05	0.9700
71	1	0.0000	0.0000	0.0000	0.0000	7	1	0.0000	138.0000	1	1.05	0.9700
72	1	0.0000	0.0000	0.0000	0.0000	8	1	0.0000	138.0000	1	1.05	0.9700
73	1	0.0000	0.0000	0.0000	0.0000	8	1	0.0000	138.0000	1	1.05	0.9700
74	1	0.0000	0.0000	0.0000	0.0000	8	1	0.0000	138.0000	1	1.05	0.9700
75	1	0.0000	0.0000	0.0000	0.0000	8	1	0.0000	138.0000	1	1.05	0.9700
76	1	0.0000	0.0000	0.0000	0.0000	8	1	0.0000	138.0000	1	1.05	0.9700
77	1	0.0000	0.0000	0.0000	0.0000	8	1	0.0000	138.0000	1	1.05	0.9700
78	1	0.0000	0.0000	0.0000	0.0000	9	1	0.0000	11.0000	1	1.05	0.9700
79	1	0.0000	0.0000	0.0000	0.0000	10	1	0.0000	33.0000	1	1.05	0.9700
80	3	0.0000	0.0000	0.0000	0.0000	11	1	0.0000	138.0000	1	1.05	0.9700
81	1	0.0000	0.0000	0.0000	0.0000	9	1	0.0000	11.0000	1	1.05	0.9700
82	1	0.0000	0.0000	0.0000	0.0000	10	1	0.0000	33.0000	1	1.05	0.9700
83	1	0.0000	0.0000	0.0000	0.0000	9	1	0.0000	11.0000	1	1.05	0.9700
84	1	0.0000	0.0000	0.0000	0.0000	10	1	0.0000	33.0000	1	1.05	0.9700

Table A.3 (a) Branch data of Bus #3 distribution system used in test cases II-V

From bus	To bus	Feeder section	Feeder type	Length (mi)	*R* (Ω/mi)	*X* (Ω /mi)	*R* (Ω)	*X* (Ω)	kV Base	MVA Base	*R* (p.u.)	*X* (p.u.)
1	2	1	1	0.3728	0.1397	0.4120	0.0521	0.1536	11	100	0.0430	0.1269
1	3	2	1	0.3728	0.1397	0.4120	0.0521	0.1536	11	100	0.0430	0.1269
1	4	3	1	0.3728	0.1397	0.4120	0.0521	0.1536	11	100	0.0430	0.1269
4	5	4	2	0.4971	0.1397	0.4120	0.0694	0.2048	11	100	0.0574	0.1693
4	6	5	3	0.5593	0.1397	0.4120	0.0781	0.2304	11	100	0.0646	0.1904
4	7	6	3	0.5593	0.1397	0.4120	0.0781	0.2304	11	100	0.0646	0.1904
7	8	7	1	0.3728	0.1397	0.4120	0.0521	0.1536	11	100	0.0430	0.1269
7	9	8	2	0.4971	0.1397	0.4120	0.0694	0.2048	11	100	0.0574	0.1693
9	10	9	2	0.4971	0.1397	0.4120	0.0694	0.2048	11	100	0.0574	0.1693
9	11	10	3	0.5593	0.1397	0.4120	0.0781	0.2304	11	100	0.0646	0.1904
11	12	11	1	0.3728	0.1397	0.4120	0.0521	0.1536	11	100	0.0430	0.1269
11	78	12	1	0.3728	0.1397	0.4120	0.0521	0.1536	11	100	0.0430	0.1269
13	14	13	2	0.4971	0.1397	0.4120	0.0694	0.2048	11	100	0.0574	0.1693
13	15	14	3	0.5593	0.1397	0.4120	0.0781	0.2304	11	100	0.0646	0.1904
15	16	15	1	0.3728	0.1397	0.4120	0.0521	0.1536	11	100	0.0430	0.1269
15	17	16	2	0.4971	0.1397	0.4120	0.0694	0.2048	11	100	0.0574	0.1693
17	18	17	3	0.5593	0.1397	0.4120	0.0781	0.2304	11	100	0.0646	0.1904
17	78	18	3	0.5593	0.1397	0.4120	0.0781	0.2304	11	100	0.0646	0.1904
19	20	19	2	0.4971	0.1397	0.4120	0.0694	0.2048	11	100	0.0574	0.1693
19	21	20	2	0.4971	0.1397	0.4120	0.0694	0.2048	11	100	0.0574	0.1693

Table A.3 (b) Branch data of Bus #3 distribution system used in test cases II-V

From bus	To bus	Feeder section	Feeder type	Length (mi)	*R* (Ω/mi)	*X* (Ω /mi)	*R* (Ω)	*X* (Ω)	kV Base	MVA Base	*R* (p.u.)	*X* (p.u.)
19	22	21	1	0.3728	0.1397	0.4120	0.0521	0.1536	11	100	0.0430	0.1269
22	23	22	1	0.3728	0.1397	0.4120	0.0521	0.1536	11	100	0.0430	0.1269
22	24	23	3	0.5593	0.1397	0.4120	0.0781	0.2304	11	100	0.0646	0.1904
24	25	24	3	0.5593	0.1397	0.4120	0.0781	0.2304	11	100	0.0646	0.1904
24	26	25	2	0.4971	0.1397	0.4120	0.0694	0.2048	11	100	0.0574	0.1693
24	27	26	2	0.4971	0.1397	0.4120	0.0694	0.2048	11	100	0.0574	0.1693
27	28	27	3	0.5593	0.1397	0.4120	0.0781	0.2304	11	100	0.0646	0.1904
27	29	28	3	0.5593	0.1397	0.4120	0.0781	0.2304	11	100	0.0646	0.1904
29	30	29	1	0.3728	0.1397	0.4120	0.0521	0.1536	11	100	0.0430	0.1269
29	81	30	1	0.3728	0.1397	0.4120	0.0521	0.1536	11	100	0.0430	0.1269
31	32	31	1	0.3728	0.1397	0.4120	0.0521	0.1536	11	100	0.0430	0.1269
31	33	32	2	0.4971	0.1397	0.4120	0.0694	0.2048	11	100	0.0574	0.1693
31	34	33	3	0.5593	0.1397	0.4120	0.0781	0.2304	11	100	0.0646	0.1904
34	35	34	3	0.5593	0.1397	0.4120	0.0781	0.2304	11	100	0.0646	0.1904
34	36	35	2	0.4971	0.1397	0.4120	0.0694	0.2048	11	100	0.0574	0.1693
36	37	36	1	0.3728	0.1397	0.4120	0.0521	0.1536	11	100	0.0430	0.1269
36	38	37	2	0.4971	0.1397	0.4120	0.0694	0.2048	11	100	0.0574	0.1693
36	39	38	3	0.5593	0.1397	0.4120	0.0781	0.2304	11	100	0.0646	0.1904
39	40	39	3	0.5593	0.1397	0.4120	0.0781	0.2304	11	100	0.0646	0.1904
39	41	40	1	0.3728	0.1397	0.4120	0.0521	0.1536	11	100	0.0430	0.1269
41	42	41	2	0.4971	0.1397	0.4120	0.0694	0.2048	11	100	0.0574	0.1693
41	81	42	1	0.3728	0.1397	0.4120	0.0521	0.1536	11	100	0.0430	0.1269
43	44	43	1	0.3728	0.1397	0.4120	0.0521	0.1536	11	100	0.0430	0.1269
43	45	44	3	0.5593	0.1397	0.4120	0.0781	0.2304	11	100	0.0646	0.1904

Table A.3 (c) Branch data of Bus #3 distribution system used in test cases II-V

From bus	To bus	Feeder section	Feeder type	Length (mi)	*R* (Ω/mi)	*X* (Ω /mi)	*R* (Ω)	*X* (Ω)	kV Base	MVA Base	*R* (p.u.)	*X* (p.u.)
43	46	45	3	0.5593	0.1397	0.4120	0.0781	0.2304	11	100	0.0646	0.1904
46	47	46	2	0.4971	0.1397	0.4120	0.0694	0.2048	11	100	0.0574	0.1693
46	48	47	2	0.4971	0.1397	0.4120	0.0694	0.2048	11	100	0.0574	0.1693
46	49	48	1	0.3728	0.1397	0.4120	0.0521	0.1536	11	100	0.0430	0.1269
49	50	49	1	0.3728	0.1397	0.4120	0.0521	0.1536	11	100	0.0430	0.1269
49	51	50	1	0.3728	0.1397	0.4120	0.0521	0.1536	11	100	0.0430	0.1269
51	52	51	2	0.4971	0.1397	0.4120	0.0694	0.2048	11	100	0.0574	0.1693
51	53	52	3	0.5593	0.1397	0.4120	0.0781	0.2304	11	100	0.0646	0.1904
53	54	53	2	0.4971	0.1397	0.4120	0.0694	0.2048	11	100	0.0574	0.1693
53	83	54	3	0.5593	0.1397	0.4120	0.0781	0.2304	11	100	0.0646	0.1904
55	56	55	3	0.5593	0.1397	0.4120	0.0781	0.2304	11	100	0.0646	0.1904
55	57	56	1	0.3728	0.1397	0.4120	0.0521	0.1536	11	100	0.0430	0.1269
55	58	57	2	0.4971	0.1397	0.4120	0.0694	0.2048	11	100	0.0574	0.1693
58	59	58	1	0.3728	0.1397	0.4120	0.0521	0.1536	11	100	0.0430	0.1269
58	60	59	3	0.5593	0.1397	0.4120	0.0781	0.2304	11	100	0.0646	0.1904
60	61	60	2	0.4971	0.1397	0.4120	0.0694	0.2048	11	100	0.0574	0.1693
60	62	61	1	0.3728	0.1397	0.4120	0.0521	0.1536	11	100	0.0430	0.1269
60	63	62	2	0.4971	0.1397	0.4120	0.0694	0.2048	11	100	0.0574	0.1693
63	64	63	3	0.5593	0.1397	0.4120	0.0781	0.2304	11	100	0.0646	0.1904
63	65	64	1	0.3728	0.1397	0.4120	0.0521	0.1536	11	100	0.0430	0.1269
63	83	65	2	0.4971	0.1397	0.4120	0.0694	0.2048	11	100	0.0574	0.1693
66	67	66	3	0.5593	0.7000	3.7000	0.3915	2.0694	138	100	0.0021	0.0109
66	68	67	1	0.3728	0.7000	3.7000	0.2610	1.3794	138	100	0.0014	0.0072
68	69	68	2	0.4971	0.7000	3.7000	0.3480	1.8393	138	100	0.0018	0.0097

Table A.3 (d) Branch data of Bus #3 distribution system used in test cases II-V

From bus	To bus	Feeder section	Feeder type	Length (mi)	*R* (Ω/mi)	*X* (Ω /mi)	*R* (Ω)	*X* (Ω)	kV Base	MVA Base	*R* (p.u.)	*X* (p.u.)
68	70	69	3	0.5593	0.7000	3.7000	0.3915	2.0694	138	100	0.0021	0.0109
70	71	70	1	0.3728	0.7000	3.7000	0.2610	1.3794	138	100	0.0014	0.0072
70	80	71	2	0.4971	0.7000	3.7000	0.3480	1.8393	138	100	0.0018	0.0097
72	73	72	1	0.3728	0.7000	3.7000	0.2610	1.3794	138	100	0.0014	0.0072
72	74	73	3	0.5593	0.7000	3.7000	0.3915	2.0694	138	100	0.0021	0.0109
74	75	74	3	0.5593	0.7000	3.7000	0.3915	2.0694	138	100	0.0021	0.0109
74	76	75	1	0.3728	0.7000	3.7000	0.2610	1.3794	138	100	0.0014	0.0072
76	77	76	1	0.3728	0.7000	3.7000	0.2610	1.3794	138	100	0.0014	0.0072
76	80	77	2	0.4971	0.7000	3.7000	0.3480	1.8393	138	100	0.0018	0.0097
78	79	100	4	0.0000	0.0000	0.1210	0.0000	0.1210	33/11	100	0.0000	0.1000
78	79	100	4	0.0000	0.0000	0.1210	0.0000	0.1210	33/11	100	0.0000	0.1000
81	82	101	4	0.0000	0.0000	0.1210	0.0000	0.1210	33/11	100	0.0000	0.1000
81	82	101	4	0.0000	0.0000	0.1210	0.0000	0.1210	33/11	100	0.0000	0.1000
83	84	102	4	0.0000	0.0000	0.1210	0.0000	0.1210	33/11	100	0.0000	0.1000
83	84	102	4	0.0000	0.0000	0.1210	0.0000	0.1210	33/11	100	0.0000	0.1000
79	82	1000	5	1.0000	0.2590	1.0000	0.2590	1.0000	33	100	0.0238	0.0918
79	82	1001	5	1.0000	0.2590	1.0000	0.2590	1.0000	33	100	0.0238	0.0918
79	84	1002	5	1.0000	0.2590	1.0000	0.2590	1.0000	33	100	0.0238	0.0918
82	84	1003	5	1.0000	0.2590	1.0000	0.2590	1.0000	33	100	0.0238	0.0918
82	80	10000	6	0.0000	0.0000	1.0890	0.0000	1.0890	138/33	100	0.0000	0.1000
82	80	10000	6	0.0000	0.0000	1.0890	0.0000	1.0890	138/33	100	0.0000	0.1000

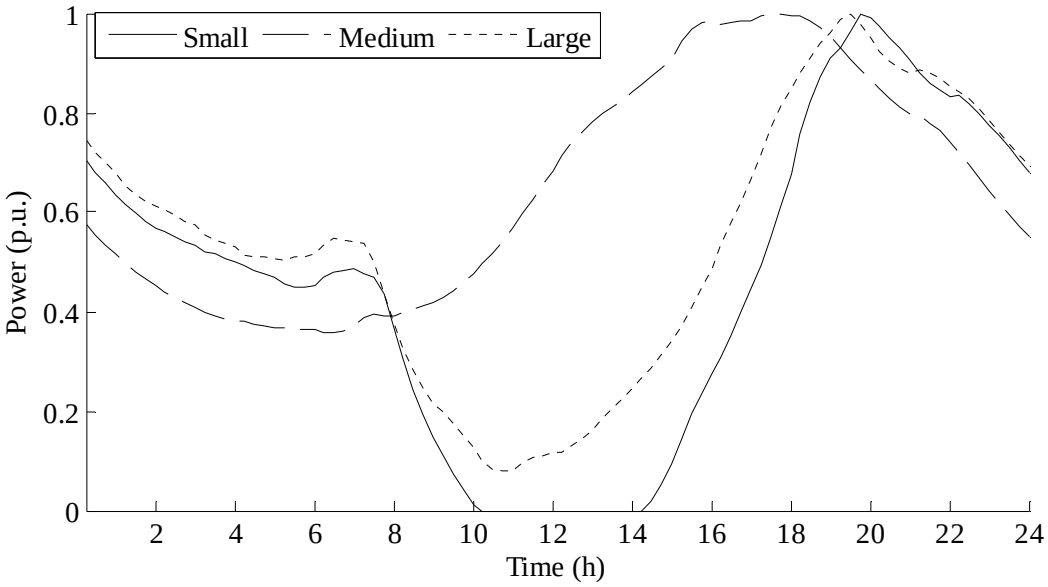

Fig. A.5 Classification of residential loads used in test cases II-V

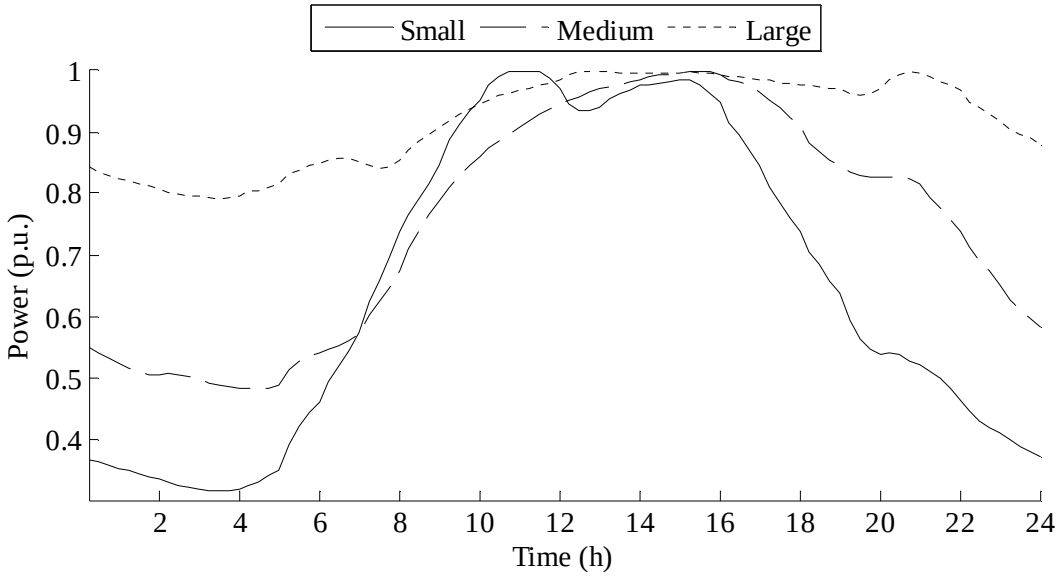

Fig. A.6 Classification of commercial loads used in test cases II-V

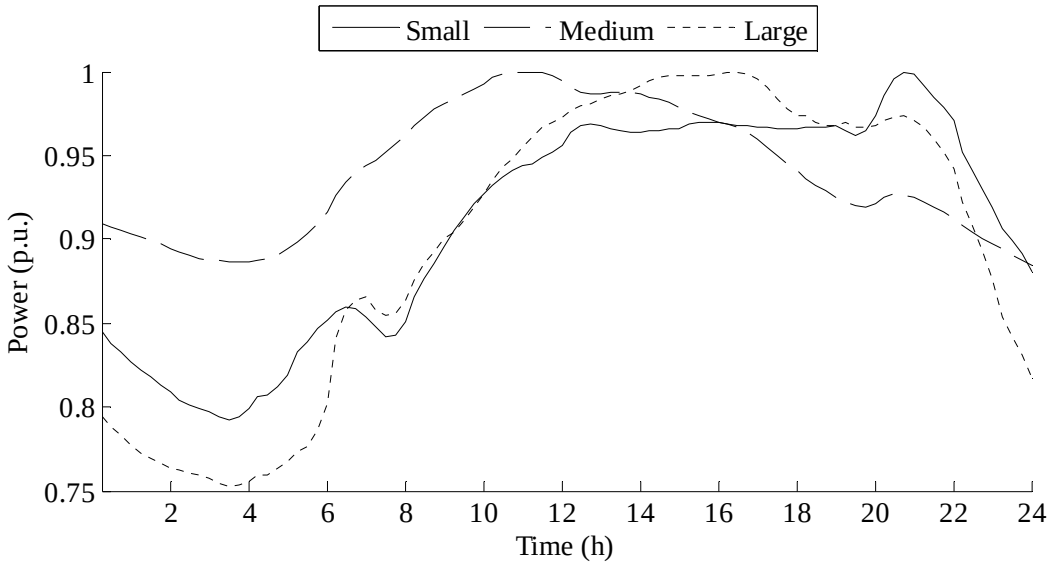

Fig. A.7 Classification of industrial loads used in test cases II-V

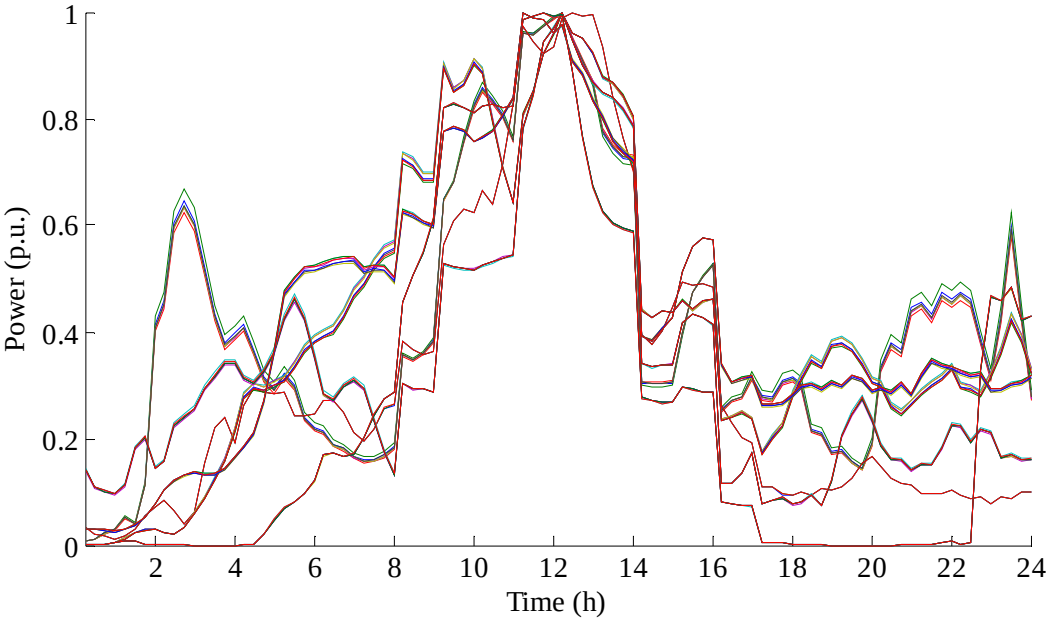

Fig. A.8 Total renewable power output depicted for all 38 load points in feeders F1-F6 of RBTS Bus #3 used in test cases II-V

APPENDIX B

ILLUSTRATIVE EXAMPLE SHOWING NBI AND SP APPLICATION

An example is shown in this appendix section that illustrates the application of the NBI method and separable programming in computing Pareto optimal solutions. Two functions $f_1(X)$ and $f_2(X)$ are chosen as shown in Figure B.1. The induvidual minima for f_1 and f_2 are shown in Table B.1. Since, the functions are non-linear the application of SP would transform the control variable from X to α, and 5 breakway points [-1.0, -0.5, 0.0, 0.5, 1.0] are chosen in the range of X, [-1, 1]. This is also shown in Table B.1. The problem is linearized and can be solved using the simplex method.

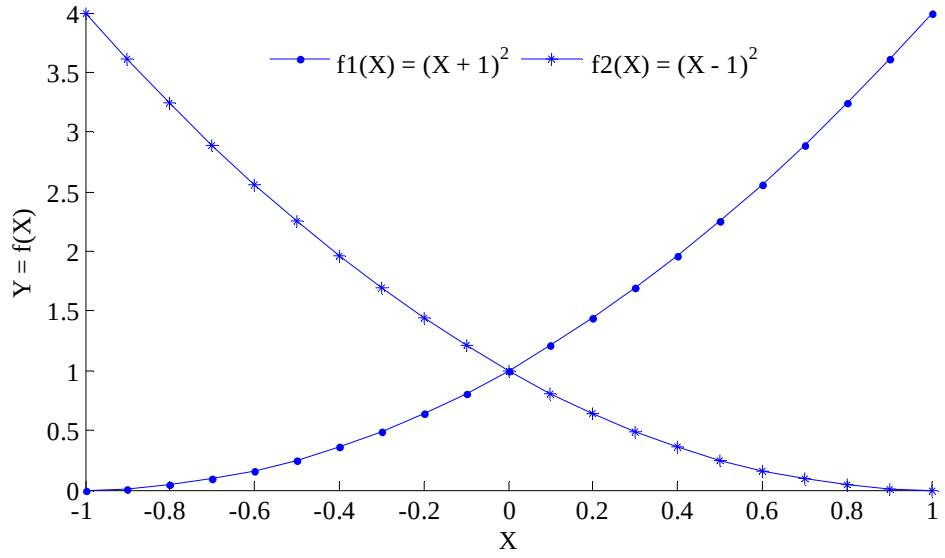

Figure B.1 Functions f_1 and f_2

Table B.1 Individual minima for f_1 and f_2 and convex hull

Function, $f_i(X)$	X^*	f_i^*	$f_i(\alpha)$
$f_1(X) = (X+1)^2$	-1	0	$0\alpha_1 + 0.25\alpha_2 + \alpha_3 + 2.25\alpha_4 + 4\alpha_5$
$f_2(X) = (X-1)^2$	1	0	$4\alpha_1 + 2.25\alpha_2 + \alpha_3 + 0.25\alpha_4 + 0\alpha_5$
Convex hull of individual minima	$\phi = \begin{bmatrix} 0 & 4 \\ 4 & 0 \end{bmatrix}$		

The transformed objective functions using the SP approximation (see (3.28) and (3.29)), is also shown in Table B.1. The transformed control variable, $x = [\alpha_1\ \alpha_2\ \alpha_3\ \alpha_4\ \alpha_5\ d]^T$. The final form of the optimization problem is maximizing the distance from the convex hull to the objective space along a normal distance, i.e., $f = [0\ 0\ 0\ 0\ 0\ -1]^I$. The equality contraints of optimization are constructed as shown in (3.41) and (3.42), and inequality constraints are constructed as shown in (3.36) and (3.37),

$$\min\ f^T x \tag{B.1}$$

such that

$$\begin{bmatrix} 0 & 0.25 & 1 & 2.25 & 4 & -0.7071 \\ 4 & 2.25 & 1 & 0.25 & 0 & -0.7071 \\ 1 & 1 & 1 & 1 & 1 & 0 \end{bmatrix} x = \phi \begin{bmatrix} w_1 \\ w_2 \end{bmatrix} \tag{B.2}$$

$$\begin{bmatrix} -1 & 0.5 & 0 & 0.5 & 1 & 0 \\ 1 & 0.5 & 0 & -0.5 & -1 & 0 \end{bmatrix} x \le \begin{bmatrix} 1 \\ 1 \end{bmatrix}. \tag{B.3}$$

For the NBI subproblems, equidistant convex weights are chosen as shown in Table B.2. The Pareto optimal solutions obtained for each of the weighting combinations, and the corresponding values obtained for the individual functions are also shown in Table B.2. The corresponding Pareto optimal front for the problem has been plotted in Figure B.2. The NBI subproblems were solved using the simplex algorithm in the MATLAB R2010 platform.

Table B.2 Pareto optimal solutions

w_1	0	1	0.1	0.9	0.2	0.8	0.3	0.7	0.4	0.6	0.5
w_2	1	0	0.9	0.1	0.8	0.2	0.7	0..3	0.6	0.4	0.5
f_1	4.0	0.0	3.24	0.04	2.56	0.16	1.96	0.36	1.44	0.64	1.00
f_2	0.00	4.0	0.04	3.24	0.16	2.56	0.36	1.96	0.64	1.44	1.00
X^*	1	-1	0.8	-0.8	0.6	-0.6	0.4	-0.4	0.2	-0.2	0

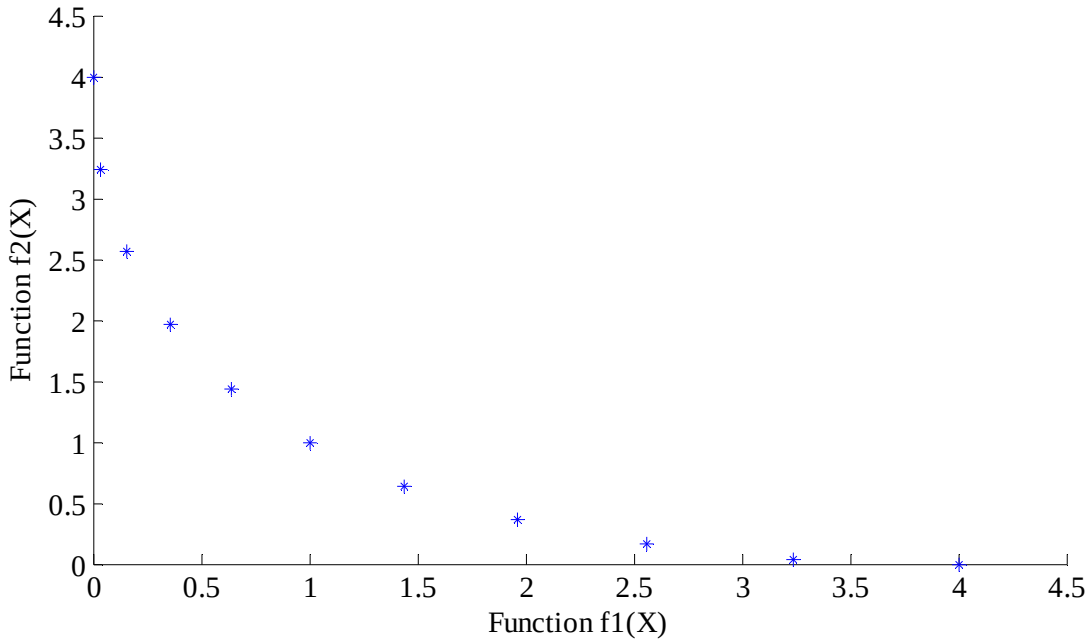

Figure B.2 Pareto optimal front for the given problem

APPENDIX C

SAMPLE MATLAB SUBROUTINES

C.1 Main Steering Routine

```
clc
clear all

global th dt topf
th = 24; % total time horizon (hours)
dt = 15/60; % length of smallest time step for optimization (hours)
delt = 1; % length of sliding window (hours)
topf = 1; % number of steps between optimal power flow (OPF)
Rp = 0; Rw = 0;

load win.mat

trload
drload

trbcase
drbcase

for i = 1: th/dt
   if mod(i, topf) == 0
      time = i;
      trlmp
   else
      if i > topf
         LMP(:, i) = LMP(:, time); %#ok<*AGROW>
      else
         % intial condition for OPF
         LMP(:, i) = [0; 11.1403; 12.1913; 12.0970; 12.2220; 12.3030];
      end
   end
   drlmp
end

for i = 1: lcount
   difference(i, :) = DLMP(list(i), :) - LMP(3, :);
   mind(i) = min(difference(i, :));
end

exitcount = zeros(sum(con), 1);  stime = zeros(sum(con), 2);
for temp = 1: lcount
   if con(temp) == 1
      tic
      mop
```

```
        stime(temp, 1) = toc;
    end
end
Rp = Rp/85;

DLMPbase = DLMP;
LMPbase = LMP;

for i = 1: 96
    loadbase(1, i) = sum(YP(:, i));
end

Rw = 4*Rw/sum(loadbase);

YP(1:38, :) = Xcon;
trbcase
drbcase

for i = 1: th/dt
    if mod(i, topf) == 0
        time = i;
        trlmp
    else
        if i > topf
            LMP(:, i) = LMP(:, time); %#ok<*AGROW>
        else
            % intial condition for OPF
            LMP(:, i) = [0; 11.1403; 12.1913; 12.0970; 12.2220; 12.3030];
        end
    end
    drlmp
end
DLMPfull = DLMP;
LMPfull = LMP;

for i = 1: 96
    loadfull(1, i) = sum(YP(:, i));
end

YP(1:38, :) = Xnoc;
trbcase
drbcase

for i = 1: th/dt
    if mod(i, topf) == 0
```

```
      time = i;
      trlmp
   else
      if i > topf
         LMP(:, i) = LMP(:, time); %#ok<*AGROW>
      else
         % intial condition for OPF
         LMP(:, i) = [0; 11.1403; 12.1913; 12.0970; 12.2220; 12.3030];
      end
   end
   drlmp
end
DLMPnoc = DLMP;
LMPnoc = LMP;


for i = 1: 96
   if i == 1
   Tf(i) = loadfull(i)*LMPfull(3, i)*0.25;
   T0(i) = loadbase(i)*LMPbase(3, i)*0.25;
   else
   Tf(i) = Tf(i-1) + loadfull(i)*LMPfull(3, i)*0.25;
   T0(i) = T0(i-1) + loadbase(i)*LMPbase(3, i)*0.25;
   end
end
save result.mat
```

C.2 Subroutine to Compute LMPs on the Transmission Network

```
pft = 0.98; f = tan(acos(pft));

mpct.bus(2, 3) = 20.0*YC(i); mpct.bus(2, 4) = f*mpct.bus(2, 3); %#ok<*IJCL>
mpct.bus(4, 3) = 40.0*YM(i); mpct.bus(4, 4) = f*mpct.bus(4, 3);
mpct.bus(5, 3) = 20.0*YN(i); mpct.bus(5, 4) = f*mpct.bus(5, 3);
mpct.bus(6, 3) = 20.0*YR(i); mpct.bus(6, 4) = f*mpct.bus(6, 3);

mpct.bus(3, 3) = sum(YP(:, i)); mpct.bus(3, 4) = sum(f*YP(:, i));

optn = mpoption('OUT_ALL', 0);
[opf opfflag(i)] = runopf(mpct, optn);
OPFR(i) = opf;

for k = 1: N
   if mpct.bus(k, 3) > 0
      LMP(k, i) = opf.bus(k, 14); %#ok<*IJCL,*AGROW>
```

```
        LMP(k, i) = LMP(k, i) + opf.bus(k, 17) - opf.bus(k, 16);

        Bt = [B(1: (k - 1), :); B(k + 1: N, :)];
        Bpr = [Bt(:, 1: k - 1) Bt(:, k + 1: N)];
        Zbase = ((mpct.bus(k, 10))^2)/mpct.baseMVA;

        T = H*A*[inv(Bpr) zeros(N - 1, 1); zeros(1, N - 1) 0];

        for l = 1: M
           LMP(k, i) = LMP(k, i) + ...
              T(l, k)*(opf.branch(l, 18) - opf.branch(l, 19));
        end
     end
end
```

C.3 Subroutine to Compute DLMPs in the Distribution System

```
pft = 0.98; f = tan(acos(pft));

mpcb.bus(list(:), 3) = YP(:, i);
mpcb.bus(list(:), 4) = f*YP(:, i);

optn = mpoption('OUT_ALL', 0);
[pf pfflag(i)] = runpf(mpcb, optn);
V = pf.bus(:, 8); d = pf.bus(:, 9)*pi/180;
Gs = pf.branch(:, 3); Bs = pf.branch(:, 4); Bsh = pf.branch(:, 5);
Pf = pf.branch(:, 14); Qf = pf.branch(:, 15);

% Converged N/R Power Flow Jacobian Matrix (Jm) from MATPOWER
Jm = full(makeJac(pf));
Jm1 = [1 zeros(1, 2*n - 2);
      zeros(2*n - 2, 1) Jm];
Jm2 = zeros(2*n, 2*n);
Jm2(1: n, 1: n) = Jm1(1: n, 1: n);
Jm2(1: n, n + 2: 2*n) = Jm1(1: n, n + 1: 2*n - 1);
Jm2(n + 2: 2*n, 1: n) = Jm1(n + 1: 2*n - 1, 1: n);
Jm2(n + 2: 2*n, n + 2: 2*n) = Jm1(n + 1: 2*n - 1, n + 1: 2*n - 1);
Jm2(n + 1, n + 1) = 1;
Jn = Jm2;

% Line Flow Sensitivity with Bus Voltage Matrix (S)
S = zeros(2*m, 2*n);
for l = 1: m
```

```
        ii = mpcb.branch(l, 1); jj = mpcb.branch(l, 2);
        S(l, ii) = ...
           V(ii)*V(jj)*(Gs(l)*sin(d(ii) - d(jj)) - Bs(l)*cos(d(ii) - d(jj)));
        S(l, j) = ...
           V(ii)*V(jj)*(Bs(l)*cos(d(ii) - d(jj)) - Gs(l)*sin(d(ii) - d(jj)));
        S(l, n + ii) = 2*V(ii)*Gs(l) ...
           - V(jj)*((Gs(l)*cos(d(ii) - d(jj)) + Bs(l)*sin(d(ii) - d(jj))));
        S(l, n + jj) = ...
           - V(ii)*((Gs(l)*cos(d(ii) - d(jj)) + Bs(l)*sin(d(ii) - d(jj))));

        S(m + l, ii) = ...
           - V(ii)*V(jj)*(Gs(l)*cos(d(ii) - d(jj)) + Bs(l)*sin(d(ii) - d(jj)));
        S(m + l, jj) = ...
           V(ii)*V(jj)*(Gs(l)*cos(d(ii) - d(jj)) + Bs(l)*sin(d(ii) - d(jj)));
        S(m + l, n + ii) = - 2*V(ii)*(Bs(l) + Bsh(l)/2) ...
           + V(jj)*((Bs(l)*cos(d(ii) - d(jj)) - Gs(l)*sin(d(ii) - d(jj))));
        S(m + l, n + jj) = ...
           V(ii)*((Bs(l)*cos(d(ii) - d(jj)) - Gs(l)*sin(d(ii) - d(jj))));
end
% Sn = -[S(:, 2: N) S(:, (N + 3): 2*N)];

% Bus Connection Matrix (L)
L = zeros(n, m);
for ii = 1: n
   for jj = 1: m
      if mpcb.branch(jj, 1) == ii
         L(ii, jj) = -1;
      elseif mpcb.branch(jj, 2) == ii
         L(ii, jj) = 1;
      end
   end
end
Lnew = [ L zeros(n, m); zeros(n, m) L; ];
L = Lnew;
% Ln = [ Lnew(2: n, :); Lnew(n + 3: 2*n, :) ];


% Jacobian Based Distribution Factors
DFJ = inv(eye(2*m) - S*inv(Jn)*L)*S*inv(Jn);
% DFJ = S*inv(Jn);
DF = DFJ(1: m, 1: n);

% PFR(i) = pf; %#ok<*IJCL>
% flow12(i) = pf.branch(12, 14);
```

```
Closs = 1;
Ccong = 1;

for bus = 1: lcount
   k = list(bus);

   DLMP(k, i) = LMP(3, i); %#ok<*IJCL,*AGROW>

   bt = [b(1: (k - 1), :); b(k + 1: n, :)];
   bpr = [bt(:, 1: k - 1) bt(:, k + 1: n)];
   zbase = ((mpcb.bus(k, 10))^2)/mpcb.baseMVA;
   Vk = pf.bus(k, 8);

   t = h*a*[inv(bpr) zeros(n - 1, 1); zeros(1, n - 1) 0];

   for j = 1: m
      Rl = pf.branch(j, 3);
      Pf = pf.branch(j, 14);
      Qf = pf.branch(j, 15);
      Pt = pf.branch(j, 16);
      Qt = pf.branch(j, 17);
      RatingA = mpcb.branch(j, 6);

      Vf = pf.bus(pf.branch(j, 1), 8);
      Df = pf.bus(pf.branch(j, 1), 9);
      Vt = pf.bus(pf.branch(j, 2), 8);
      Dt = pf.bus(pf.branch(j, 2), 9);

      if Rl == 0
      Il = 0;
      else
      Il = sqrt(abs(Pf - Pt)/(mpcb.baseMVA*Rl*2));
      end
      DLMP_loss(j) = abs(DF(j, k))*(2*Il*Rl)/(Vk*pft);

      DLMP(k, i) = DLMP(k, i) + Closs*DLMP_loss(j) + Ccong*abs(DF(j, k));
   end
end
```

C.4 Subroutine to Compute Pareto Solutions at a Pre-assigned Load Point

```
X_ld(temp, :) = YP(temp, :);
dlmp = DLMP(list(temp), :);
```

```
n = th/dt;
X_dg = [0 0 0 0 0 0 0 0 848 1949 1994 2927 3222 3143 1323 1582 412 ...
   0 0 0 0 0 0 0];
X_dg = 0.5*max(X_ld(temp, :))*X_dg/max(X_dg);
Xdg = zeros(1, n);
j = 1;
for i = 1: n
   if mod(i, n/th) ~= 0
      Xdg(i) = X_dg(j);
   else
      Xdg(i) = X_dg(j);
      j = j + 1;
   end
end
X_d(temp, :) = Xdg + 0.5*wind_f(temp, 1:96);
X_dpu(temp, :) = X_d(temp, :)/max(X_d(temp, :));
X = X_ld(temp, :) - X_d(temp, :);
Rp = Rp + max(X_d(temp, :));
Rw = Rw + sum(X_d(temp, :))*0.25;
Em = 0.5; Pm = 0.25; so = 0.5; eff = 0.95;
n = 1/dt; l = 3;
x = [-Pm 0 Pm];

A = zeros(5*th, l*th + 2); b = zeros(5*th, 1);
for i = 1: th
   A(i, ((i - 1)*l + 1): i*l) = x; b(i) = Pm;
   A(th + i, ((i - 1)*l + 1): i*l) = -x; b(th + i) = Pm;
   for j = 1: i
      A(2*th + i, ((j - 1)*l + 1): j*l) = x;
      A(3*th + i, ((j - 1)*l + 1): j*l) = -x;
   end
   b(2*th + i) = (1-so)*Em;
   b(3*th + i) = so*Em;
   A(4*th + i, ((i - 1)*l + 1): i*l) = x; b(4*th + i) =...
      -max(X(((i - 1)*n + 1): i*n));
   A(4*th + i, th*l + 1) = -1;
end

aeq = zeros(th, l*th + 1); beq = ones(th, 1);
for i = 1: th
   aeq(i, ((i - 1)*l + 1): i*l) = [1 1 1];
end

F1 = zeros(th*l + 2, 1); Fm = zeros(4, 1);
F2 = F1; F3 = F1; F4 = F1; F = F1;
```

```
F1(th*l + 1) = 1;
cr = 0.3*min(dlmp) + 0.7*max(dlmp);
for i = 1: th
   F3(((i - 1)*l + 1): i*l) = x*sum(dlmp(((i - 1)*n + 1): i*n))*dt;
   F4(((i - 1)*l + 1): i*l) = abs(x)*(1 - eff);
   if dlmp(i) > cr
      F2(((i - 1)*l + 1): i*l) = x;
   end
end
C = dlmp*X'*dt;
Ep = sum(X)*dt;

ub = [ones(l*th, 1); inf; inf];
lb = [zeros(l*th, 1); -inf; -inf];

X1 = linprog(F1(1:(l*th + 1)), A(:, 1:(l*th + 1)), b, aeq, beq,...
   lb(1:(l*th + 1)), ub(1:(l*th + 1)));
Fm(1) = F1(1:(l*th + 1))'*X1;
X2 = linprog(F2(1:(l*th + 1)), A(:, 1:(l*th + 1)), b, aeq, beq,...
   lb(1:(l*th + 1)), ub(1:(l*th + 1)));
Fm(2) = F2(1:(l*th + 1))'*X2 + Ep;
X3 = linprog(F3(1:(l*th + 1)), A(:, 1:(l*th + 1)), b, aeq, beq,...
   lb(1:(l*th + 1)), ub(1:(l*th + 1)));
Fm(3) = F3(1:(l*th + 1))'*X3 + C;
X4 = linprog(F4(1:(l*th + 1)), A(:, 1:(l*th + 1)), b, aeq, beq,...
   lb(1:(l*th + 1)), ub(1:(l*th + 1)));
Fm(4) = F4(1:(l*th + 1))'*X4;

phi = [F1(1:(l*th + 1))'*X1 F1(1:(l*th + 1))'*X2 F1(1:(l*th + 1))'*X3 ...
      F1(1:(l*th + 1))'*X4;
      F2(1:(l*th + 1))'*X1 F2(1:(l*th + 1))'*X2 F2(1:(l*th + 1))'*X3 ...
      F2(1:(l*th + 1))'*X4;
      F3(1:(l*th + 1))'*X1 F3(1:(l*th + 1))'*X2 F3(1:(l*th + 1))'*X3 ...
      F3(1:(l*th + 1))'*X4;
      F4(1:(l*th + 1))'*X1 F4(1:(l*th + 1))'*X2 F4(1:(l*th + 1))'*X3 ...
      F4(1:(l*th + 1))'*X4];
phi = phi - (Fm - [0 Ep C 0]')*[1 1 1 1];

flag = 1;
s = 5;
P = (1/6)*s*(s + 1)*(s + 2);
W = zeros(4, P);
for i = 1: -0.25: 0
   for j = 0: 0.25: (1 - i)
      for k = 0: 0.25: (1 - i - j)
```

```
            W(:, flag) = [i j k (1 - i - j - k)]';
            flag = flag + 1;
        end
    end
end

N = phi*[1 1 1 1]';
u = N / norm(N, 2);
Aeq = zeros(4 + th, th*l + 2); Beq = zeros(4 + th, 1);
Aeq(1:4, :) = [F1(1:(th*l + 1))' u(1);
               F2(1:(th*l + 1))' u(2);
               F3(1:(th*l + 1))' u(3);
               F4(1:(th*l + 1))' u(4)];

XS = zeros(th*l + 2, P); Xsol = zeros(th, P); Xnorm = zeros(1, P);
feval = zeros(1, P); exitflag = feval;

for i = 1: P
Beq(1:4) = phi*W(:, i);
Aeq(5:(4 + th), 1:(l*th + 1)) = aeq;
Beq(5:(4 + th)) = beq;

F(th*l + 2) = -1;

options = ...
    optimset('LargeScale', 'off', 'Simplex', 'on', 'Display', 'iter');
[XS(:, i), feval(i), exitflag(i)] = ...
    linprog(F, A, b, Aeq, Beq, lb, ub, [], options);
if exitflag(i) == 1
    exitcount(temp) = exitcount(temp) + 1;
    for j = 1: th
        Xsol(j, i) = x*XS((l*(j - 1) + 1): l*j, i);
    end
    Xnorm(i) = norm(Xsol(:, i), 2);
end
end
flag = 1;
for i = 1: P
    if exitflag(i) == 1
        if flag == 1
            mn = Xnorm(i);
            mx = Xnorm(i);
        elseif Xnorm(i) < mn
            mn = Xnorm(i);
        elseif Xnorm(i) > mx
```

```
            mx = Xnorm(i);
        end
        flag = flag + 1;
    end
end

for i = 1: P
    if Xnorm(i) == mx
        Xs = Xsol(:, i)';
        Wopt(temp, :) = W(:, i)'; %#ok<*AGROW>
    end
end
for i = 1: th
    Xcon(temp, ((i - 1)*n + 1): i*n) = X(((i - 1)*n + 1): i*n) + ...
        Xs(i)*ones(1, n);
    Xnoc(temp, ((i - 1)*n + 1): i*n) = X(((i - 1)*n + 1): i*n);
end
```